AN INVESTIGATION OF AN EXISTING ALUMINUM LATTICE DOME UNDER SNOW LOADS

by

Byron Lloyd Cook

Thesis submitted to the Faculty of the
Virginia Polytechnic Institute and State University
in partial fulfillment of the requirements for the degree of

MASTER OF ENGINEERING

in

Civil Engineering

APPROVED:

S.M. Holzer, Chairman

R.H. Plaut

D.A. Garst

September, 1991

Blacksburg, Virginia

ACKNOWLEDGMENTS

I would like to express my sincere gratitude to Dr. Siegfried Holzer for his encouragement. Also, I would like to thank all of the professors in the Structural Division at Virginia Tech.

I am grateful for all the people who helped me put this thesis together: Tammy Barrett for typing some of the manuscript, Yancey Hull for drawing all of the illustrations, and Mario Godinez for editing.

I would like to thank my wife, Julie, who typed some of the manuscript, plotted the graphs, and gave me encouragement when I needed it.

Finally, I want to dedicate this thesis to the memory of my father, Charles F. Cook, Jr., for he directed me into Civil Engineering and challenged me to pursue an advanced degree.

TABLE OF CONTENTS

LIST OF FIGURES

LIST OF TABLES

CHAPTER 1

INTRODUCTION

1.1 History and Background

Most structures today consist of beam and column construction. Analysis of these structures assumes that the loads and member behavior can be transformed into two-dimensional analysis. But, with the advent of the computer and the use of finite element methods, structural analysis has changed radically (35). With the use of the computer, the transformation of two-dimensional thinking in structural design to the spatial treatment of force flow is now possible. The computer can be programmed to deal with the complex interaction of these physical phenomenons.

With the rapid advancement of computer technology, the use of a group of structures, called space structures, has increased. The definition of a space structure by Subramanian (35) is as follows:

> **A space structure is a structured system in the form of a three-dimensional assembly of elements (as opposed to a continuous surface), resisting loads which can be applied at any point, inclined at any angle to the surface of the structure and acting in any direction. Rolled, extruded or fabricated sections comprise the member elements.**

The three-dimensional character includes flat surfaces with loading perpendicular to the plane as well as curved surfaces.

Space structures can be divided into three broad categories:

1) Skeleton (lattice) frameworks;

2) Stressed skin systems; and,

3) Suspended (cable or membrane) structures (35).

Of these three, the skeleton, or lattice framework is most widely used. Lattice framework structures can be subdivided into three categories:

1) Double-layer Grids;

2) Lattice Barrel Vaults; and,

3) Lattice Domes.

Domes are one of the oldest of these structural forms and have been used in architecture from earliest times. They enclose a maximum amount of space with a minimum surface and can be very economical in terms of material (9,35).

Historically, domes represent an ideology of their own with a specific symbolic meaning. In the Roman, Christian, and Islamic worlds, they were associated with temples, churches, mosques, memorials, baptisteries, tombs, baths, and other meeting places; they were not just functional solutions for covering large spaces (29). The introduction of iron opened up a new era of lattice domes in the latter part of the nineteenth century (19, 29, 35). Today, lattice domes are

used for churches, civic centers, planetaria, aquariums, gymnasia, sports arenas, skating rinks, swimming pools, theaters, restaurants, sedimentation basins and tank tops.

Lattice domes, because they are network structures as opposed to continuous structures, are relatively lightweight. A 130 foot lattice dome may weigh 15 times less, but be equally as strong as the same size dome made of concrete (30).

1.2 Objectives

Structural analysis is a mathematical representation of the structure and the applied loads whose behavior is sufficiently close to that of the original structure. To accomplish this, many assumptions and idealizations must be made. For example, member properties may be treated as linear when they are actually curvilinear, or an end condition may be treated as fixed or pinned when actually it is somewhere between these two. The collapse of a large dome in Bucharest, Romania, in 1963 is an example of the variations in live load distribution (18). A possible reason for the failure is an incorrect model of the applied loads. The major goal of this paper is to study a modeling method which approximates the actual physical phenomena. The modeling method is divided into two categories: the applied loads and the physical dome.

The modeling of the applied loads used in my study is an extension of the derivation by Hao (14). Hao transformed the

applied pressures into a joint load. Instead of a point load at the joints, the applied load is transformed into a linearly varying distributed load applied along the members. A derivation of this model is presented in Chapter 3 of this paper.

The modeling of the physical dome was done by the stiffness matrix method. STAAD-III, a commercial stiffness matrix structural program, was used. The power and extent of the program is greater than the traditional student-written programs. Simple models were investigated in order to accrue sufficient familiarity with the program before any analysis of the dome was performed. A parametric study of joint stiffness versus deflection and internal forces was done, and is included in Chapter 5.

CHAPTER 2

DOME DESCRIPTION

2.1 Introduction

This chapter contains the physical description of the dome used in this study. Many papers have performed finite element analysis of lattice domes. All of these lattice domes were of a theoretical nature not an existing dome. A commercial dome by a company called Conservatek was chosen for this study.

2.2 Geometry

Lattice domes are a subset of space structures in which either the joints or the members lie on a surface of revolution. The arrangement of the members defines the category of the dome. There are several ways to categorize domes. Makowski (18) uses inventors' names and geometric patterns. A more systematic method is presented by Schueller (29). Schueller organizes lattice domes according to the nature of their surface structure. Figure 2.1 is a guide to the different categories of domes. Figure 2.2 gives examples of the major lattice dome systems: Schwedler, Lattice, Lamella, Grid, and Geodesic.

The Schwedler dome, shown in Figure 2.2a, is named after its inventor. The defining feature of the Schwedler dome is

Figure 2.1 Dome Category Guide

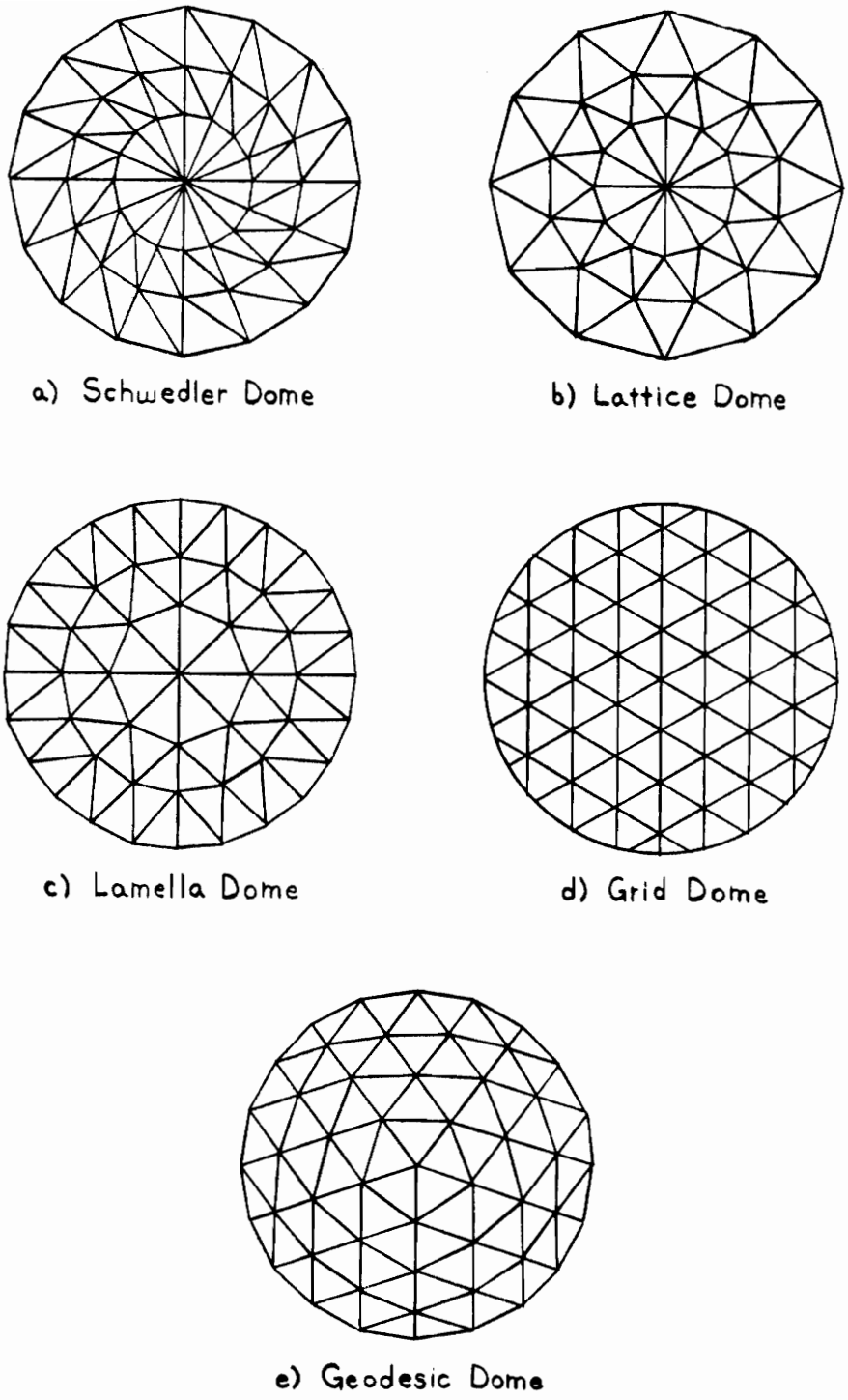

Figure 2.2 Examples of Major Dome Systems

the radial ribs with concentric rings. The trapezoidal bays are divided by a diagonal member, thus forming a triangular mesh.

The lattice dome, shown in Figure 2.2b, is characterized by a set of concentric rings. The top ring is divided by a set of radial ribs from the apex. The remaining concentric circles are divided by diagonal members which joins any two concentric rings into a triangular mesh.

The lamella dome, shown in Figure 2.2c, is a derivation of the Schwedler dome. Lamella domes are a curvilinear system of ribbed domes, characterized by:

1) Only a few of the ribs running from the rim to the crown of the dome as meridional spherical sector dividers;
2) All other ribs running as intra-sector parallel lines; and,
3) A diamond grid being thus formed (31), each diamond may be subdivided into triangles.

The grid dome, shown in Figure 2.2d, is the simplest form. A grid is projected onto a sphere creating the geometry.

The geodesic dome, shown in Figure 2.2e, combines the feature of lamella domes in having triangular grids with individual struts of different lengths, and the feature of lattice domes in locating individual struts comprising the

triangular grids on, or very near, great circles (31). R. Buckminster Fuller invented and patented this system. He considered the icosahedron as the most efficient fundamental volume-controlling device of nature because it provides the most volume with the least surface (29). The icosahedron is projected on the surface of a sphere, thus dividing the sphere into 20 equilateral spherical triangles, which is the maximum number of equilateral triangles into which a sphere can be divided. Each of these triangles can be subdivided into six triangles by drawing medians and bisecting the sides of each original triangle. These medians follow great circles, which are the extensions of the sides of the basic equilateral triangles into which a spherical icosahedron can be divided. Using this method of construction it is possible to form 15 complete great circles regularly arranged on the surface of the sphere. In geodesic domes, the members forming the framework are usually straight along the chords of a geodesic arc (35). The geodesic sphere can be truncated to yield a ⅝, ½, or ⅝ geodesic dome.

The plan view for a Conservatek Alumadome is depicted in Figure 2.3 and the profile is depicted in Figure 2.4. The coordinates of the center of each connection are given in Table 2.1. The type of geometry is a lattice dome which consists of 3 tiers. The dome has a diameter of 60 feet and a

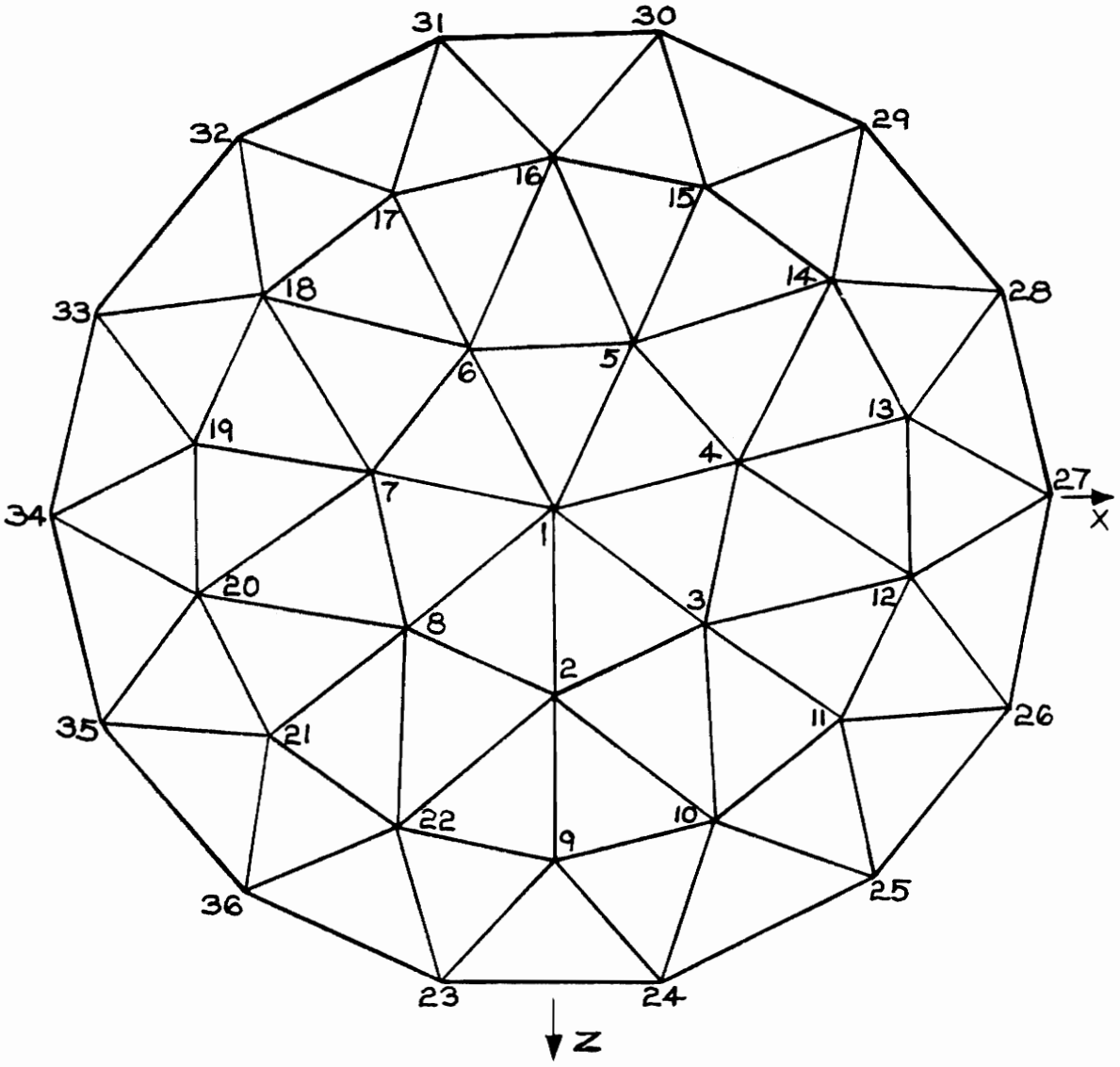

Figure 2.3 Plan View for the Conservatek Alumadome

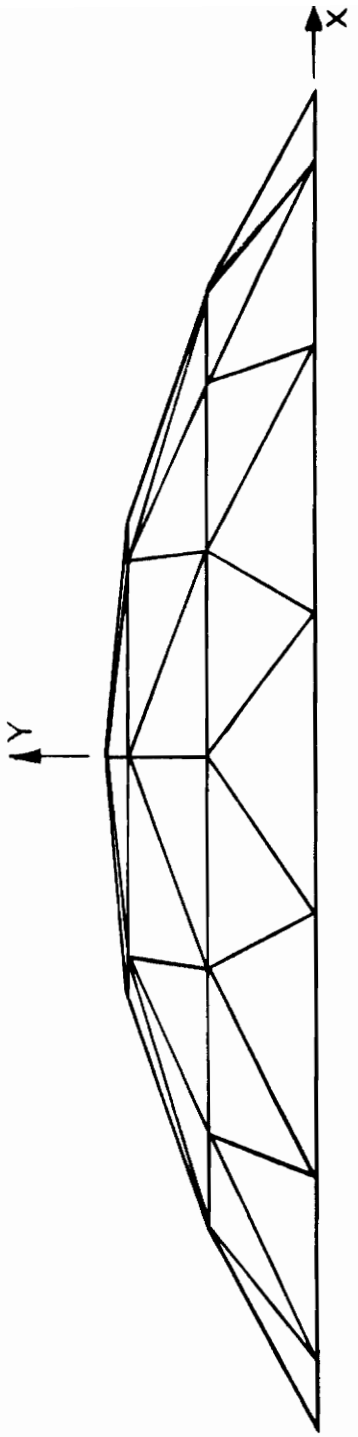

Figure 2.4 Profile of the Conservatek Alumadome

JOINT	X (INCH)	Y (INCH)	Z (INCH)
1	0	105.4793	0
2	0	92.1595	130.3312
3	101.8970	92.1595	81.2602
4	127.0635	92.1595	-29.0014
5	56.5486	92.1595	-117.4243
6	-56.5486	92.1595	-117.4243
7	-127.0635	92.1595	-29.0014
8	-101.8970	92.1595	81.2602
9	0	53.2459	254.1230
10	110.2598	53.2459	228.9569
11	198.6814	53.2459	158.4431
12	247.7516	53.2459	56.5477
13	247.7516	53.2459	-56.5477
14	198.6814	53.2459	-158.4431
15	110.2598	53.2459	-228.9569
16	0	53.2459	-254.1230
17	-110.2598	53.2459	-228.9569
18	-198.6814	53.2459	-158.4431
19	-247.7516	53.2459	-56.5477
20	-247.7516	53.2459	56.5477
21	-198.6814	53.2459	158.4431
22	-110.2598	53.2459	228.9569
23	-78.6077	0	344.4030
24	78.6077	0	344.4030
25	220.2539	0	276.1898
26	318.2762	0	153.2738
27	353.2599	0	0
28	318.2762	0	-153.2738
29	220.2539	0	-276.1898
30	78.6077	0	-344.4030
31	-78.6077	0	-344.4030
32	-220.2539	0	-276.1898
33	-318.2762	0	-153.2738
34	-353.2599	0	0
35	-318.2762	0	153.2738
36	-220.2539	0	276.1898

TABLE 2.1 JOINT COORDINATES

height of 9.25 feet. There is a tension ring of 14 members and 77 interior members.

2.3 Longitudinal Members

The structural behavior of space structures results in approximately half the members acting in compression, which requires struts with significant buckling capability (37). Tubular members are more commonly used in single-layer structures because the cross-sectional properties are the same in all directions. This means that they are adaptable to a number of connection mechanisms, and eliminate the lateral-torsional buckling problem. Unfortunately, tubular members are not as compatible as I-beams or rectangular tubes in attaching cladding.

The type of material used for domes has varied through history. Wood domes were built in the Middle Ages. Masonry was the traditional material used until the development of steel in the 19th century. The high strength, low alloy structural steels and heat treated constructional alloy steels invented in the twentieth century resulted in larger and lighter domes. Within the last five decades heat treated and tempered aluminum alloys, high strength alloys, and rolled and extruded sections of aluminum have been introduced successively, resulting in lightweight, non-corrosive metallic domes (35). With the advent of laminated wood structures,

wood became another economical dome material.

The longitudinal members in the Conservatek Alumadome are aluminum I-beams. The mechanical properties are in accordance with the Aluminum Standards and Data, 8th Edition (2). Two types of members are used in the dome and they have the following cross-sectioned properties:

Type 1

Depth = 6 in

Area = 2.114 in^2

Major Moment of Inertia
(about local z-axis) = 10.46 in^4

Minor Moment of Inertia
(about local y-axis) = 0.748 in^4

Torsional Moment of Inertia = 0.014 in^4

Type 2

Depth = 6 in

Area = 3.68 in^2

Major Moment of Inertia
(about local z-axis) = 21.52 in^4

Minor Moment of Inertia
(about local y-axis) = 3.801 in^4

Torsional Moment of Inertia = 0.064 in^4

The members are of the aluminum alloy 6061-T6 with a Modulus of Elasticity of 10.1 x 10^3 ksi. All interior members have the cross-sectional properties of Type 1. All tension ring members have the cross-sectional properties of Type 2.

2.4 Connections

The function of the connections is to adequately transfer all forces and moments applied at the ends of the members meeting at a joint, to interconnect all the members coming into the joint with ease, and to provide the necessary accuracy during construction. Much consideration is needed to fabricate them at moderate prices and of unobtrusive appearance (20). There are several ways to categorize connections. Arciszewski (3) divides the connector system into 3 parts: joint elements, end-pieces of joint elements, and end-pieces of bars. Subramanian (35) uses existing connectors to make categories. He then establishes tables of typical characteristics to classify systems. The categories are as follows:

1) Welded cast connectors;
2) Welded node connectors;
3) Screw connected node connectors;
4) Pressed metal connectors;
5) Key connected node connectors; and,
6) Connectors using gusset plates.

The MERO joint belongs to the screw connected node category; the UNISTRUT system belongs to the pressed metal node connector category; the TRIODETIC system belongs to the key connected node category; and the TESEP, TUB ACCORD, CASH, and TOD systems belong to the connectors using gusset plates

category.

The Conservatek Alumadome uses gusset plate connectors. The structural members are connected by 2 gusset plates, one for each flange, by a minimum of 4 bolts per flange. Figure 2.5 shows a plan view of the connection and Figure 2.6 shows a cross-section of the connection.

2.5 Cladding

There is no ideal type of cladding for a dome. The materials used are not only influenced by the architectural concept, and the geographical location of the structure, but also by all of the parameters of the structural analysis (snow, wind, earthquakes, and other climatic influences) (11). Cladding is divided into two classes:

1) Flexible skin

2) Rigid roofing

Flexible skins are either stretched over the framework or suspended below. Examples of flexible skins are PVC laminated fabric and PTFE laminated glass-reinforced membranes.

Rigid cladding systems are based upon the use of individual panels of a dome. Examples of rigid cladding materials commonly used are acrylic, plywood and aluminum. Apart from the difficulty of sealing such panels, most lattice domes consist of members which are designed to carry axial end loads (12). Bending moments must be avoided and, in practice,

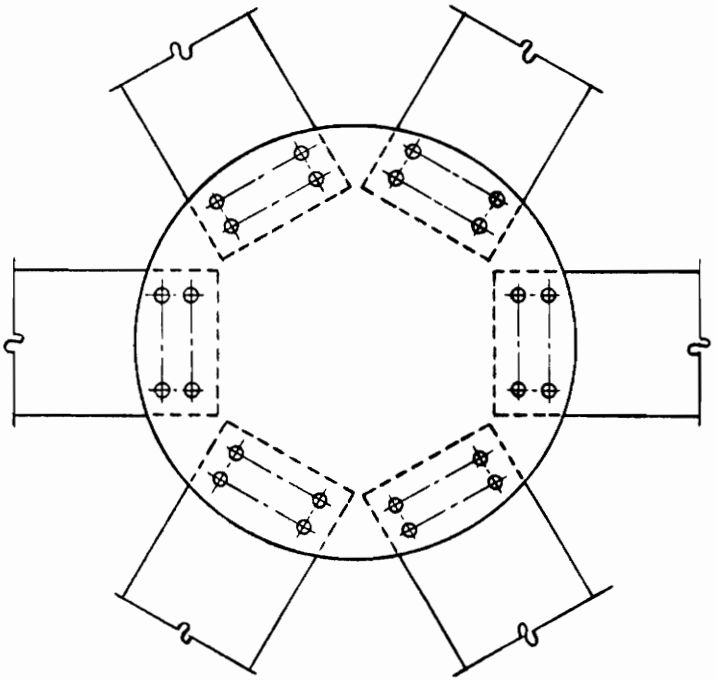

Figure 2.5 Plan View of the Gusset Plate Connection

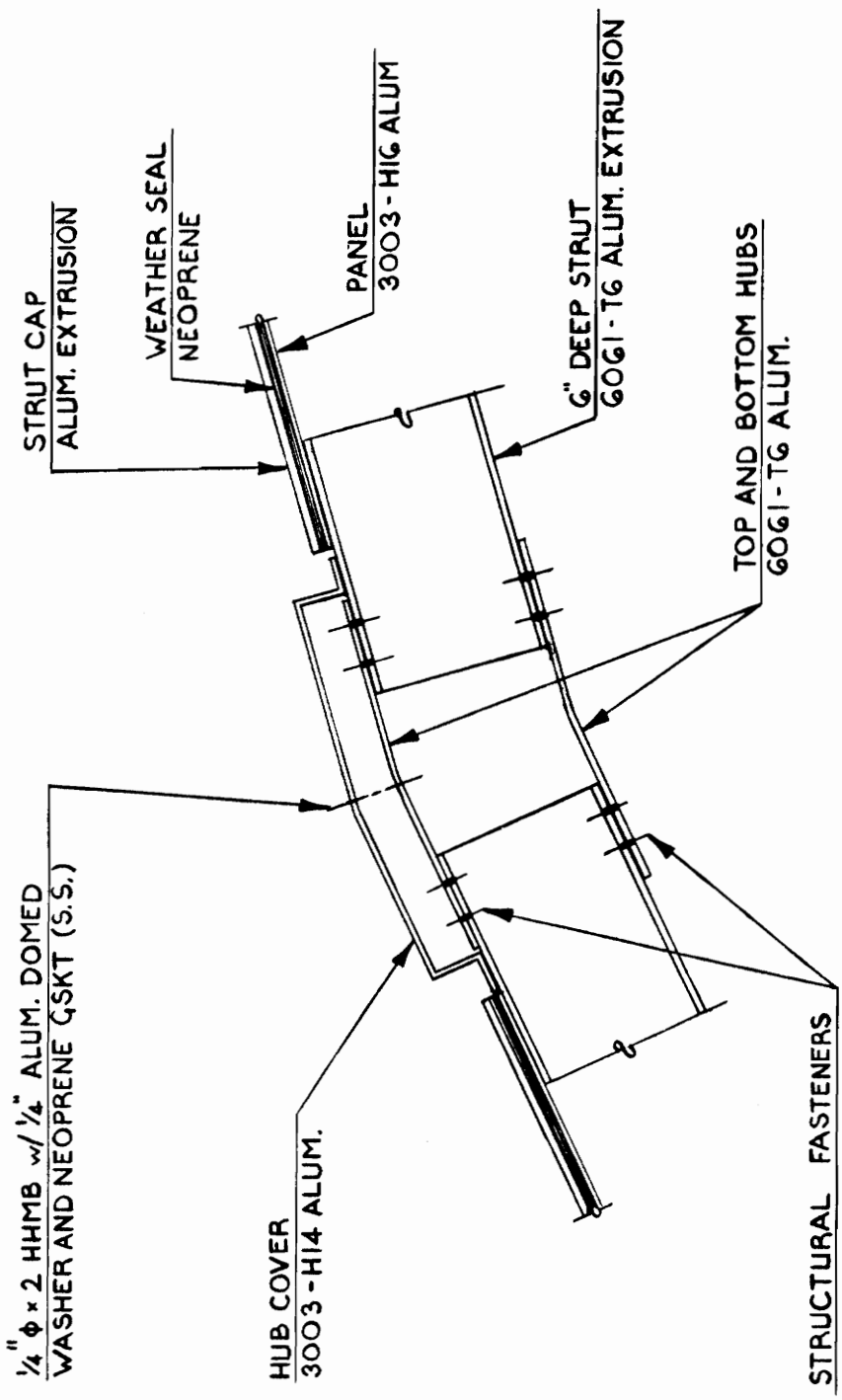

Figure 2.6 Cross-Section of the Gusset Plate Connection

this means that cladding support points must be restricted to the joint positions. To achieve this, it is necessary either to adopt a panel system which reflects the structural network or to provide an auxiliary system of purlins or support bars (12).

The Conservatek Alumadome cladding panels are attached continuously along their edges to the structural member by means of clamping bars which engage the panels in an interlocking joint. A cross-section of the joint is shown in Figure 2.7.

Since the panel is connected along the structural member, bending moments in the longitudinal member must be taken into consideration. A derivation of transforming pressure loads into member loads is presented in Chapter 3.

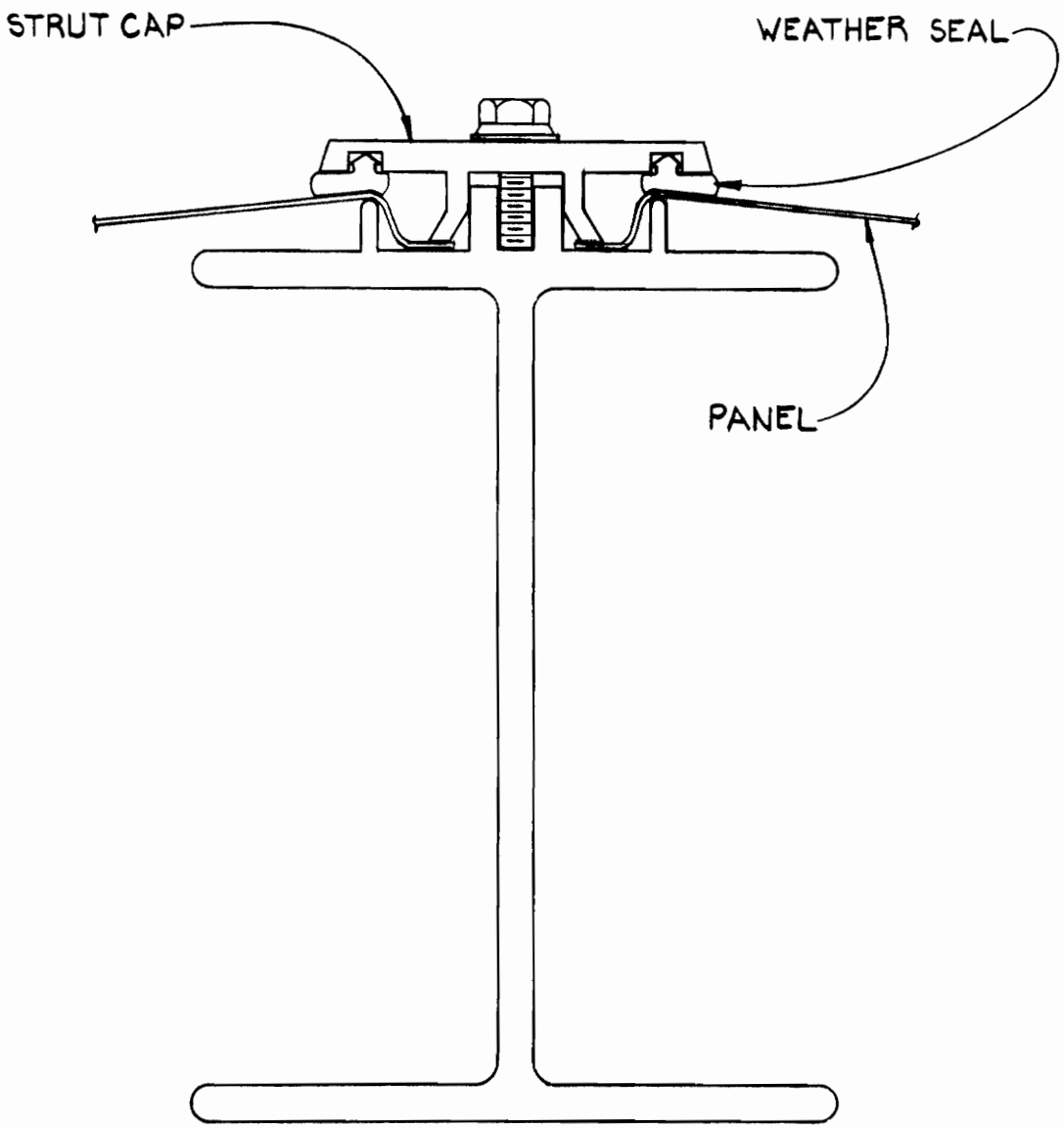

Figure 2.7 Cross-Section of the Panel Joint

CHAPTER 3

LOADS

3.1 Introduction

A structure must be able to resist the many types of forces applied to it. According to the Alumadome Specification (2), the magnitude of the loads applied to the structure shall be determined in accordance with ANSI A58.1-1982 (22). According to Makowski (18), the critical load combinations for a dome are as follows:

1) Snow load over the whole dome;

2) Unbalanced snow load (It is usual to allow for the possibility of a build-up of snow on one side of the dome); and,

3) Wind load.

On the assumption that the dome can support its own self-weight, the dead load will not be examined. The snow load over the whole dome and a linearly varying snow load over ½ of the dome was examined.

3.2 Transformation of Loads

The distributed load applied on each panel must be transformed into a series of forces. Transforming the distributed load into a load vector is a realistic assumption for many domes since many suspend a load carrying sheet from

the joints of a dome (36). For these domes, the load is truly applied at the nodes. However, Figure 2.8 indicates that the panel is attached along the members. Bending strain, therefore, cannot be neglected. Renton (26) and McConnel and Klimke (21) discuss this topic.

One of the objectives of this thesis is to develop a model of the loads along the members. Hao (14) transforms pressure loads at nodes into equivalent nodal forces. The normal forces at each corner of a panel are expressed as follows:

$$R_1 = \frac{2P_1A}{12} + \frac{1P_2A}{12} + \frac{1P_3A}{12} \qquad (3.1)$$

$$R_2 = \frac{1P_1A}{12} + \frac{2P_2A}{12} + \frac{1P_3A}{12} \qquad (3.2)$$

$$R_3 = \frac{1P_1A}{12} + \frac{1P_2A}{12} + \frac{2P_3A}{12} \qquad (3.3)$$

where R_i = nodal force at node i acting normal to the plane of the panel

P_i = pressure at node i

A = area of the panel.

By reversing the direction of the reactive forces at the nodes, these loads are the equivalent loads applied at the nodes.

With the aid of Figure 3.1, one can use statics to solve for the reactions along each member by taking the moment about the appropriate side. Each member length is designated by the joint from which it is opposite (i.e. l_1, l_2, l_3). For each

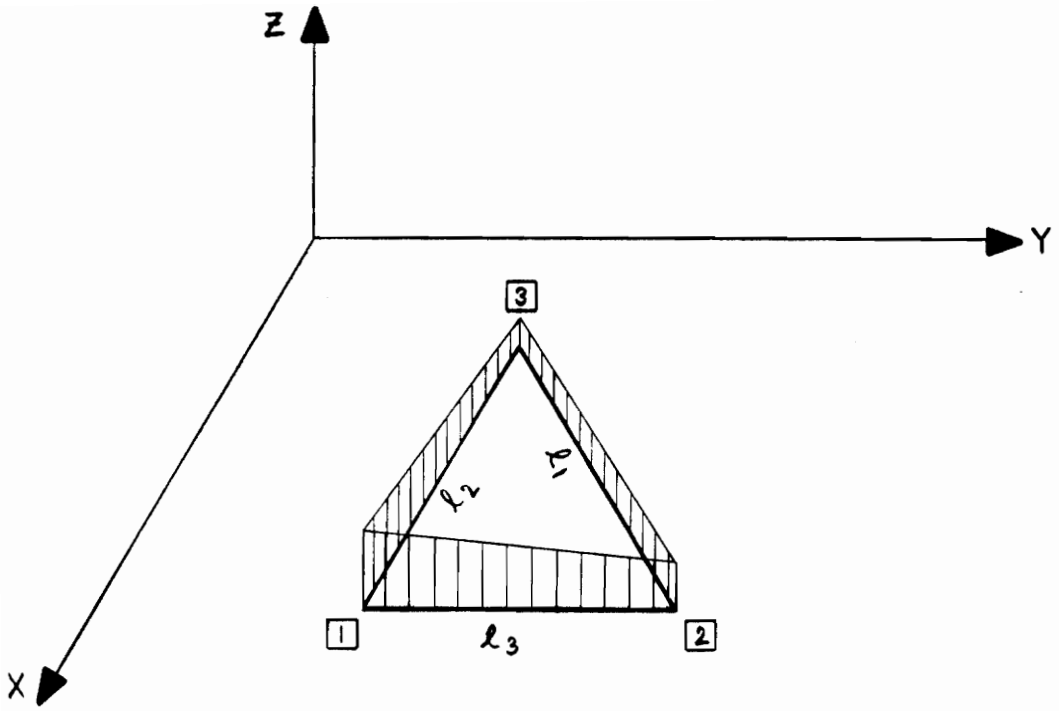

(a) Domain

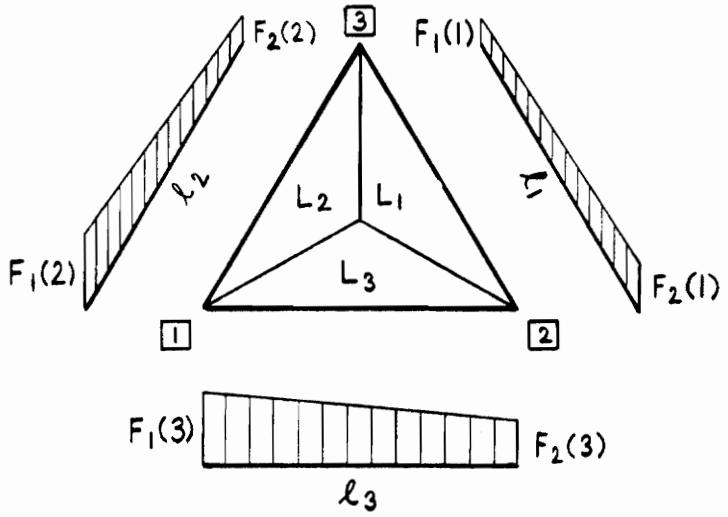

(b) Image

Figure 3.1 Panel Load Coordinates

member, the distributed force is defined at each end, F_1 and F_2. The force at the 2-end of member 3 is shown as $F_2(3)$. By taking the moment about the 1-2 side of the panel, one obtains the equilibrium equation

$$M_{R3} = M_{F1}^{\ 2} + M_{F2}^{\ 2} + M_{F1}^{\ 1} + M_{F2}^{\ 1} \tag{3.4}$$

where M_{R3} is the moment due to R_3. By the principle of superposition, the forces along member 2 can be divided into two triangular loads; one triangular load has the force of $F_1(2)$ at the 1-end and zero at the 2-end, and the other triangular load has the force of $F_2(2)$ at the 2-end and zero at the 1-end. Both of these forces vary linearly between the ends. The moment due to the triangular force $F_1(2)$ is $M_{F1}^{\ 2}$ and the moment due to the triangular force $F_2(2)$ is $M_{F2}^{\ 2}$. The moment due to the forces along member 1 are computed in the similar way and are called M^1_{F1} and M^1_{F2}.

From Figure 3.2a, one can calculate the moment M_{R3}:

$$M_{R3} = R_3 h_3. \tag{3.5}$$

The area of the panel is:

$$A = \frac{l_3 h_3}{2} \tag{3.6}$$

Solving for h_3 in Eq. 3.6 and substituting it into Eq. 3.5, one obtains

$$M_{R3} = \frac{2AR_3}{l_3} \tag{3.7}$$

The moment $M_{F2}^{\ 2}$ can be calculated from Figure 3.2b. Using natural coordinates, the coordinates along member 2 are:

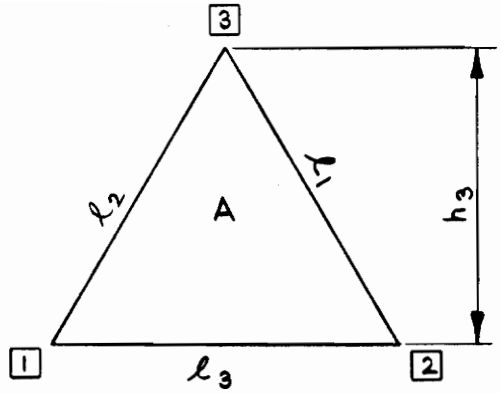

(a) Moment M_{R3}

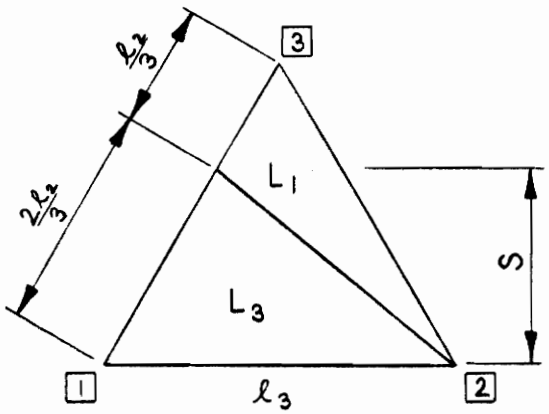

(b) Moment M^2_{F2}

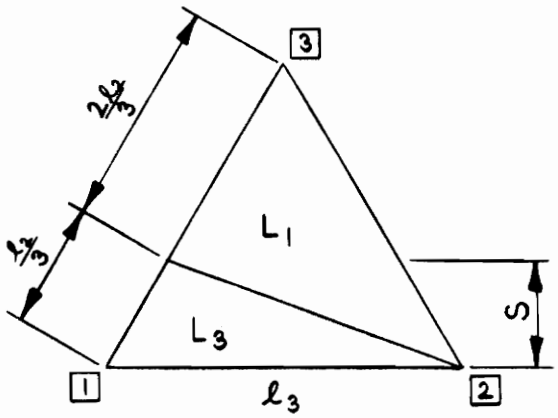

(c) Moment M^2_{F1}

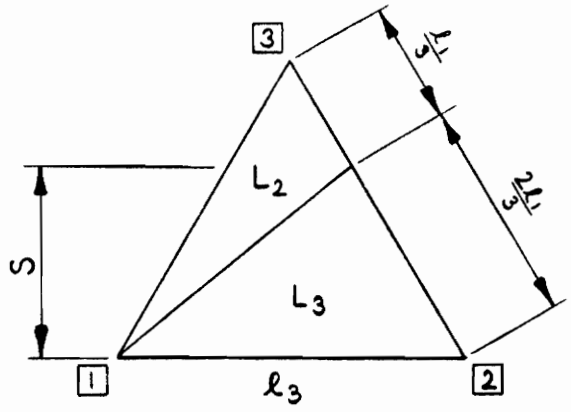

(d) Moment M^1_{F1}

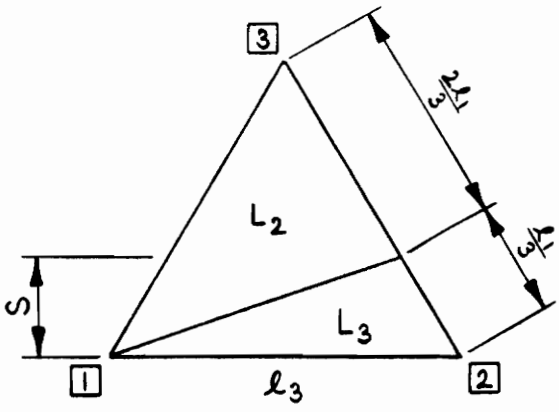

(e) Moment M^1_{F2}

Figure 3.2 Panel Moment Diagrams

$$L_2 = 0; \qquad L_1 + L_3 = 1 \tag{3.8}$$

Since the location of the centroid of a right triangle is ⅓ of the base from the apex at the 2-end of the member 2, the values of L_1 and L_3 are

$$L_1 = \frac{1}{3}; \qquad L_3 = \frac{2}{3}. \tag{3.9}$$

The moment due to the 2-end force along member 2 is

$$M^2_{F2} = \frac{F_2(2)\ l_2 S}{2}. \tag{3.10}$$

The area at the centroid of the 2-end force is

$$A_3 = \frac{l_3 S}{2}, \tag{3.11}$$

since

$$L_3 = \frac{A_3}{A} = \frac{2}{3}. \tag{3.12}$$

By substituting Eq. 3.11 into Eq. 3.12, one obtains

$$S = \frac{4A}{3l_3}. \tag{3.13}$$

Substituting Eq. 3.13 into Eq. 3.10, the moment M_{F2}^2 can be expressed as

$$M^2_{F2} = \frac{2l_2 A F_2(2)}{3l_3}. \tag{3.14}$$

From Figure 3.2c, the moment M^2_{F1} can be calculated. Using natural coordinates, the coordinates along member 2 are

$$L_2 = 0, \quad L_1 + L_3 = 1. \tag{3.15}$$

This time, the load is at the 1-end of the member. So the coordinates of L_1 and L_3 are:

$$L_1=\frac{2}{3}, \text{ and } L_3 = \frac{1}{3}. \tag{3.16}$$

The moment due to the 1-end force along member 2 is

$$M^2_{F1} = \frac{F_1(2)l_2S}{2} \tag{3.17}$$

The area at the centroid of the 1-end force is

$$A_3 = \frac{l_3S}{2} \tag{3.18}$$

since

$$L_3 = \frac{A_3}{A} = \frac{1}{3} \tag{3.19}$$

substituting Eq. 3.18 into Eq. 3.19, one obtains

$$S = \frac{2A}{3l_3} \tag{3.20}$$

Substituting Eq. 3.32 into Eq. 3.29, the moment M^2_{F1} can be expressed as

$$M^2_{F1} = \frac{l_2}{3l_3} A\ F_1(2) \tag{3.21}$$

The moments due to the forces along member 1 are similarly calculated. From Figure 3.2d and Figure 3.2e, the moments M^1_{F1} and M^1_{F2} can be calculated. The moment due to the 1-end force along member 1 is

$$M^1_{F1} = \frac{2l_2}{3l_3} AF_1(1) \tag{3.22}$$

The moment due to the 2-end force along member 1 is

$$M^1_{F2} = \frac{l_1}{3l_3} AF_2(1) \tag{3.23}$$

Substituting Eqs. 3.7, 3.14, 3.21, 3.22, 3.23 into Eq. 3.4, dividing each side by 2A and multiplying each side by l_3,

one can reduce Eq. 3.4 to

$$\frac{1}{6}l_2F_1(2) + \frac{2}{6}l_2F_2(2) + \frac{2}{6}l_1F_1(1) + \frac{1}{6}l_1F_2(1) = R_3 \quad (3.24)$$

Similarly, the equilibrium equations about the other sides of the panel are solved. The results are:

$$\frac{1}{6}l_2F_1(2) + \frac{2}{6}l_2F_2(2) + \frac{2}{6}l_1F_1(1) + \frac{1}{6}l_1F_2(1) = R_3, \quad (3.25)$$

$$\frac{1}{6}l_3F_1(3) + \frac{2}{6}l_3F_2(3) + \frac{1}{6}l_1F_1(1) + \frac{2}{6}l_1F_2(1) = R_2, \text{ and} \quad (3.26)$$

$$\frac{2}{6}l_2F_1(2) + \frac{1}{6}l_2F_2(2) + \frac{2}{6}l_3F_1(3) + \frac{1}{6}l_3F_2(3) = R_1. \quad (3.27)$$

Since the applied load is continuous, the beam loading has to be continuous as well; therefore,

$$F_1(3) = F_1(2) = F_1, \quad (3.28)$$

$$F_2(3) = F_2(1) = F_2, \text{ and} \quad (3.29)$$

$$F_2(2) = F_1(1) = F_3. \quad (3.30)$$

By substituting Eqs. 3.28, 3.29, and 3.30 into Eqs. 3.25, 3.26, and 3.27, one obtains the following equations:

$$\frac{1}{6}l_2F_1 + \frac{1}{6}l_1F_2 + \frac{2}{6}(l_1 + l_2)\,F_3 = R_3, \quad (3.31)$$

$$\frac{1}{6}l_3F_1 + \frac{2}{6}(l_1 + l_3)F_2 + \frac{1}{6}F_3 = R_2, \text{ and} \quad (3.32)$$

$$\frac{2}{6}(l_2 + l_3)F_1 + \frac{1}{6}l_3F_2 + \frac{1}{6}l_2F_3 = R_1. \quad (3.33)$$

Alternative solution of Eqs. 3.31, 3.32, and 3.33 are in Appendix A. Substituting Eqs. 3.1, 3.2, 3.3 into Eqs. 3.31, 3.32, 3.33 and solving for F_1, F_2, F_3 results in the following equations:

$$F_1 = \frac{1}{(l_1 + l_2)(l_1 + l_3)(l_2 + l_3) + l_1 l_2 l_3} \left[\frac{1}{12} P_1 A \left(6l_1^2 + 7l_1 l_2 + 7l_1 l_3 + 4l_2 l_3\right) + \frac{1}{12} P_2 A \left(3l_1^2 + 4l_1 l_2 + l_1 l_3 - 2l_2 l_3\right) + \frac{1}{12} P_3 A \left(3l_1^2 + l_1 l_2 + 4l_1 l_2 - 2l_2 l_3\right)\right], \quad (3.34)$$

$$F_2 = \frac{1}{(l_1 + l_2)(l_1 + l_3)(l_2 + l_3) + l_1 l_2 l_3} \left[\frac{1}{12} P_1 A \left(3l_2^2 + 4l_1 l_2 - 2l_1 l_3 + l_2 l_3\right) + \frac{1}{12} P_2 A \left(6l_2^2 + 7l_1 l_2 + 4_1 l_3 + 2l_2 l_3 + 7l_2 l_3\right) + \frac{1}{12} P_3 A \left(3l_2^2 + l_1 l_2 - 2l_1 l_3 + 4l_2 l_3\right)\right], \quad (3.35)$$

$$F_3 = \frac{1}{(l_1 + l_2)(l_1 + l_3)(l_2 + l_3) + l_1 l_2 l_3} \left[\frac{1}{12} P_1 A \left(3l_3^2 - 2l_1 l_2 + 4l_1 l_3 + l_2 l_3\right) + \frac{1}{12} P_2 A \left(3l_3^2 - 2l_1 l_2 + {}_1 l_3 + 4l_2 l_3\right) + \frac{1}{12} P_3 A \left(6l_3^2 + 4_1 l_2 + 7l_1 l_3 + 7l_2 l_3\right)\right] \quad (3.36)$$

where l_1, l_2, l_3 are the lengths of the triangular panel; A is the area of the triangle; and P_1, P_2, P_3 are the design pressures at nodes 1, 2, and 3, respectively.

3.3 Snow Loads

Snow loads are one of the most important live loads for domes. The determination of snow load distribution is extremely difficult. Several known examples of the collapse of domes show that the failure was caused by the unbalanced accumulation of snow. In 1963, a large lattice dome in

Bucharest, Romania collapsed because of the unpredictability of the snow distribution (32). The ANSI A58.1-1982 Code (22) has a provision for unbalanced snow loads. The snow load in this report will be calculated based on Category I, unheated structures.

The loading conditions for the dome will be uniform load and an unbalanced snow load covering half of the dome. For the uniform load, a ground snow load of 35 psf was chosen. A uniform snow load of 29.52 psf was calculated. For the unsymmetric snow load, the snow distribution is shown in Figure 3.3a. In Figure 3.3b, the crossed-hatched panels are the ones to which the unbalanced snow load will be applied. The design pressures at the nodes are shown in Table 3.1.

3.4 Computer Program Description

As discussed in Section 3.2, pressured loads are transformed into non-uniform distributed loads. A BASIC computer program was written for the above transformation (See Appendix E). As with many structural analysis programs, the following information was required:

1) Number of joints;
2) Number of elements;
3) Joint Coordinates;
4) Member Incidence; and,
5) Loads.

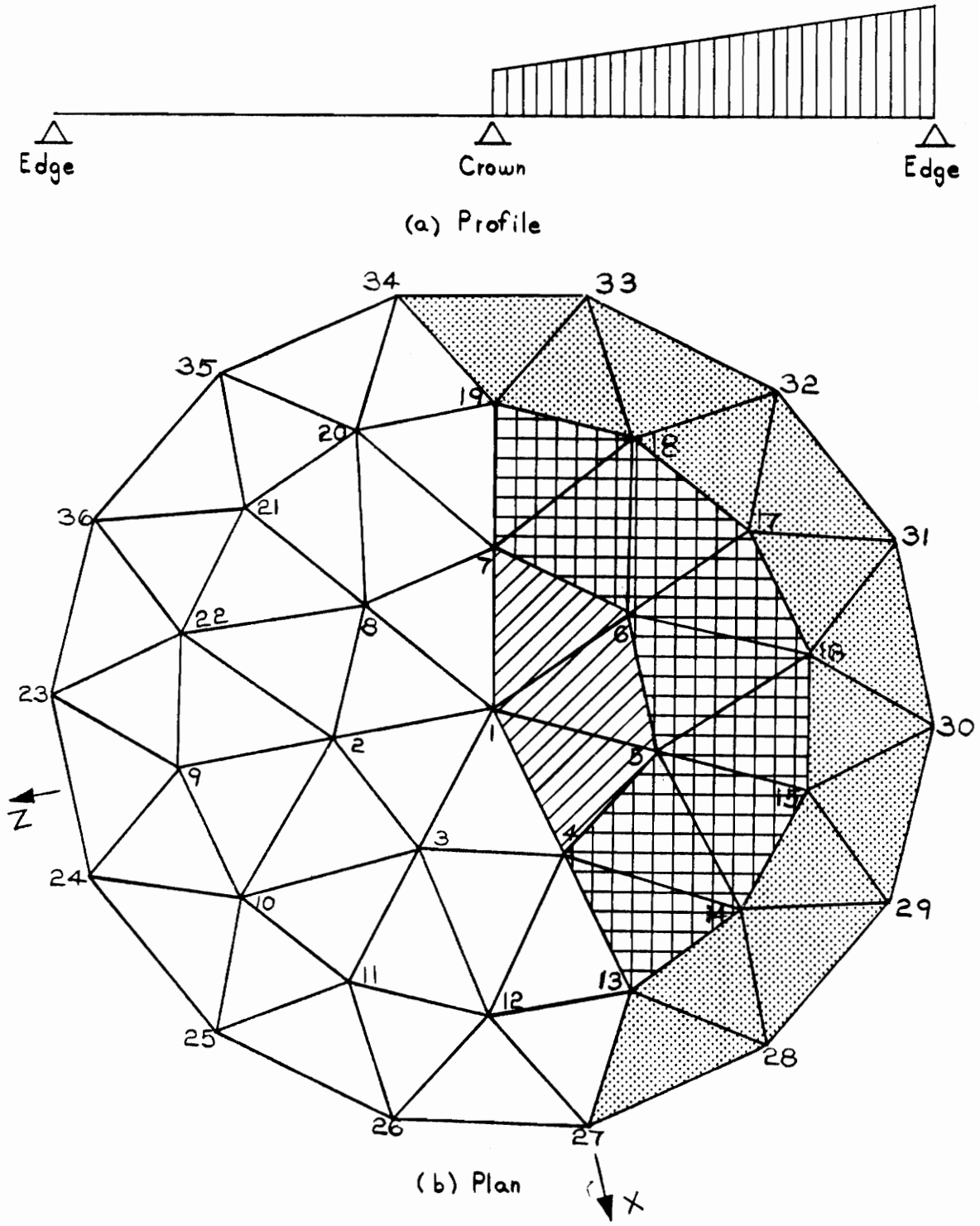

Figure 3.3 Unbalanced Snow Distribution

NODE	PRESSURE (psf)
1	17.6400
4	21.1060
5	31.6735
6	31.6735
7	21.1060
13	24.3981
14	36.5757
15	45.0029
16	48.0105
17	45.0029
18	36.5757
19	24.3981
27	17.6400
28	35.9579
29	50.6478
30	58.8000
31	58.8000
32	50.6478
33	35.9579
34	17.6400

Table 3.1 Unbalanced Snow Pressures

In this particular computer program, additional information was required. The number of panels in the structure was needed. A panel is defined by three members making a triangle. In addition to the number of panels, the relationship of joint numbers and member numbers to the panel had to be defined. The Panel Element Incidence relates element numbers to the panel number. The Panel Joint Incidence relates joint number to the panel number. The relationship of element number and joint number is shown in Figure 3.1.

The output of the computer program is in tabular form. An echo of the input is first printed with the element lengths and panel area as calculated in the program. The concentrated loads at joints derived by Hao (14) are printed with joint numbers. The linearly varying distributed loads along members are printed next. For each element, the end distributed force value is printed with its corresponding joint number. Using these values, a linear equation of the distributed force was calculated and the slope and intercept was printed. The variable is the x-coordinate (coord (1)). If the element is perpendicular to the x-coordinate, the z-coordinate (coord(3)) is used.

CHAPTER 4

MODELING WITH STAAD

4.1 Introduction

STAAD-III is a large and powerful structural program developed by Research Engineering, Inc. It is a comprehensive structural engineering program capable of performing analyses of planer and three-dimensional structures comprised of beam, truss, and thin-shell elements. There is a large amount of documentation which is covered in its Users' Manual (34). All words and phrases which appear in capital letters are key words and parameters for this program.

Before STAAD-III could be used on the Conservatek dome, it was necessary to understand the parameters and analysis of relatively simple structures. An eight member pyramid, Figure 4.1, was modelled using STAAD-III and all the parameters were investigated on the pyramid before using them on the dome.

4.2 Beams

All STAAD-III beam elements allow both bending and axial load. First order beam theory, which assumes that the cross section does not deform in its section, is used. Beam elements may also be subjected to shear and bending in two arbitrary perpendicular planes, and they may also be subjected to torsion. These deformations are independent in linear

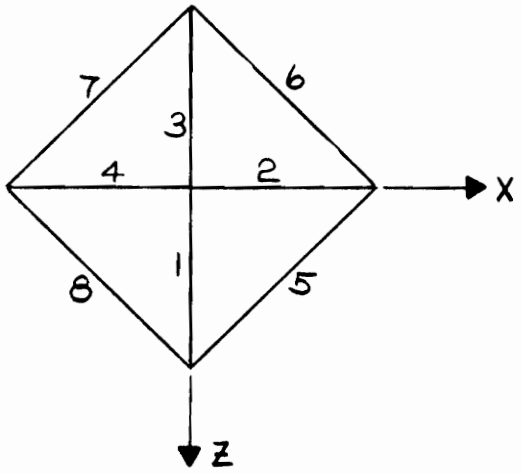

(a) Plan View

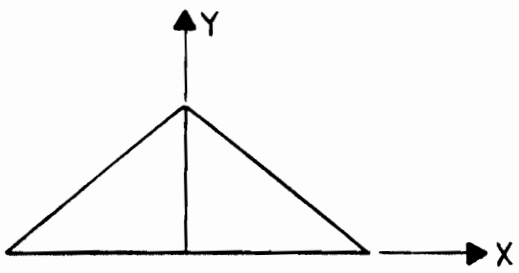

(b) Profile View

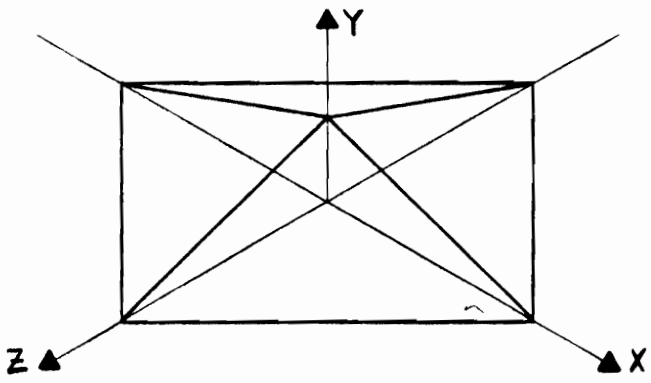

(c) Isometric View

Figure 4.1 Pyramid Model

response when the cross-sections are free to warp (15). The warp is treated as a small relative rotation between the normal to the plane of the cross-section and the beam axis.

For beams in space, the direction of the local Z-Axis of the beam must be defined. Figure 4.2 shows the local coordinates of the member cross-section. The relationship between the local coordinates to the global coordinates is defined as the BETA angle.

When the local X-Axis is parallel to the global Y-Axis, as in the case of a column in a structure, the BETA angle is the angle through which the local Z-Axis has been rotated about the local X-Axis from a position of being parallel and in the same positive direction of the global Z-Axis.

When the local Z-Axis is not parallel to the global Y-Axis, the BETA angle is the angle through which the local coordinate system has been rotated about the local X-Axis from a position of having the local Z-Axis parallel to the global X-Z plane and the local Y-Axis in the same positive direction as the global Y-Axis. Figure 4.3 details the positions for the BETA angle equals 0 degrees or 90 degrees.

An alternative way to provide the member orientation is to input the coordinates of an arbitrary reference point (EF) located in the member X-Y plane but not on the axis of the member. From the location of the reference point (REF), the program automatically calculates the orientation of the member

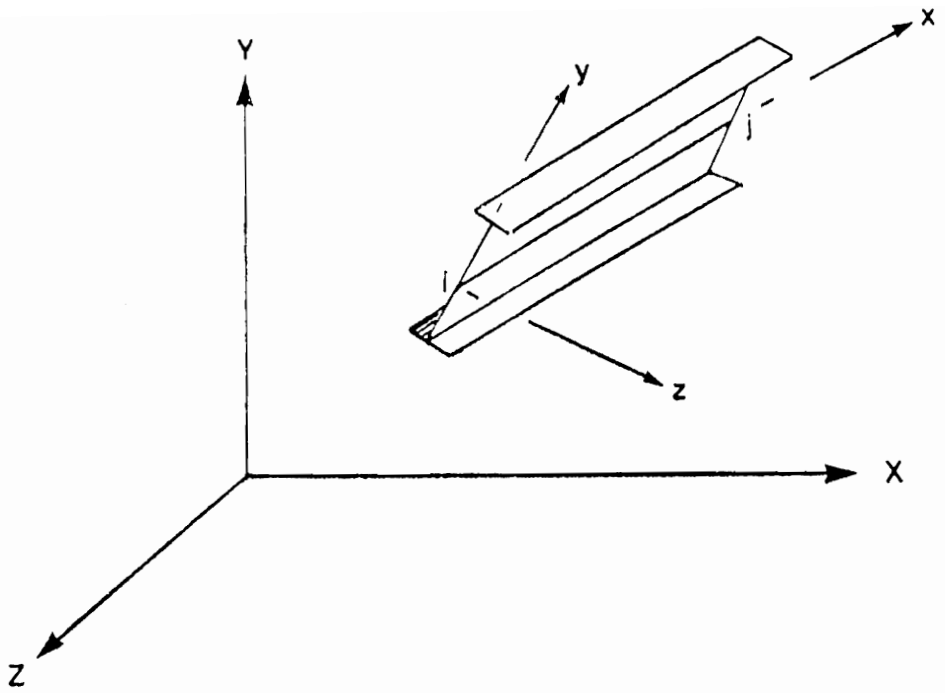

Figure 4.2 Local Coordinates of Cross-Section

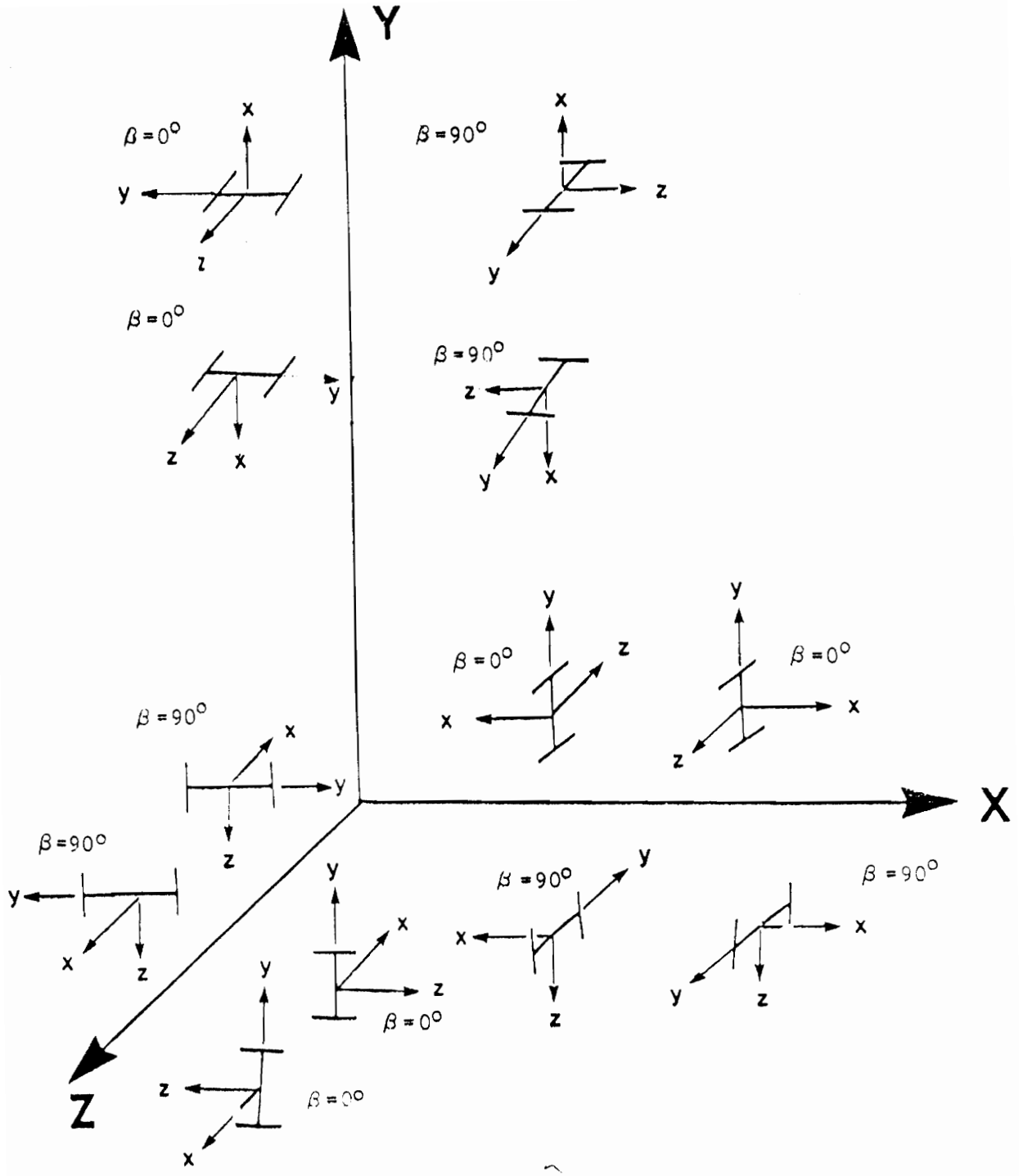

Figure 4.3 Relationship Between Global and Local Axis

X-Y plane.

STAAD-III provides a library of cross-sections for use with the beam elements. Cross-sections can be called from standard steel sections from AISC. The cross-section types are:

- o I-Section
- o Angle Section
- o Double Angle Section
- o T-Section
- o Channel Section
- o Double Channel Section
- o Tube Section
- o Pipe Section.

MEMBER PROPERTIES in the program can be provided by giving prismatic properties directly. The user then specifies the following properties:

AX = Cross Sectional Area

IZ = Moment of Inertia Around Local Z-Axis (major axis moment of inertia)

IY = Moment of Inertia Around Local Y-Axis (Minor Axis Moment of Inertia)

IX = Torsional Constant (Effective Torsional Moment of Inertia)

AY = Effective Shear Area in Local Y-Axis

AZ = Effective Shear Area in Local Z-Axis

YD = Depth in Local Y-Axis

ZD = Depth in Local Z-Axis

If the shear areas are input, the program will automatically consider shear deformations in the analysis, and if they are left out, shear deformation will be ignored. In a frame structure, the ratio of shear deflection to bending deflection is so small that, in most cases, it can be ignored (34). The depths in the two major directions, YD and ZD, are used in the program to calculate the section moduli. These are needed only to calculate member stresses or to perform concrete design. The user can omit YD and ZD if stress or design of these members is of no interest. The default value is 10 inches for YD and ZD.

Depending on the type of structure, a minimum of cross-sectional properties must be supplied. In a SPACE structure, the minimum properties are the cross-sectional area (AX), the torsional constant (IX), the moment of inertia around the local Y-Axis (IY), and the moment of inertia around the local Z-Axis (IZ).

Following the cross-sectional properties, the material CONSTANTS are entered. The material CONSTANTS are: modulus of elasticity (E); weight density (DEN); Poisson's ratio (POISS); coefficient of thermal expansion (ALPHA); beta angle (BETA); and coordinates for any reference point (REF). The modulus of elasticity, E, must be provided or the analysis will not be performed. Weight density (DEN) is used only when selfweight

of the structure is to be taken into account. Poisson's ratio (POISS) is used to calculate the shear modulus. The coefficient of thermal expansion (ALPHA) is used to calculate the expansion of the members if temperature loads are applied. The temperature unit for temperature load and ALPHA must be the same.

The member section properties for the interior members and the tension ring are given in Section 2.3. The longitudinal members are divided into two equal elements with a joint at the midpoint in order to model the internal forces and deflections. The modulus of elasticity is 10,100 ksi. The reference point option REF was used in defining the BETA angle. The geometry of a dome is ideal for its use, but a shift of the Y coordinates is required.

4.3 Connections

As shown in Figure 2.5 and Figure 2.6, the Conservatek dome uses two gusset plates for connecting the members. One method of modeling this connection is to use a plate element. STAAD-III has two types of plate elements and a triangular and quadrilateral element. For the Conservatek dome, a four-node element, a five-node element, a six-node element and a seven-node plate element would be necessary to model the connection.

A connecting element was used for the joint. The length of the connecting element is equal to the radius of the gusset

plates, 3 inches. Since the actual stiffness of the gusset plates can not be easily modeled as a beam element, the stiffness was chosen to be a function of the longitudinal member's cross-sectional properties.

The method to model a member with pinned ends is to use the MEMBER RELEASE command. Individual force components at either end of the member can be set to zero with MEMBER RELEASE command. By specifying release components, individual degrees of freedom are removed from the analysis. Release components are given in the local coordinate system for each member.

4.4 Loads

As discussed in Chapter 3, the distributed pressure load is transformed into a non-uniform distributed member force. STAAD-III can accept joint loads, member loads, temperature loads and fixed-end member loads. STAAD-III can also generate the selfweight of the structure and use it as uniformly distributed member loads in analysis.

STAAD-III has three types of member loads that may be applied directly to a member. These loads are uniformly distributed loads, concentrated loads, and linearly varying loads, including trapezoidal. Uniform loads act on the full or partial length of a member. Concentrated loads act at any intermediate, specified point. Linearly varying loads act

over the full length of a member.

Any number of loads may be specified to act upon a member in any independent loading condition. Member loads can be specified in the member coordinate system or the global coordinate system. Positive forces act in the positive coordinate directions, local or global.

For a linear varying load, the user has the choice of two commands: LIN or TRAP. The LIN command specifies a linearly decreasing or increasing load or a triangular load. This command is only applied in the local direction. The TRAP command defines a trapezoidal linearly-varying load which may act over the full or partial length of a member and in a local, global, or projected direction. By specifying the starting load value at the "a"-end of the member and the ending load value at the "b"-end, the TRAP command produces the same loading as the LIN command but in the global coordinates.

4.5 Computational Constraints

The use of additional elements in the structural model certainly increases the computational cost, and might be prohibitive in a large model. However, too simple a structure will not show the response which is characteristic of a lattice dome. When models are limited in size, structural characteristics are being imposed which are not always

obvious. The significance of the imposed restraints is reduced in larger models.

The volume of output is a potential problem. There are options which control the output. The user has the option of printing any of the input information (joint coordinates, member incidence, member properties, material properties, supports) or the coordinates of the center of gravity of the structure for all or a list of joints and members. Like the input selection, the output print options are similar. The output print options are: JOINT DISPLACEMENTS, MEMBER FORCES, SUPPORT REACTIONS, MEMBER SECTION FORCES, MEMBER STRESSES and ANALYSIS RESULTS. The ANALYSIS RESULTS command combines the first three commands and is the most commonly used.

CHAPTER 5

STRUCTURAL ANALYSIS RESULTS

5.1 Introduction

In order to gain experience and confidence with STAAD-III, a series of very small problems were done. These were simple beams and two-dimensional frames and trusses. The results of the simple computer models were compared to hand calculations and were found to be reasonably close.

5.2 Test Problem

A three-dimensional, eight-member structure in the form of a pyramid, as discussed in Chapter 4, was modeled using STAAD-III. The geometry of the pyramid is based on the top tier of the dome. The cross-elements of the pyramid have the same length and slope as those of the top tier. The cross-section of the cross-element is the same as that of the interior member of the dome. The tension members of the pyramid have the same cross-section as the tension ring of the dome.

The loading of the pyramid is similar to that of the dome. The balanced snow load is the same. The unbalanced snow load for the pyramid uses the same load at the apex (17.64 psf) and the same load as the first tier of the dome at the base (31.67 psf). Members 1, 2, 3, 5 and 6 have the applied unbalanced snow load; see Figure 4.1 for member

locations. Although this is different from what the loads would be calculated from ANSI (22), the results will give a representation of the action of the top tier.

The pyramid was modelled the same way as discussed in Chapter 4 (see Figure 4.1). A connector element at each end models the connection and the member is subdivided into two elements. The pyramid was modelled with pinned ends by using the MEMBER RELEASE command and releasing the moment about the local z-axis. The pyramid was also modeled with the connector element having the same cross-sectional properties as the member (framed ends). The results are shown in Table 5.1, Table 5.2, and Table 5.3. Only vertical displacements were investigated at the midpoint of the member and at the apex (Table 5.1). The internal forces investigated were the axial force, moment about the major axis (moment about the local z-axis) and the moment about the minor axis (moment about the local y-axis). The internal forces were examined at each midpoint of the member (Table 5.2 and Table 5.3).

The displacements of the framed pyramid at the apex and at the midpoint of members 5, 6, 7 and 9 are greater than the pinned end cross-frame. Although the results seem backwards to what they should be, this is due to rigid body motion. The connector element at the apex and the bottom wants to retain its original slope. This forces the element to translate but not to rotate.

MIDSPAN OF MEMBER	JOINT	BALANCED	UNBALANCED
1	PINNED FRAMED	-0.54829 -0.44230	-0.21869 -0.18141
2	PINNED FRAMED	-0.54829 -0.44230	-0.34278 -0.30355
3	PINNED FRAMED	-0.54829 -0.44230	-0.21869 -0.18141
4	PINNED FRAMED	-0.54829 -0.44230	-0.09459 -0.05927
5	PINNED FRAMED	-0.26700 -0.31345	-0.25668 -0.26106
6	PINNED FRAMED	-0.26700 -0.31345	-0.25668 -0.26106
7	PINNED FRAMED	-0.26700 -0.31345	-0.00003 -0.01440
8	PINNED FRAMED	-0.26700 -0.31345	-0.00003 -0.01440
APEX	PINNED FRAMED	-0.48715 -0.50271	-0.18919 -0.20111

TABLE 5.1 Displacements, Balanced & Unbalanced Snow

MEMBER	JOINT	AXIAL	MOMENT ABOUT LOCAL Z-AXIS	MOMENT ABOUT LOCAL Y-AXIS
1	PINNED FRAMED	5769.00 5952.30	18,085.91 12,454.33	- -
2	PINNED FRAMED	5769.00 5952.30	18,085.91 12,454.33	- -
3	PINNED FRAMED	5769.00 5952.30	18,085.91 12,454.33	- -
4	PINNED FRAMED	5769.00 5952.30	18,085.91 12,454.33	- -
5	PINNED FRAMED	-4057.03 -4187.32	14,795.18 18,102.36	2,155.16 1,059.30
6	PINNED FRAMED	-4057.03 -4187.32	14,795.18 18,102.36	2,155.16 1,059.30
7	PINNED FRAMED	-4057.03 -4187.32	14,795.18 18,102.36	2,155.16 1,059.30
8	PINNED FRAMED	-4057.03 -4187.32	14,795.18 18,102.36	2,155.16 1,059.30

TABLE 5.2 Balanced Snow, Forces

MEMBER	JOINT	AXIAL	MOMENT ABOUT LOCAL Z-AXIS	MOMENT ABOUT LOCAL Y-AXIS
1	PINNED FRAMED	2239.82 2380.51	7,370.27 5,230.11	- 30.32
2	PINNED FRAMED	2239.90 2383.68	14,740.78 12,503.49	- -
3	PINNED FRAMED	2239.82 2380.51	7,370.27 5,230.11	- 30.32
4	PINNED FRAMED	2239.74 2377.33	-0.30 -2,043.30	- -
5	PINNED FRAMED	-1575.53 -1681.45	14,220.98 15,269.89	2,074.75 1,078.09
6	PINNED FRAMED	-1575.53 -1681.45	14,220.98 15,269.89	2,074.75 1,078.09
7	PINNED FRAMED	-1575.53 -1669.61	0.96 821.98	- 93.48
8	PINNED FRAMED	-1575.53 -1669.61	0.30 821.98	- 93.48

TABLE 5.3 Unbalanced Snow, Forces

The results in Tables 5.2 and 5.3 were anticipated. The axial force is larger in the framed pyramid than in the pinned end cross frame. The moment at the midpoint of the pinned end pyramid is larger than the framed pyramid. The exceptions are in members 5, 6, 7, and 8. The increase in these members is from secondary moments from the cross-members.

5.3 Dome Modelled with Truss Elements

The Conservatek dome was first modelled with truss elements. One truss element was used to model each member. The member was defined from connection center to connection center. The loads were applied as concentrated forces at the center of the joints. These forces, see Table 5.4, were calculated by the computer program in Appendix E and the theory was discussed in Chapter 3. The base was not constrained in the X-Z plane.

The axial forces of the dome under the balanced snow loads were as expected. All the interior members were in compression and the tension ring members were in tension. The dome under the unbalanced snow load only had four members in tension under the load area (Figure 5.1).

For the dome under balanced snow, the positions of the highest forces are shown in Figure 5.2. The locations of the highest tension and compression were not surprisingly at the

JOINT	LOAD (POUNDS)
1	3,916
2	2,740
3	2,740
4	2,740
5	2,740
6	2,740
7	2,740
8	2,740
9	2,283
10	2,740
11	2,283
12	2,740
13	2,283
14	2,740
15	2,283
16	2,740
17	2,283
18	2,740

JOINT	LOAD (POUNDS)
19	2,283
20	2,740
21	2,283
22	2,740
23	1,370
24	1,370
25	1,370
26	1,370
27	1,370
28	1,370
29	1,370
30	1,370
31	1,370
32	1,370
33	1,370
34	1,370
35	1,370
36	1,370

(a) BALANCED SNOW LOAD

JOINT	LOAD (POUNDS)
1	1,312
2	-
3	-
4	1,923
5	3,846
6	3,846
7	1,923
8	-
9	-
10	-
11	-
12	-
13	2,771
14	5,275
15	4,534
16	5,275
17	4,534
18	5,275

JOINT	LOAD (POUNDS)
19	2,771
20	-
21	-
22	-
23	-
24	-
25	-
26	-
27	1,067
28	3,141
29	3,141
30	3,141
31	3,141
32	3,141
33	3,141
34	1,067
35	-
36	-

(b) UNBALANCED SNOW LOAD

TABLE 5.4 APPLIED LOADS FOR TRUSS MODEL

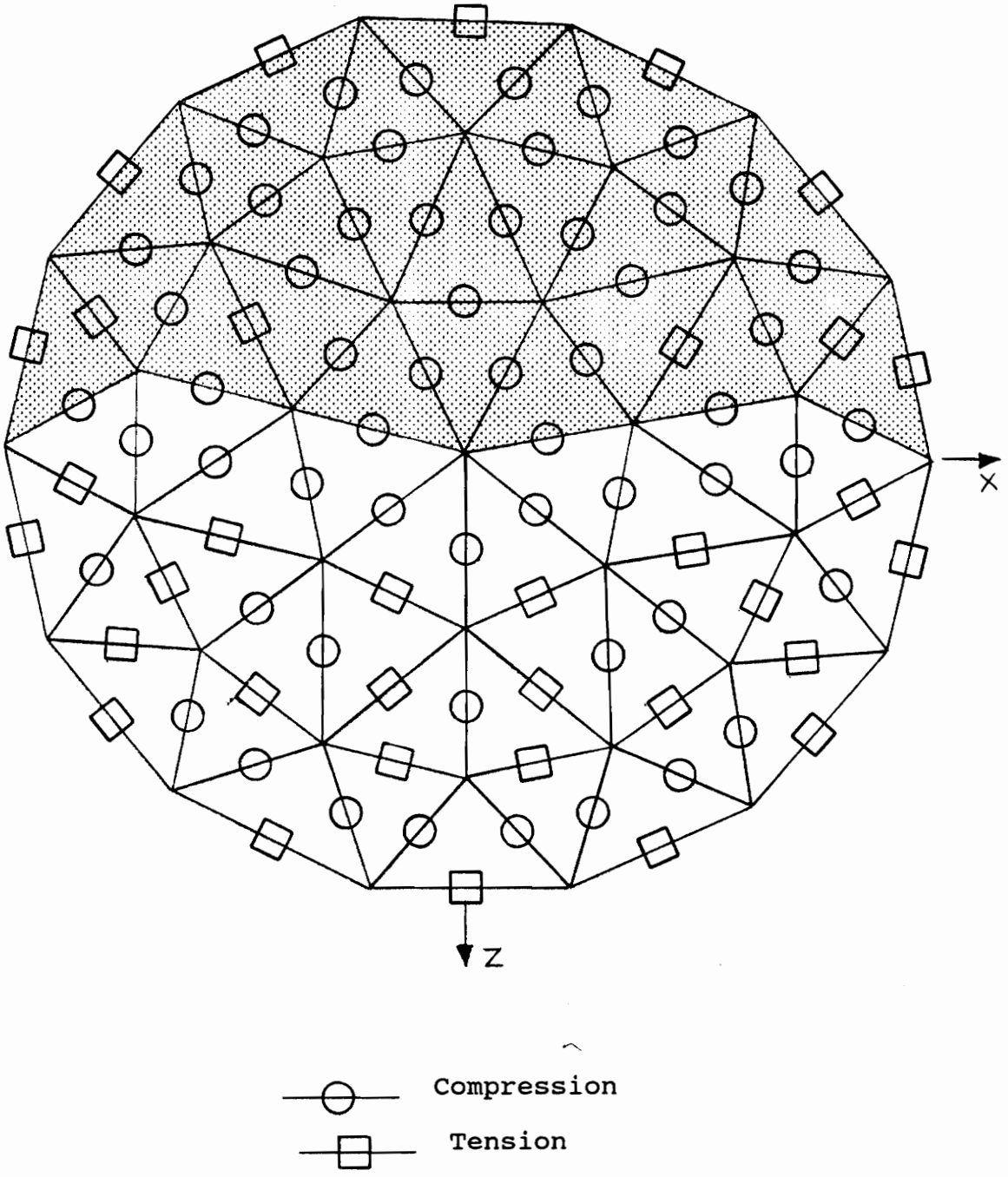

Figure 5.1 Axial Forces of Truss Model Under Unbalanced Snow

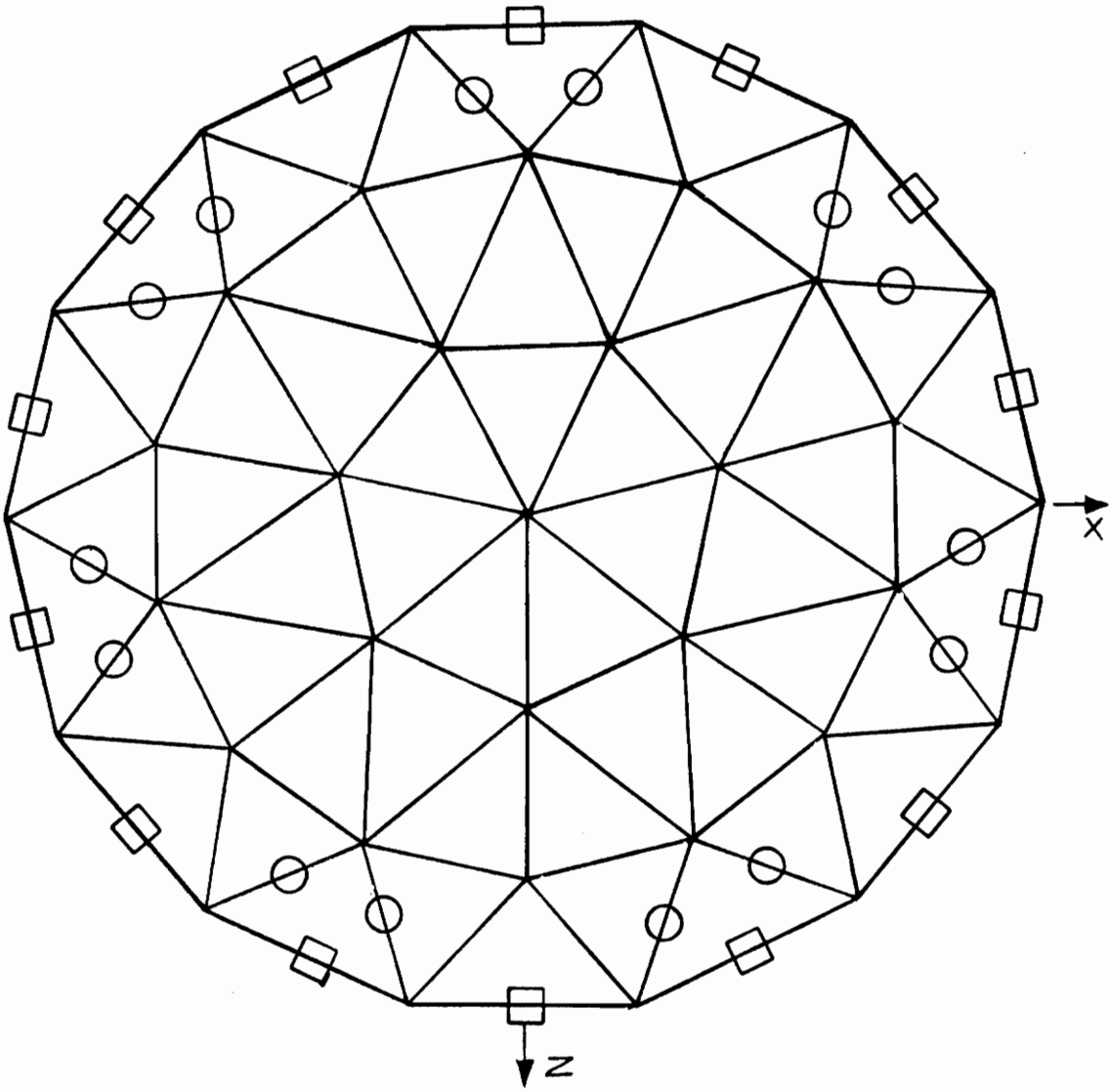

Figure 5.2
Truss Model Under Balanced Snow:
Position of Member with Greatest Forces

bottom tier. It was unexpected, however, that the compression load was in the second tier rather than in the first tier. The locations of the maximum and minimum vertical displacements other than at the supports are shown in Figure 5.3.

The positions of the highest forces of the dome under the unbalanced snow load are shown in Figure 5.4. Their locations were expected. The locations of the maximum and minimum vertical displacements other than at the supports are shown in Figure 5.5. Here again, the locations of the maximum and minimum, which are on opposite sides of the dome, were expected.

5.4 Dome Modelled with Beam Elements

The Conservatek dome was then modelled with beam elements. The loads were applied as linearly varying distributed forces along each element. These forces were calculated by the computer program in Appendix E and the theory was discussed in Chapter 3. The base was not constrained in the X-Z plane.

The internal forces in the beam model were compared to the specifications for aluminum structures by the Aluminum Association (2) for only the pinned end model and the frame-end model (K=1). STAAD-III has the ability to calculate the maximum and minimum values of internal forces of an element.

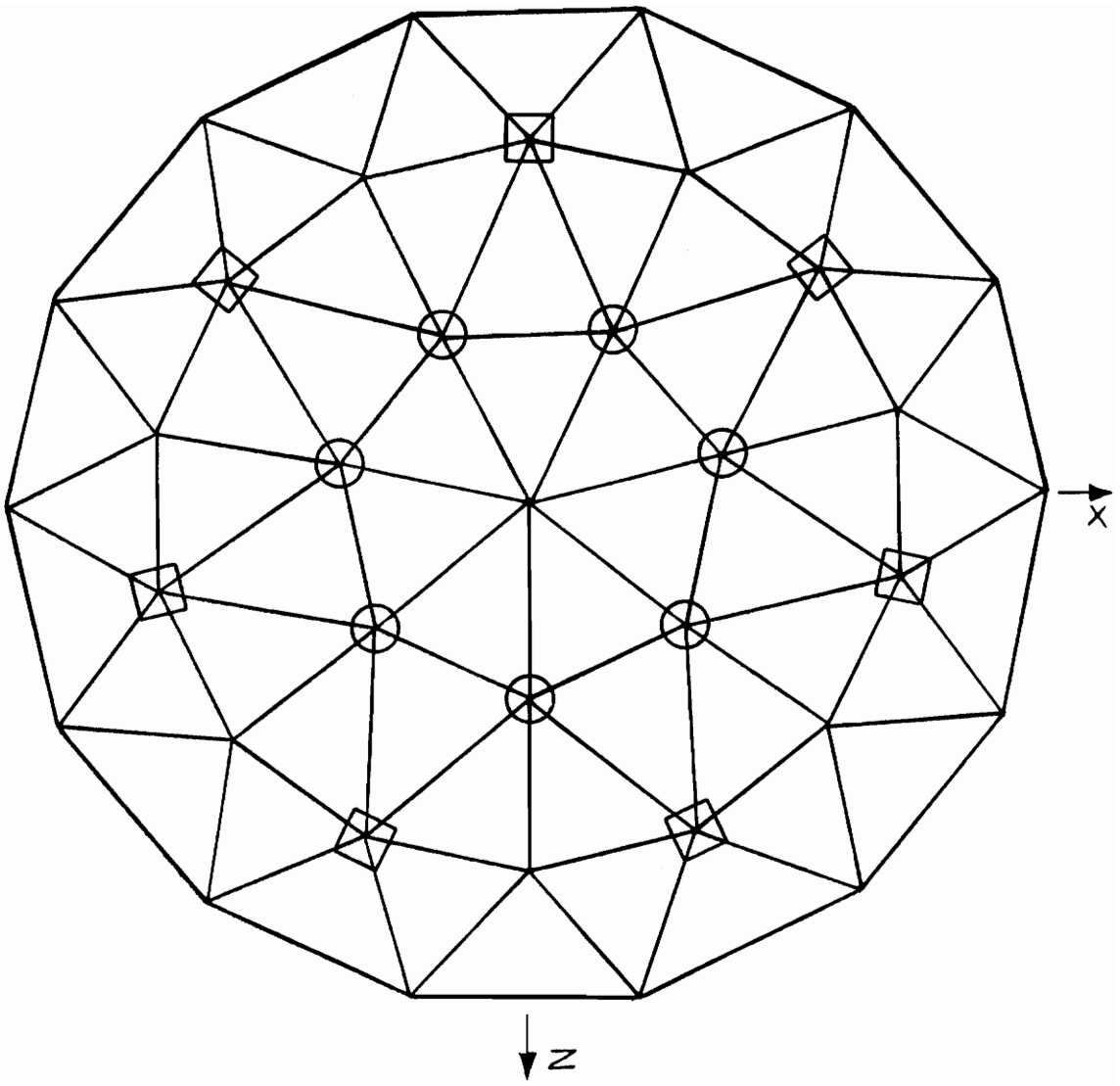

○ Greatest Vertical Displacement

□ Least Vertical Displacement

Figure 5.3
Truss Model Under Balanced Snow:
Position of Nodes with Greatest and Least Displacement

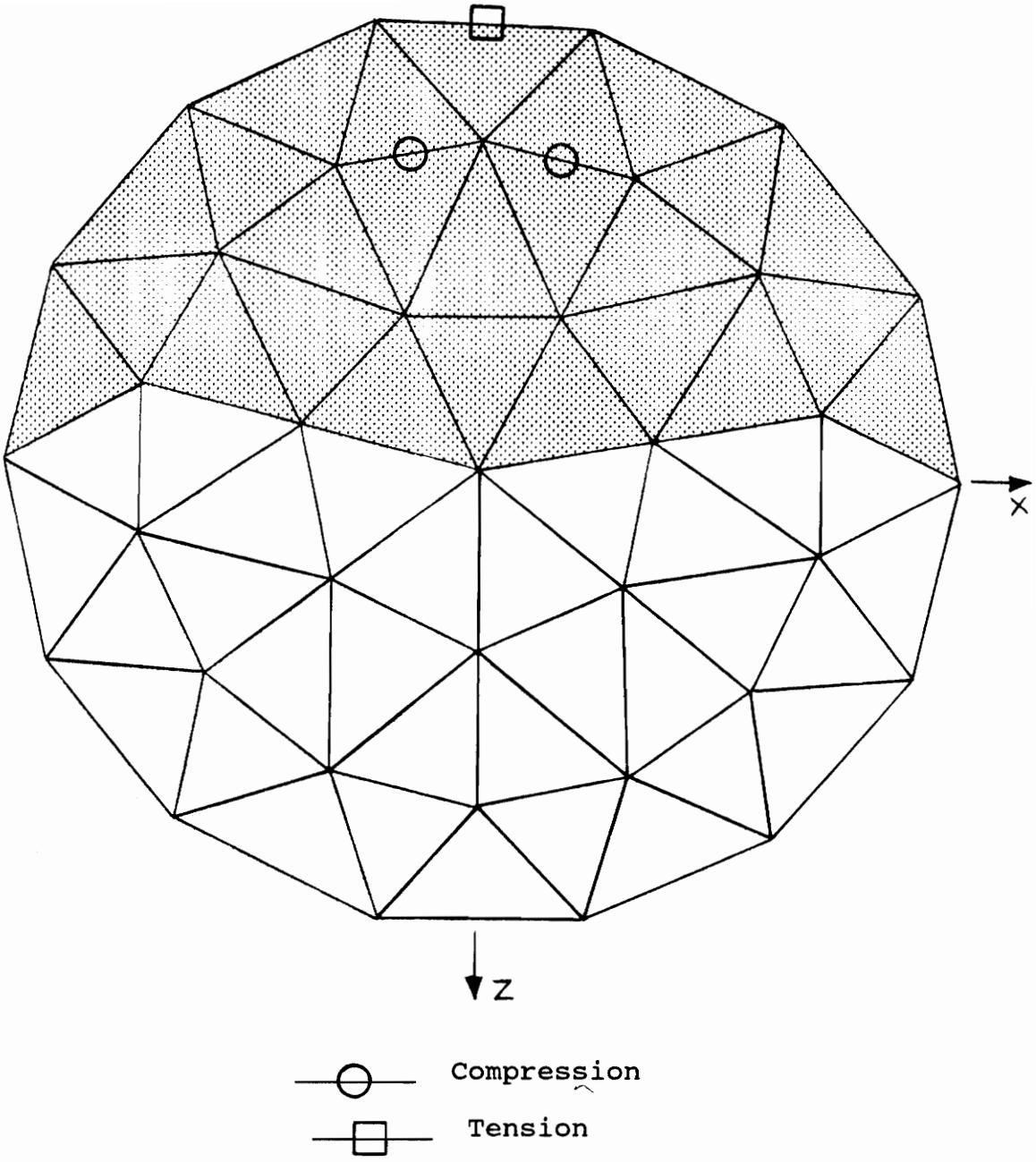

Figure 5.4
Truss Model Under Unbalanced Snow:
Position of Members with Greatest Forces

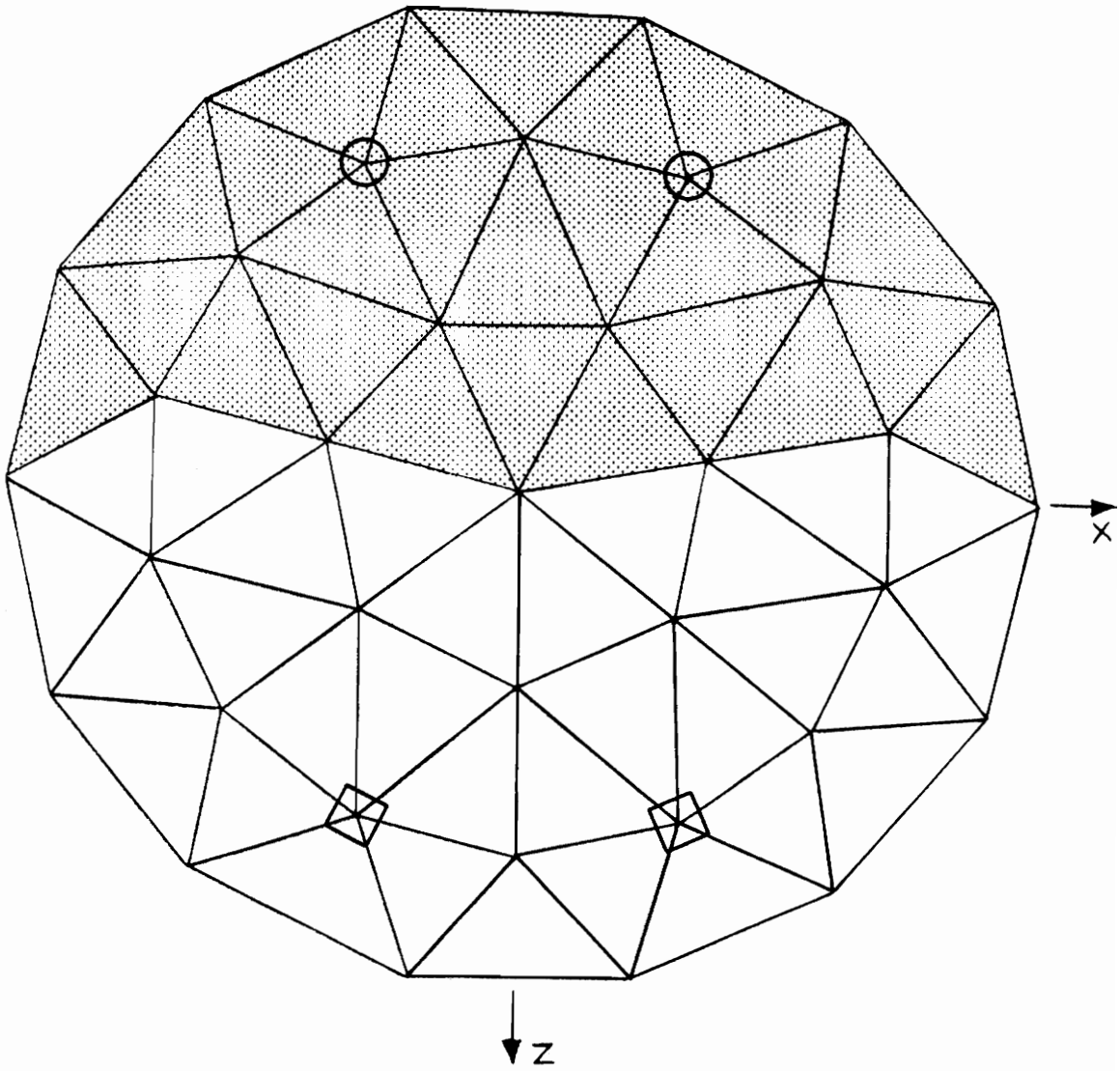

Figure 5.5
Truss Model Under Unbalanced Snow:
Position of Nodes with Greatest and Least Displacement

Using the maximum forces in each member, the ratio of applied stresses to allowable stresses were calculated. Only the axial stresses and the stresses due to the moment about the local Z-axis were used because the section modulus about the local Y-axis was not given nor could it be calculated from the information given. Critical stress due to biaxial bending and compression could occur. For the pinned end model (K=0), Figures 5.6 and 5.7 show the location of the maximum stress ratio for the balanced snow and the unbalanced snow, respectively. The balanced snow maximum stress ratio uses only 49.5% of the allowable overall stress. The unbalanced snow maximum stress ratio is 1.024 which is 2.4% over the allowable overall stress. For the framed-end model (K=1), Figures 5.8 and 5.9 show the location of the maximum stress ratios for the balanced snow and the unbalanced snow, respectively. The balanced snow maximum stress ratio is 0.417, which is less than that of the pinned end model. The location of the maximum stressed members is one tier lower than for the pinned end model. The location of the maximum stressed member in the rigid end model is the same as the pinned end model. The stress ratio for the rigid end is 0.921 which is lower than that for the pinned end model.

A parametric study of joint stiffness in the dome was performed. The connector element stiffness ranged from K=0, pinned ends to K=4.0. The cross-sectional properties of the

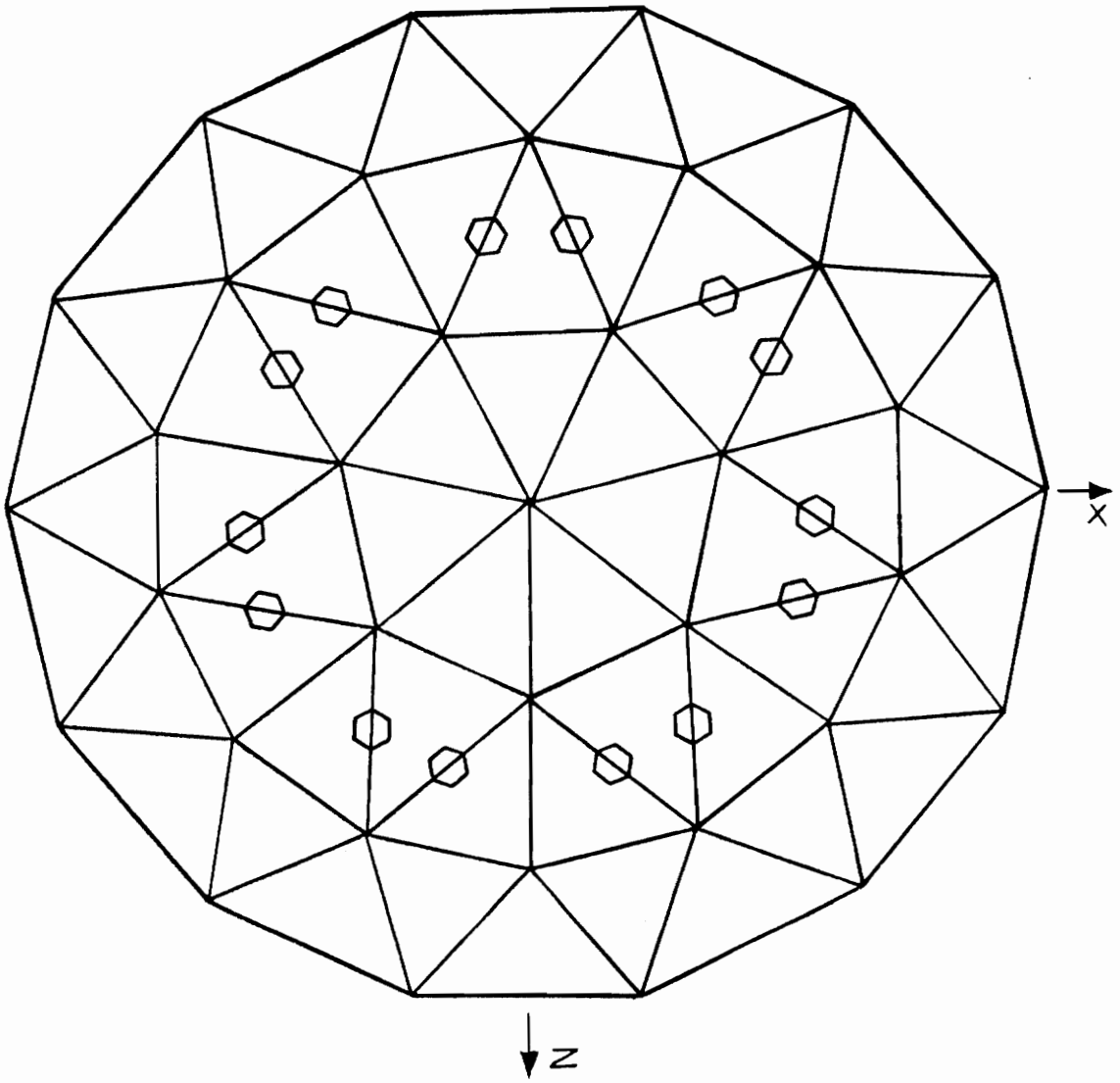

Highest Stress Ratio = 0.495

Figure 5.6
Pinned-End Model (K=0) Under Balanced Snow:
Members with Highest Stress Ratio

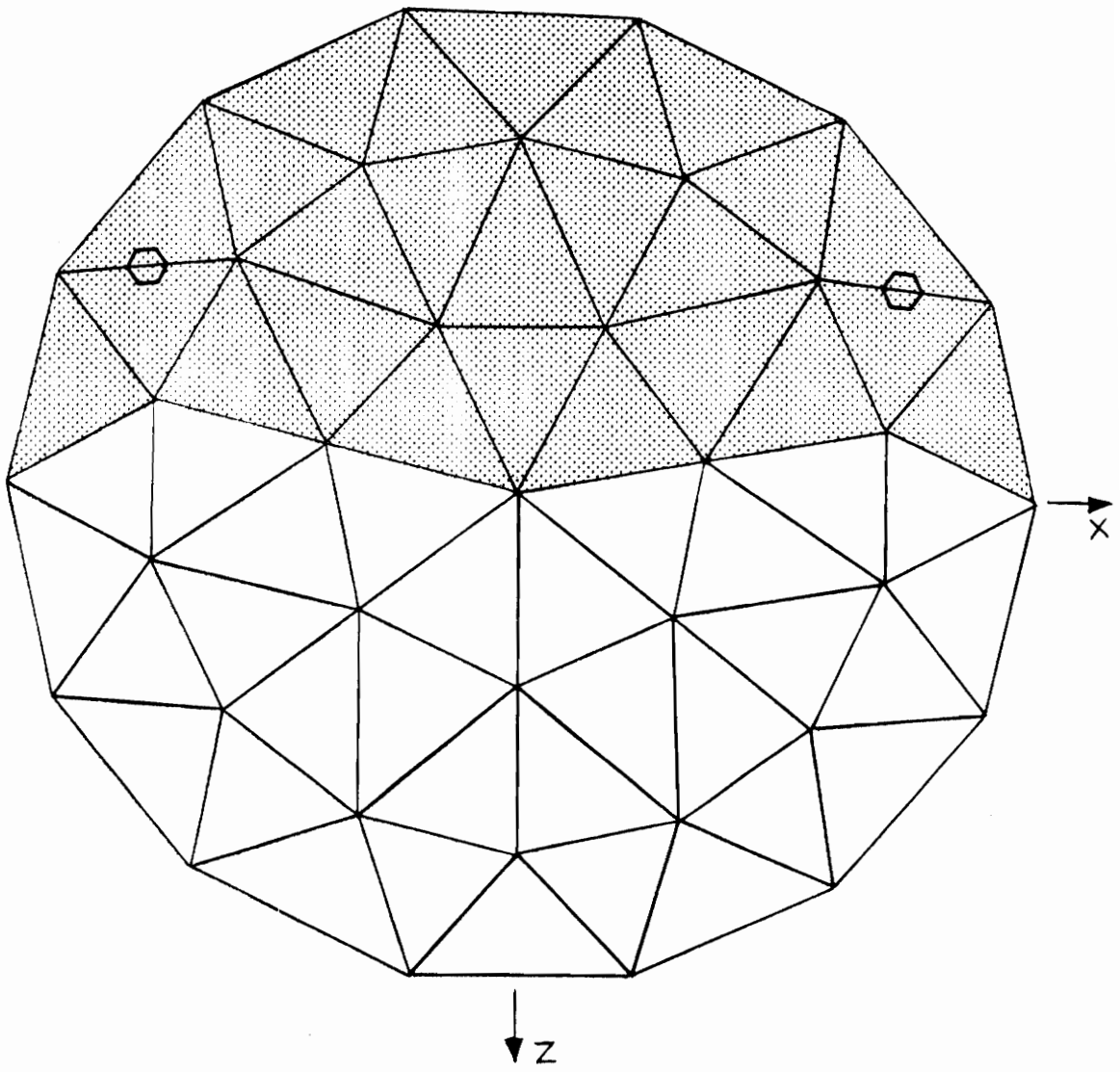

Highest Stress Ratio = 1.024

Figure 5.7
Pinned-End Model (K=0) Under Unbalanced Snow:
Members with Highest Stress Ratio

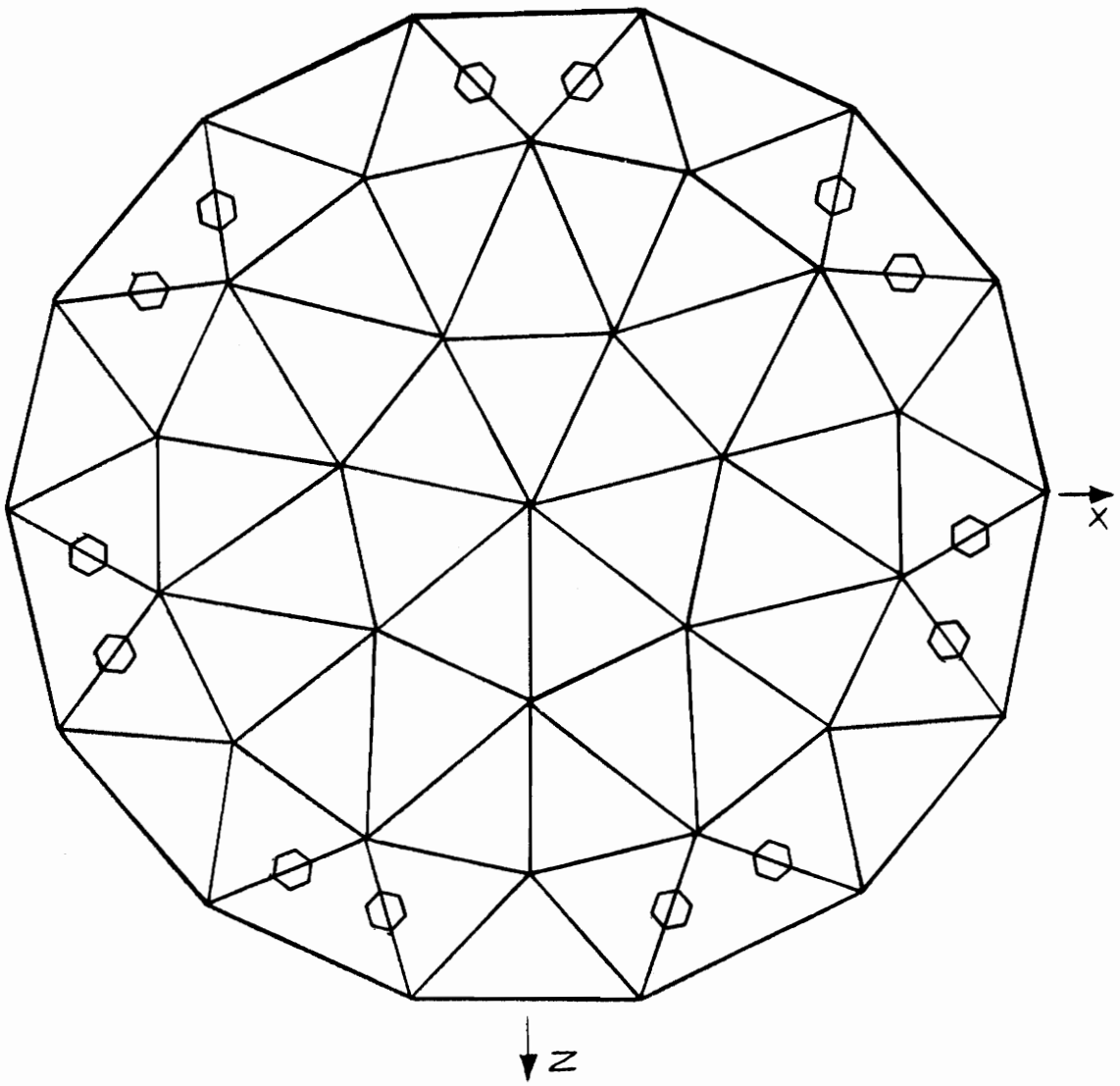

Figure 5.8
Framed-End Model (K=1) Under Balanced Snow:
Members with Highest Stress Ratio

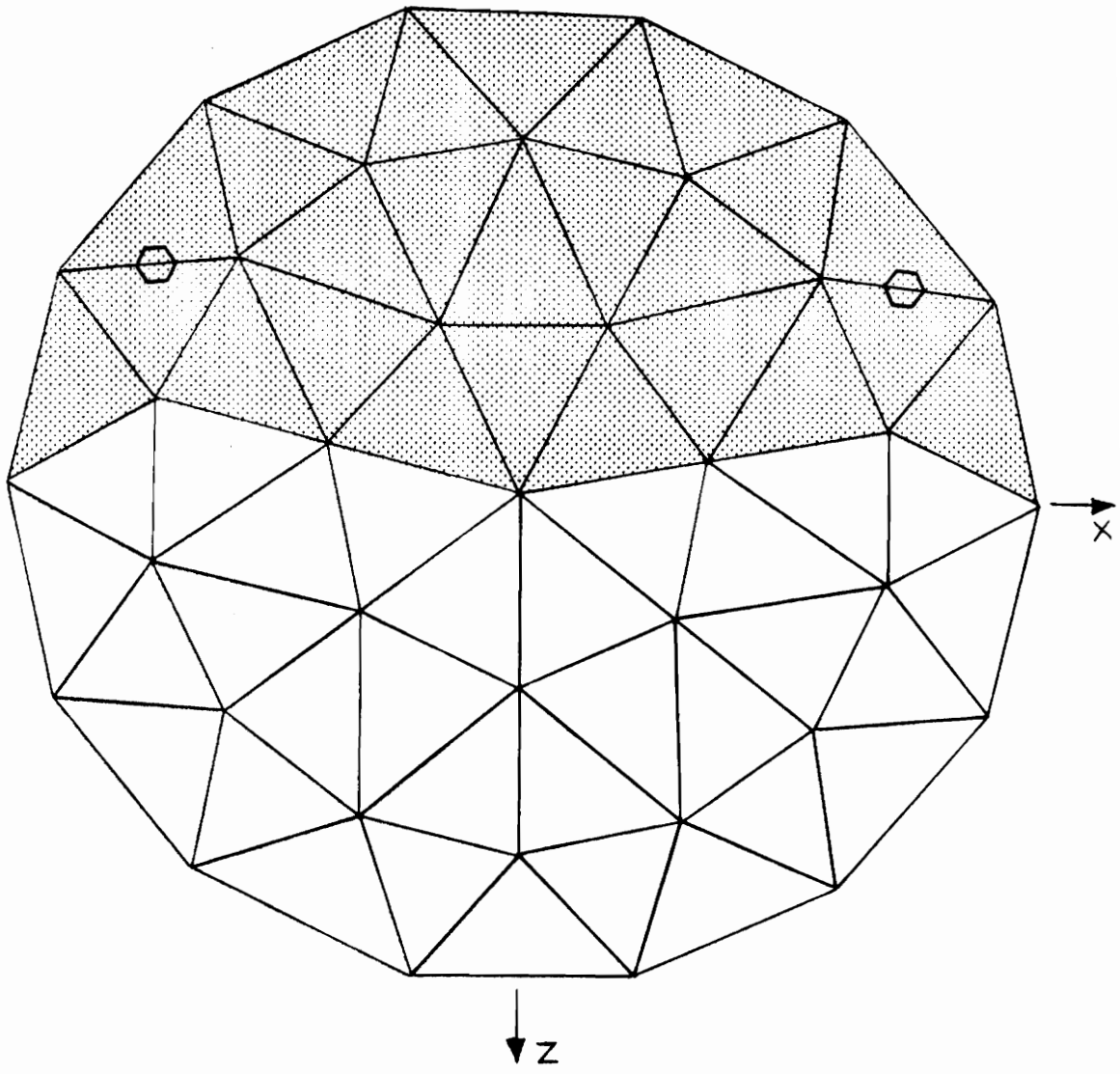

Highest Stress Ratio 0.921

Figure 5.9
Framed-End Model (K=1) Under Unbalanced Snow:
Members with Highest Stress Ratio

connector element was a function of the member element properties. The area, moment of inertia about the local z-axis, the moment about the local y-axis, and the torsional moment of inertia were all multiplied by the stiffness factor K.

Since the output of the runs was voluminous, certain results of the dome were selected. For displacements, only the vertical displacement was examined and only at the joint center. For internal forces, only the axial force, the moment about the local z-axis and the moment about the local y-axis were examined at the midpoint of the member. The moment about the local z-axis will be referred to as the major moment and the moment about the local y-axis will be referred to as the minor moment.

The location of the maximum deflection for the balanced snow load case is along the top ring of the dome (Figure 5.10). The maximum deflection was at the same location for all connector stiffnesses. The stiffness-deflection curve shows that the maximum deflection decreases as the connector stiffness increases from K=0.5 to K=4.0, see Figure 5.11. The maximum deflection at K=0 is approximately the same as at K=2.5.

Regardless of the connector stiffness, the maximum compression is along the top ring of the dome, see Figure 5.12. Unlike deflection, the axial compression increases as

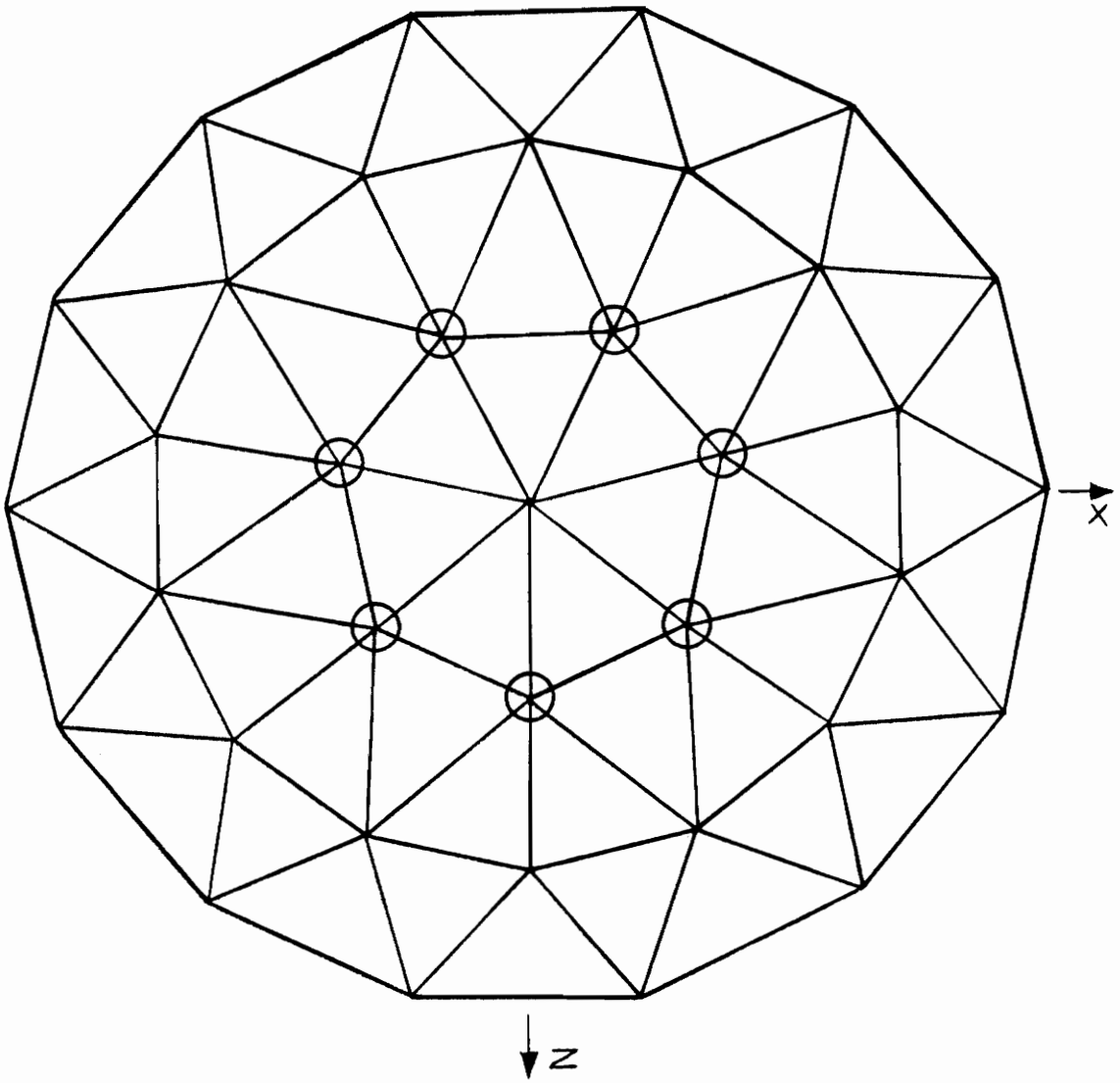

Figure 5.10
Balanced Snow:
Position of Nodes with Greatest Displacement

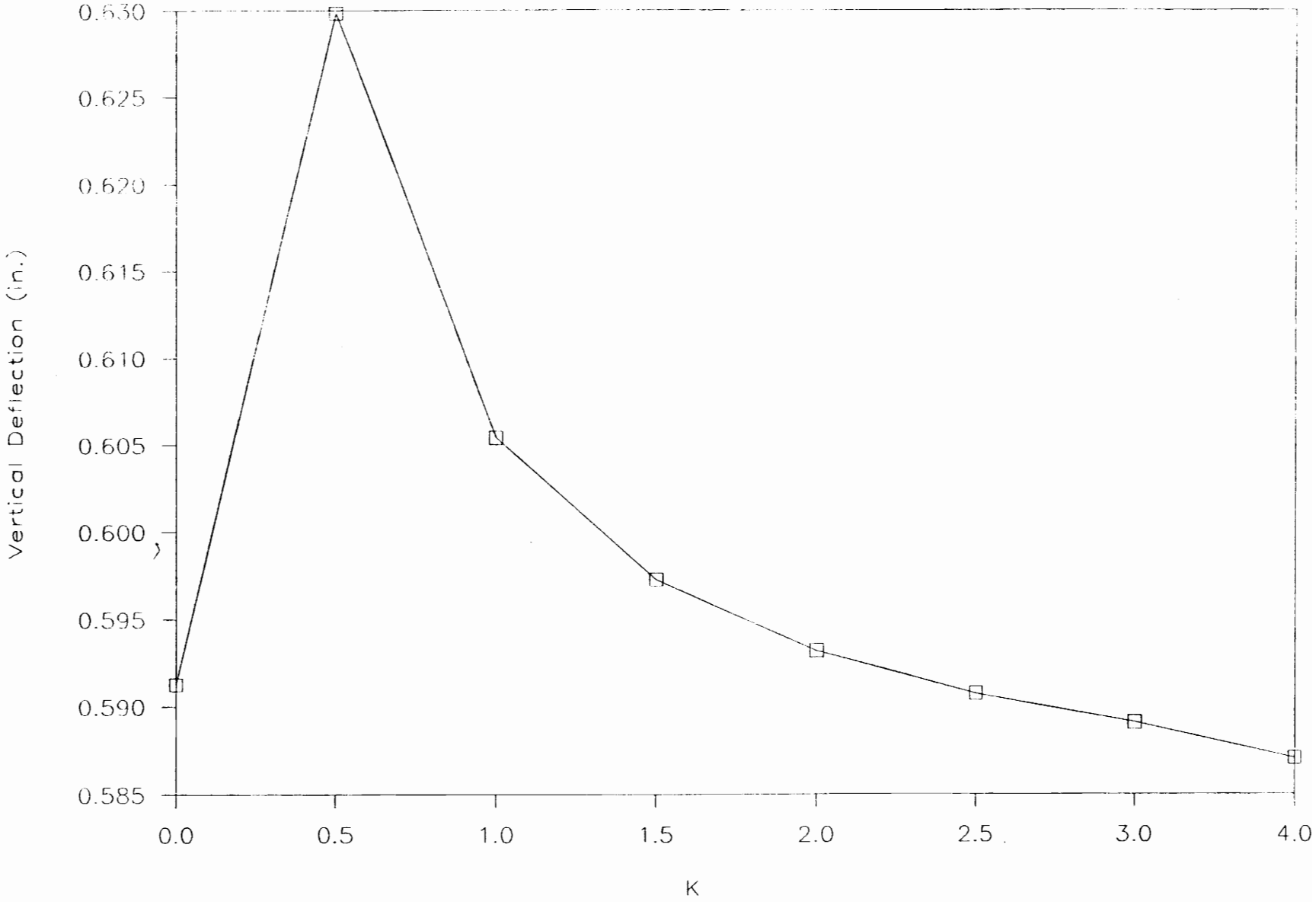

Figure 5.11
Balanced Snow: Stiffness-Displacement Curve

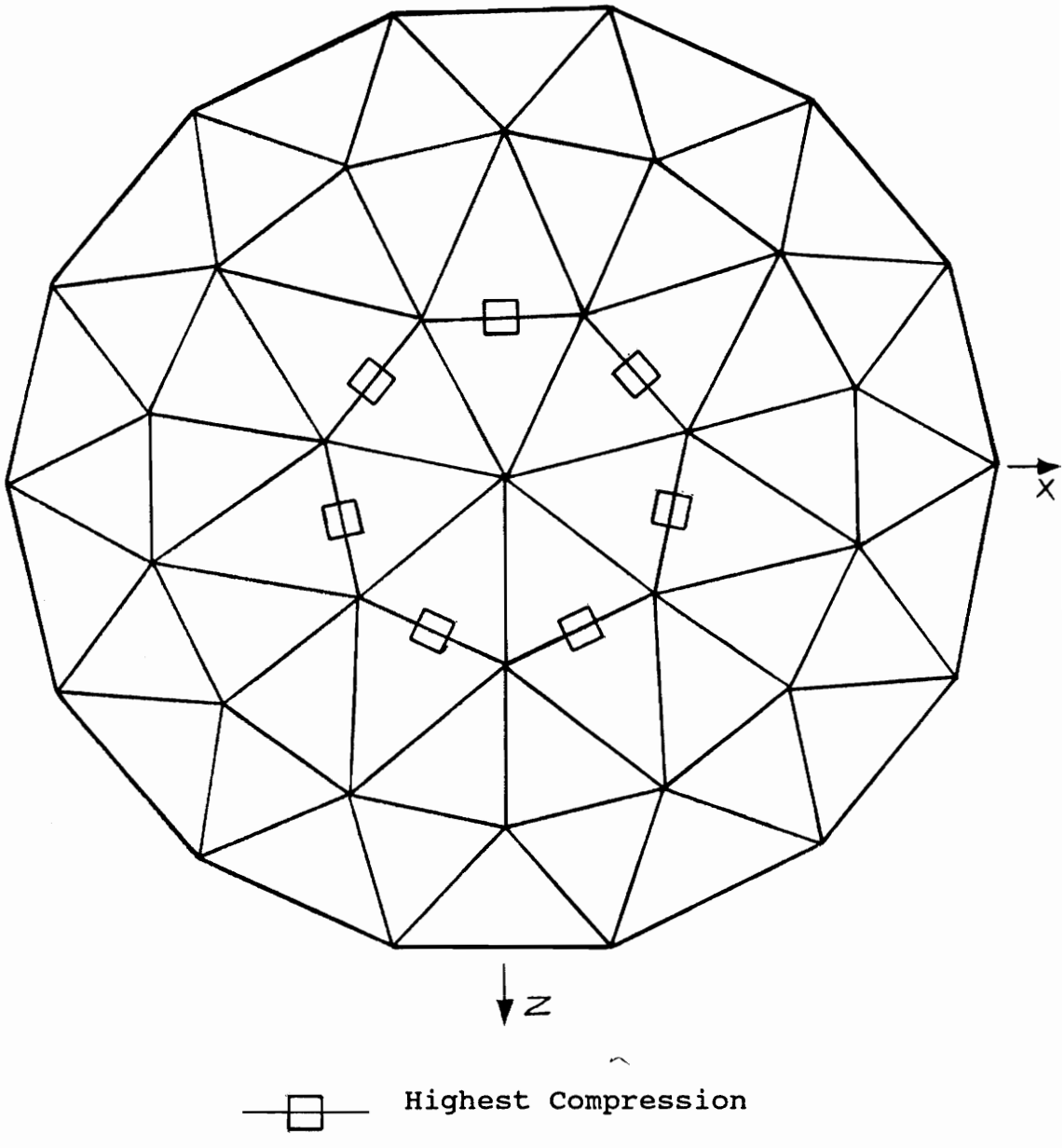

Figure 5.12
Balanced Snow:
Position of Members with Highest Compression

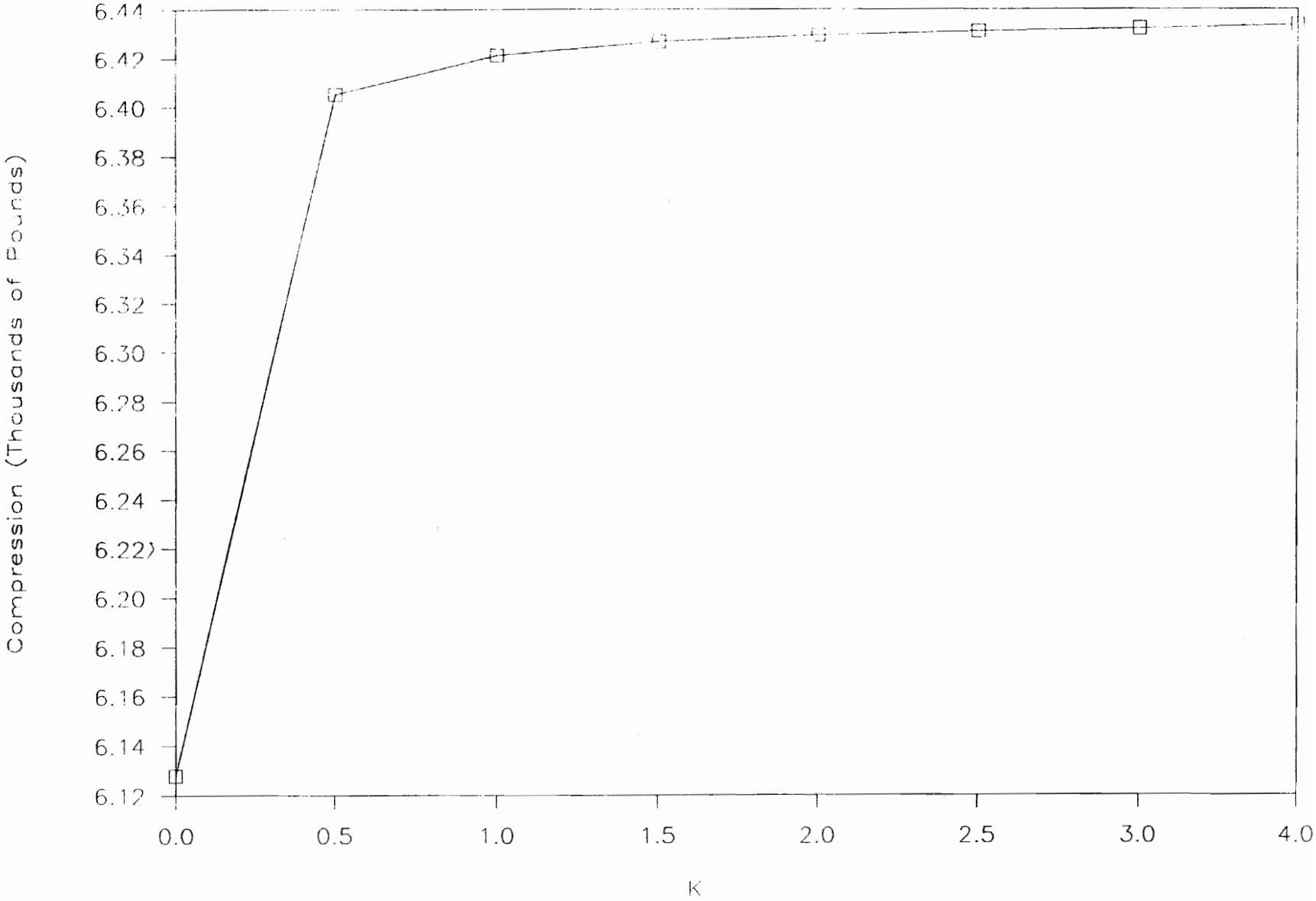

Figure 5.13
Balanced Snow: Stiffness-Compression Curve

the stiffness of the connector element increases. A big jump in compression is made between K=0, pinned end model, to K=0.5to K=4.0, see Figure 5.13. From K=0.5 to K=4.0 the curve levels out, and an increase of 0.43% occurs between the two points.

The location of the maximum tension is naturally at the tension ring, at the hexagon portions of the dome (see Figure 5.14). The stiffness-tension curve, Figure 5.15, is similar to the stiffness-compression curve in which the maximum tension increases and a big jump occurs from K=0 to K=0.5. It is an increase of 0.46%.

For the maximum major moment, the location depends on the stiffness of the connector element. The location of the maximum major moment for K=0, pinned end model, is along the diagonal members of the second tier with a value of 20,215 lb.in, see Figure 5.16. The bottom tier members are the members with the maximum major moment for K=0.5 to K=4.0, see Figure 5.17. The major moment at the midpoint of the member decreases as the stiffness of the connector element increases. See Figure 5.18 for the stiffness-major moment curve. This is similar to a simply supported beam in which the ends are slowly restrained. The value of the major moment at the bottom tier for K=0 is 14,650 lb. in. The percent difference between K=0 and K=0.5 is 23.4%.

Unlike the major moment, the minor moment does not depend

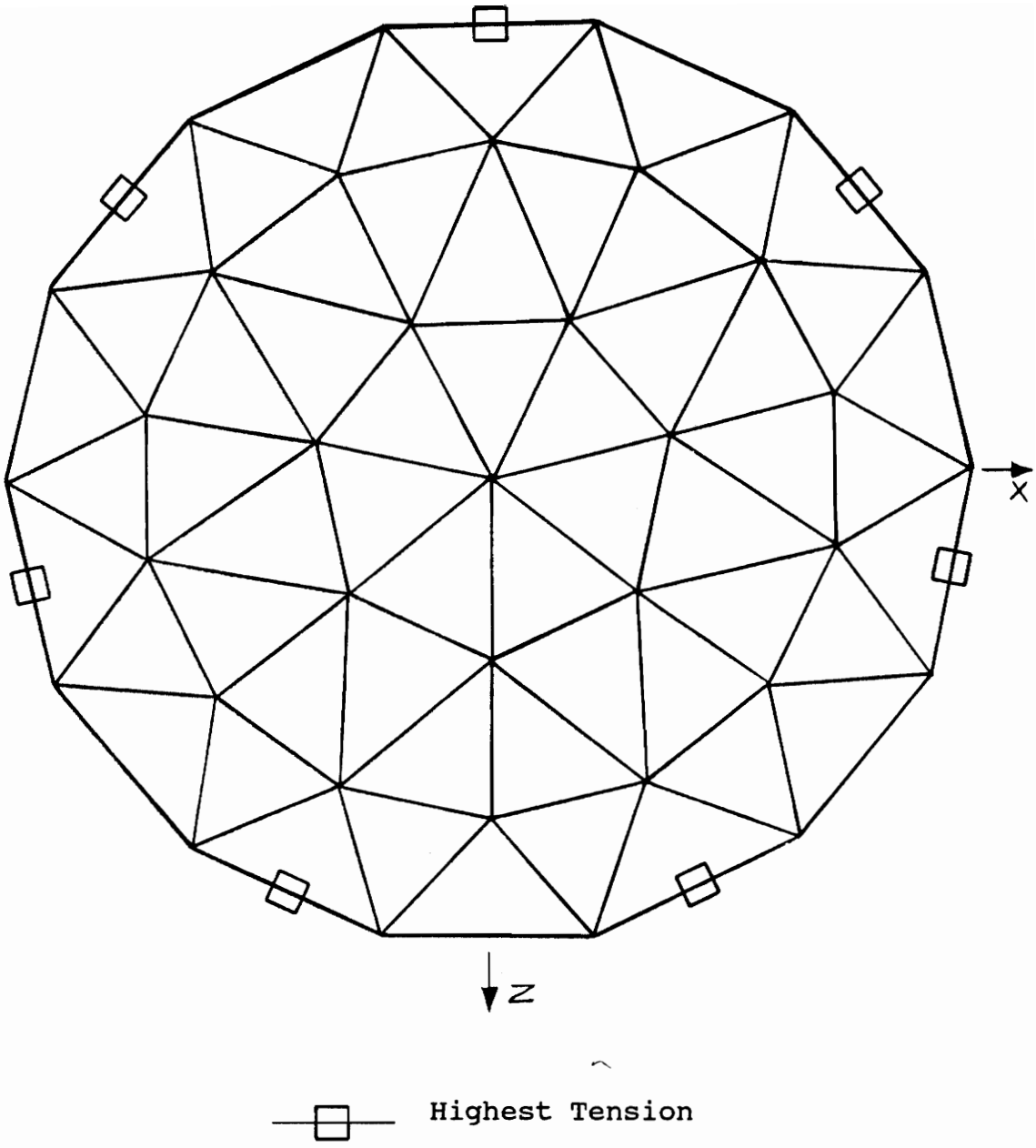

Figure 5.14
Balanced Snow:
Position of Members with Highest Tension

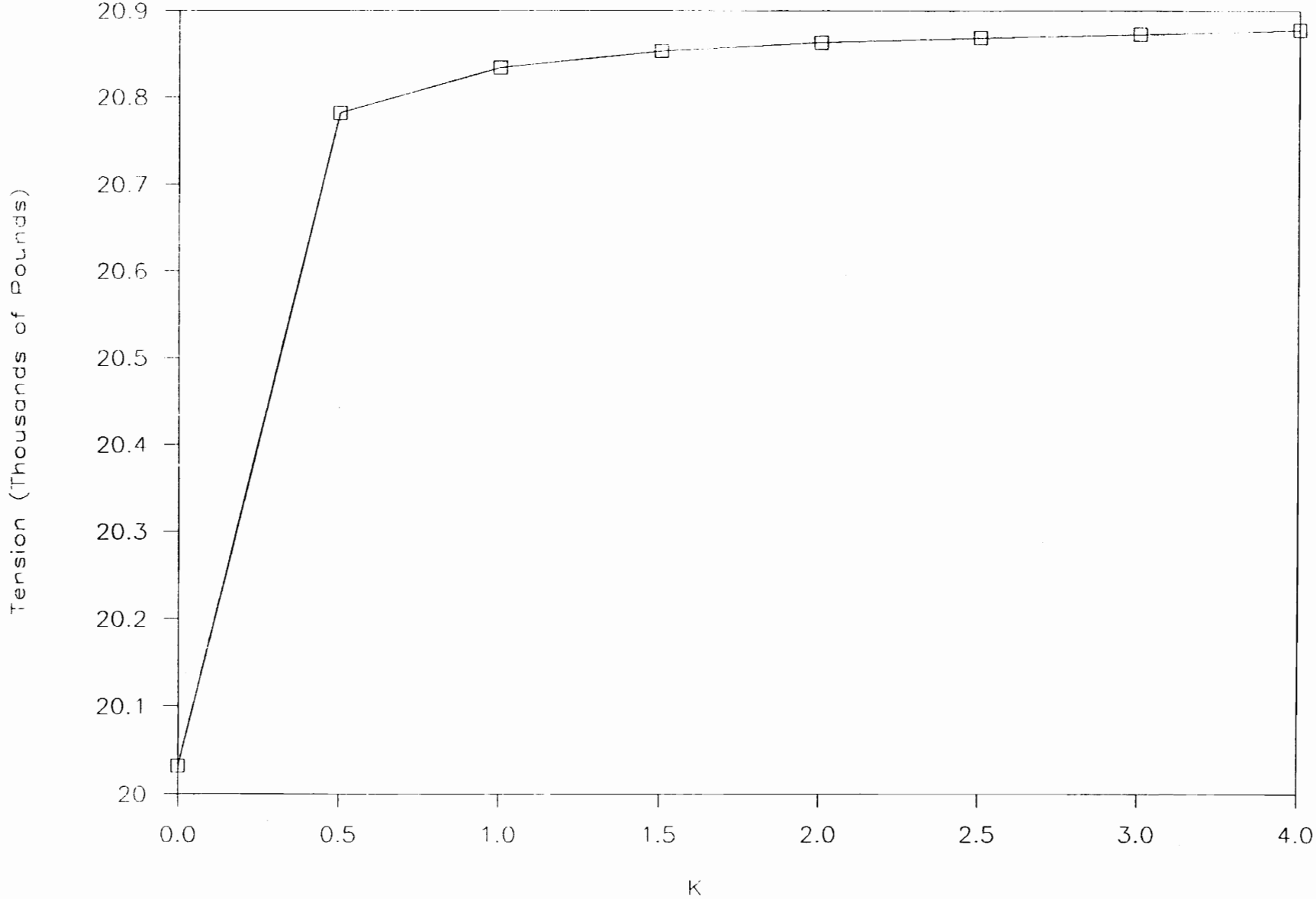

Figure 5.15
Balanced Snow: Stiffness-Tension Curve

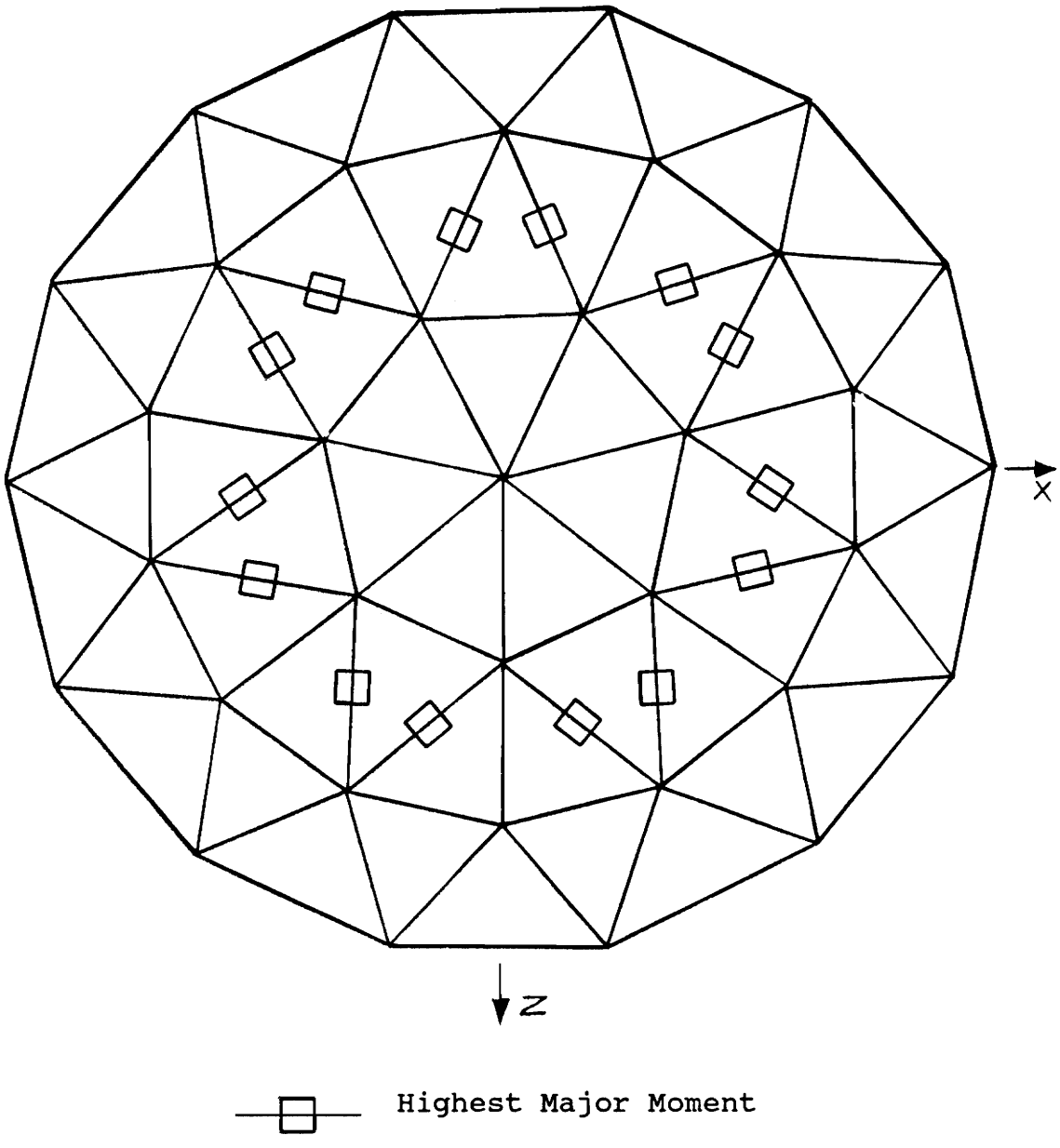

Figure 5.16
Balanced Snow: Position of Members with
Highest Major Moment for Pinned-End Model (K=0)

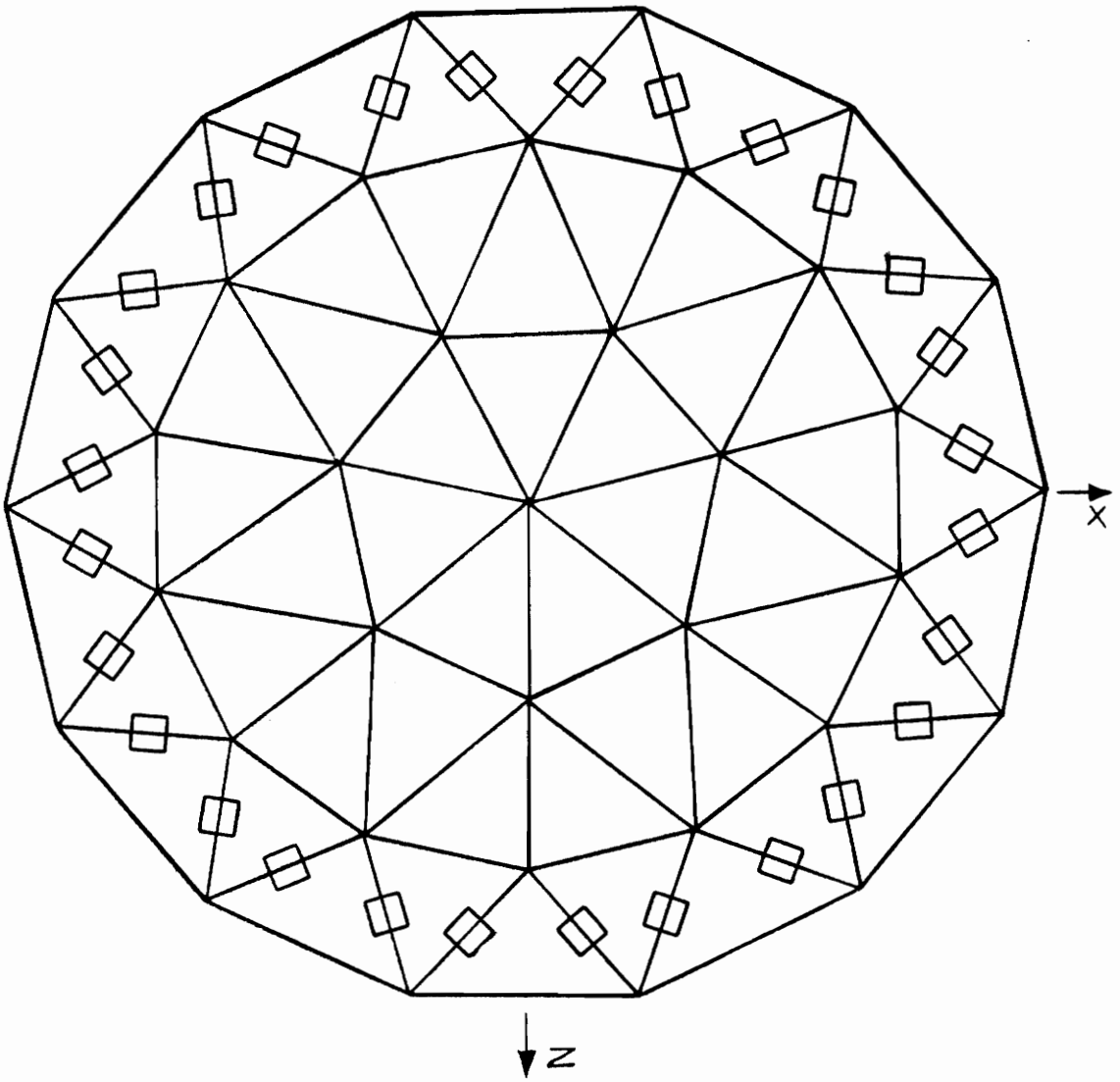

Highest Major Moment

Figure 5.17
Balanced Snow:
Position of Members with Highest Major Moment

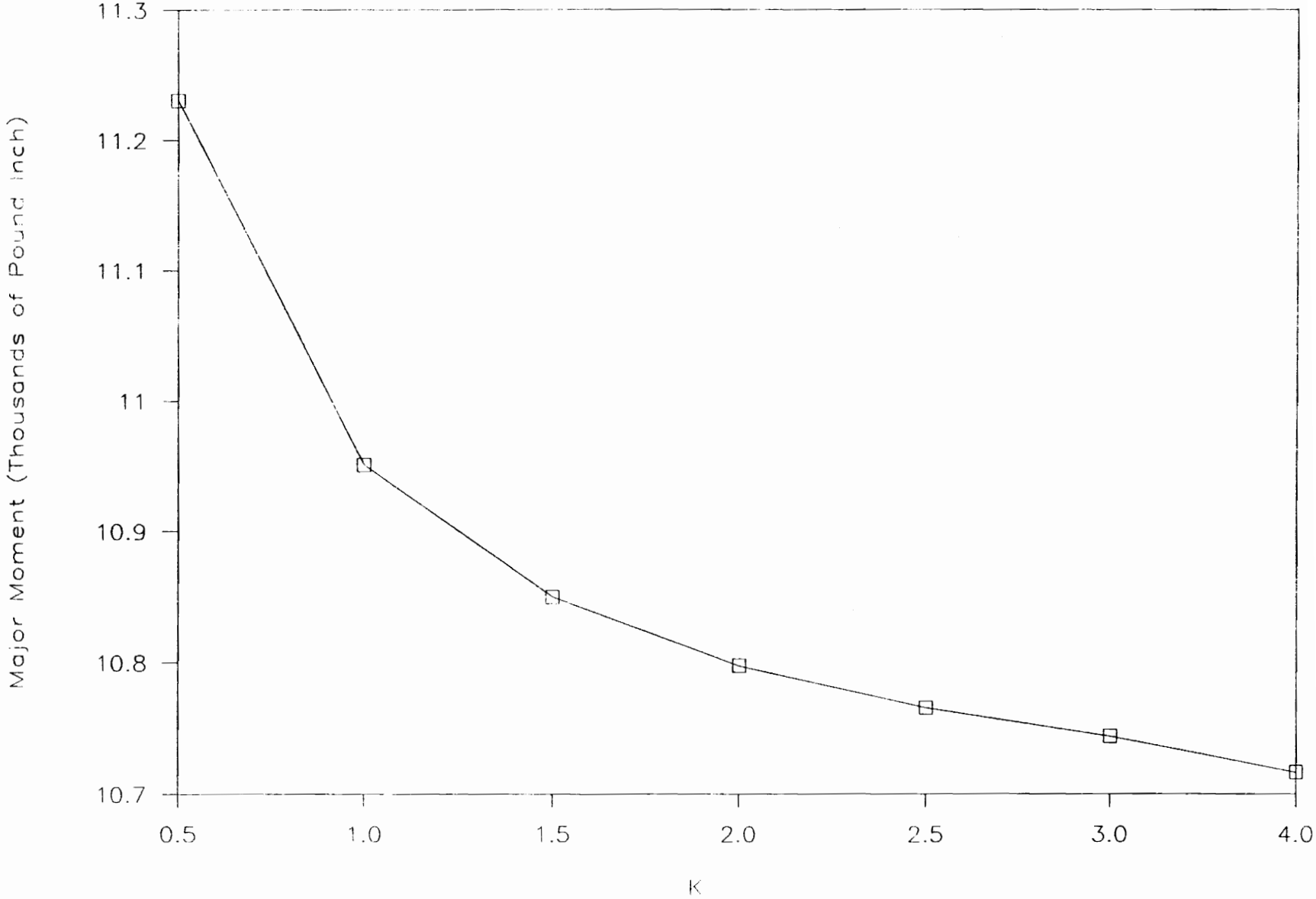

Figure 5.18
Balanced Snow: Stiffness-Major Moment Curve

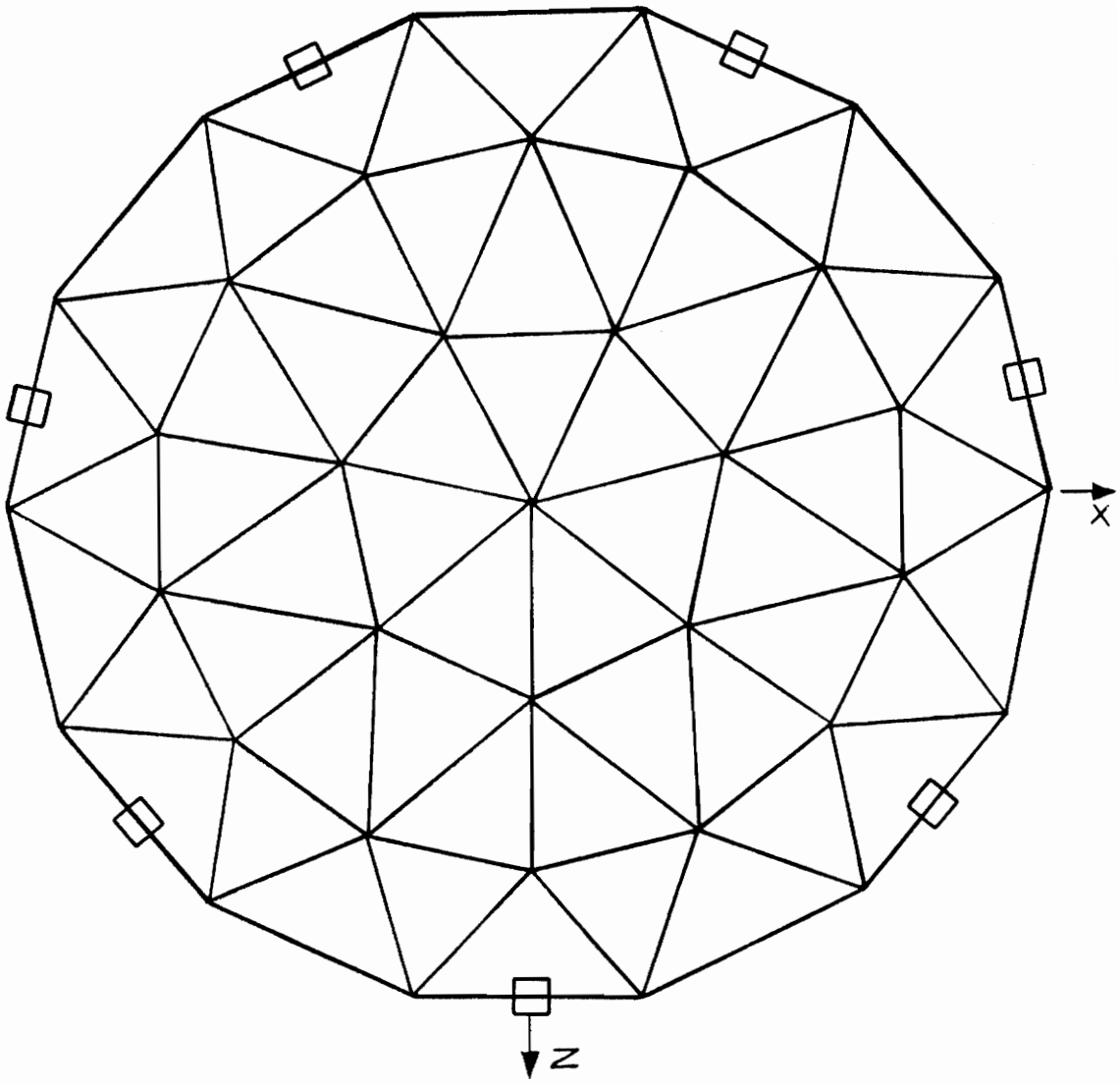

Highest Minor Moment

Figure 5.19
Balanced Snow:
Position of Members with Highest Minor Moment

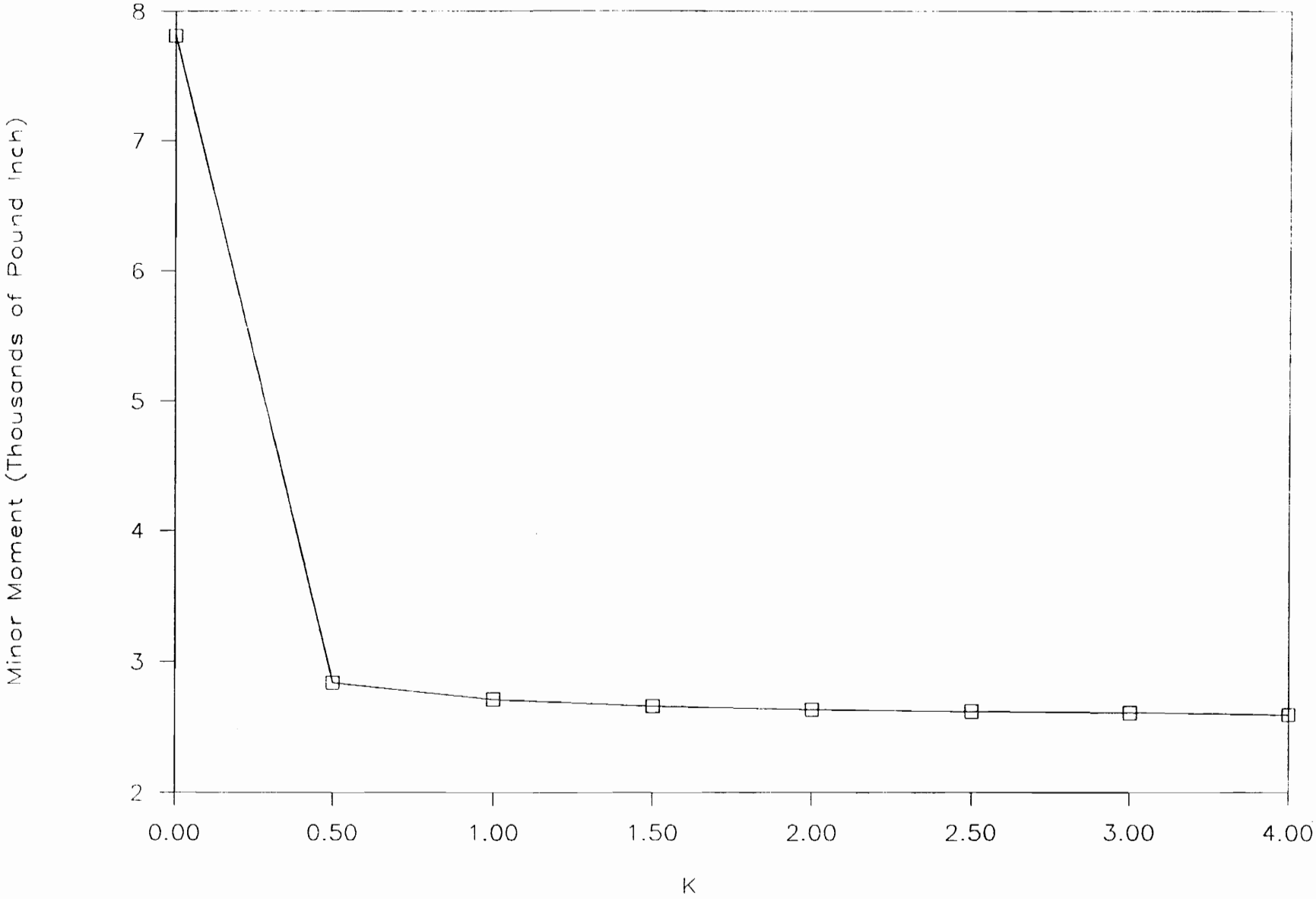

Figure 5.20
Balanced Snow: Stiffness-Minor Moment Curve

on the stiffness of the connector element. The location of the maximum minor moment is at the tension ring, at the pentagon portions of the dome (see Figure 5.19). The stiffness-minor moment curve, Figure 5.20, is similar to the stiffness-major moment curve in which the minor moment at the midpoint of the member decreases as the stiffness of the connector element increases.

The location of the maximum deflection is dependent on the joint stiffness for the dome under the unbalanced snow load. The pinned end model (K=0) is different than for the joint stiffness K=0.5 to K=4.0. Figure 5.21 shows the location of the maximum deflection for K=0 to be on the second ring in the middle portion of the load with a value of 0.784 in. The location of the maximum deflection for K=0.5 to 4.0 is on the second ring on either side of the center node as shown in Figure 5.22. The stiffness-deflection curve for K=0.5 to K=4.0 is similar to the balanced snow load because the deflection decreases as the connector element stiffness increases, see Figure 5.23. The deflection at the nodes on each side of the midpoint for K=0 is 0.780 in. The percentage difference between K=0 and K=0.5 is 11.8%.

The location of the maximum compression is along the second ring at the center of the loading area, see Figure 5.24. The stiffness-compression curve is similar to the balanced snow stiffness-compression curve in that there is a

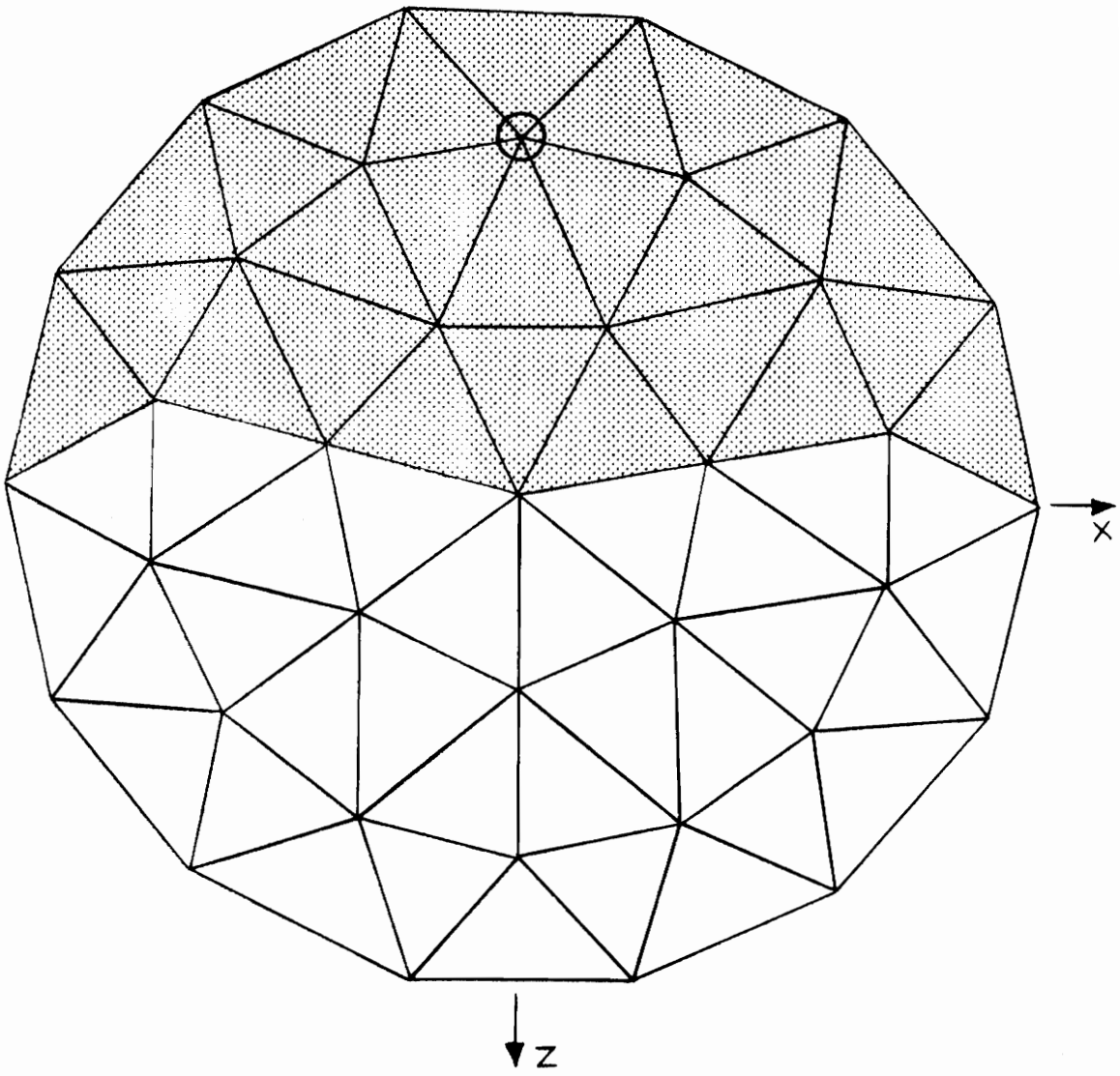

◯ Greatest Vertical Displacement

Figure 5.21
Unbalanced Snow: Position of Node with
Greatest Displacement for Pinned-End Model (K=0)

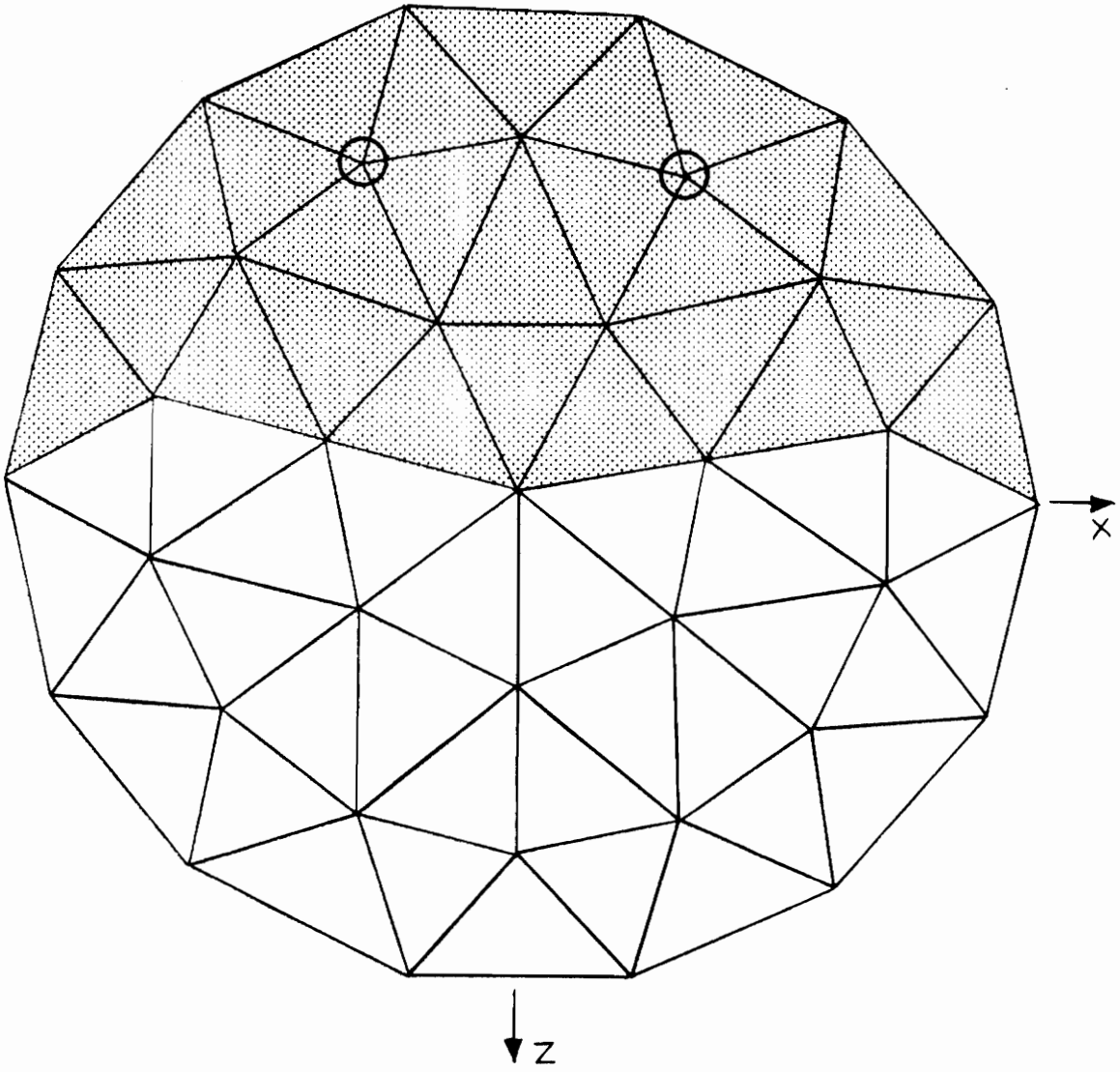

○ Greatest Vertical Displacement

Figure 5.22
Unbalanced Snow:
Position of Nodes with Greatest Displacement

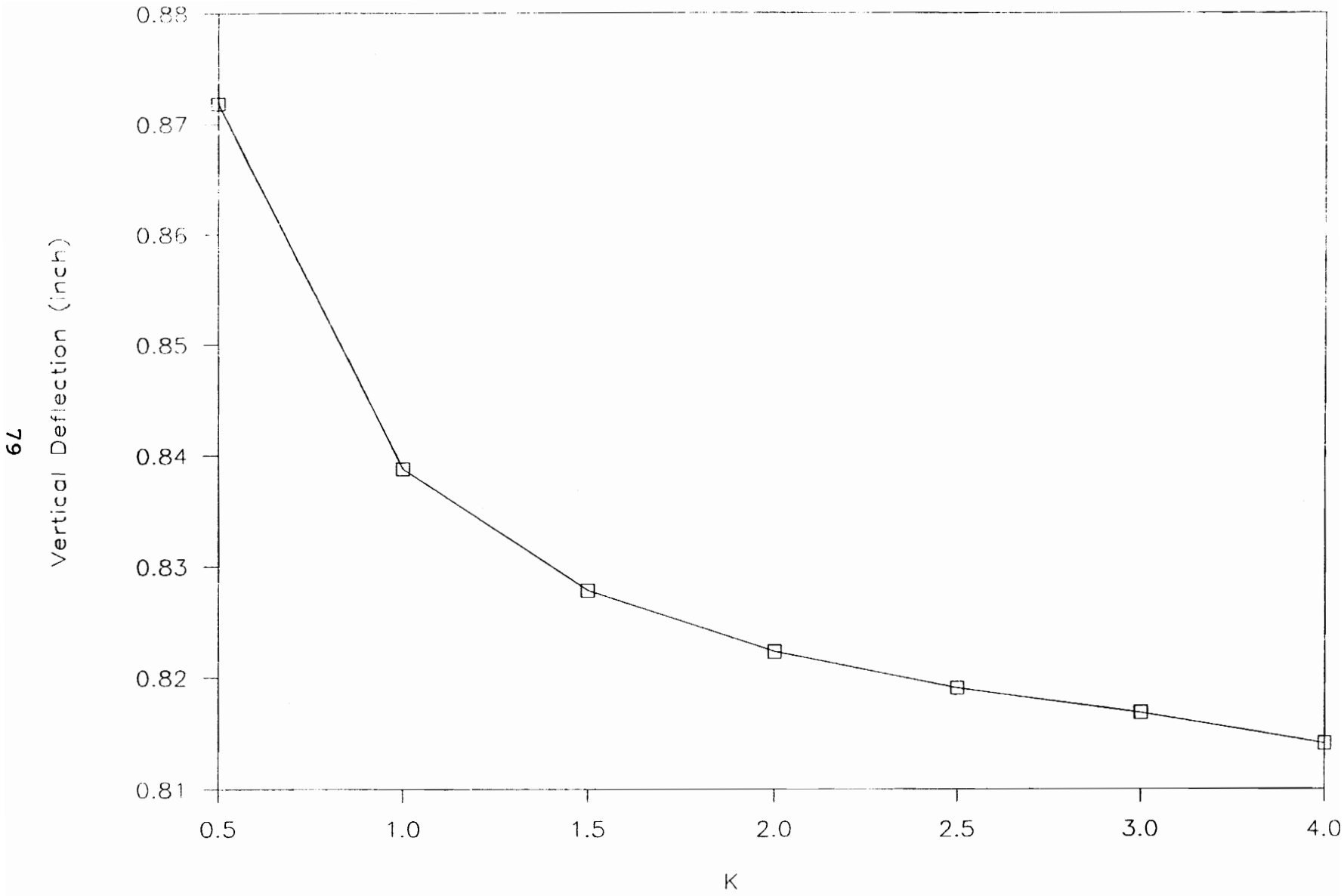

Figure 5.23
Unbalanced Snow: Stiffness-Displacement Curve

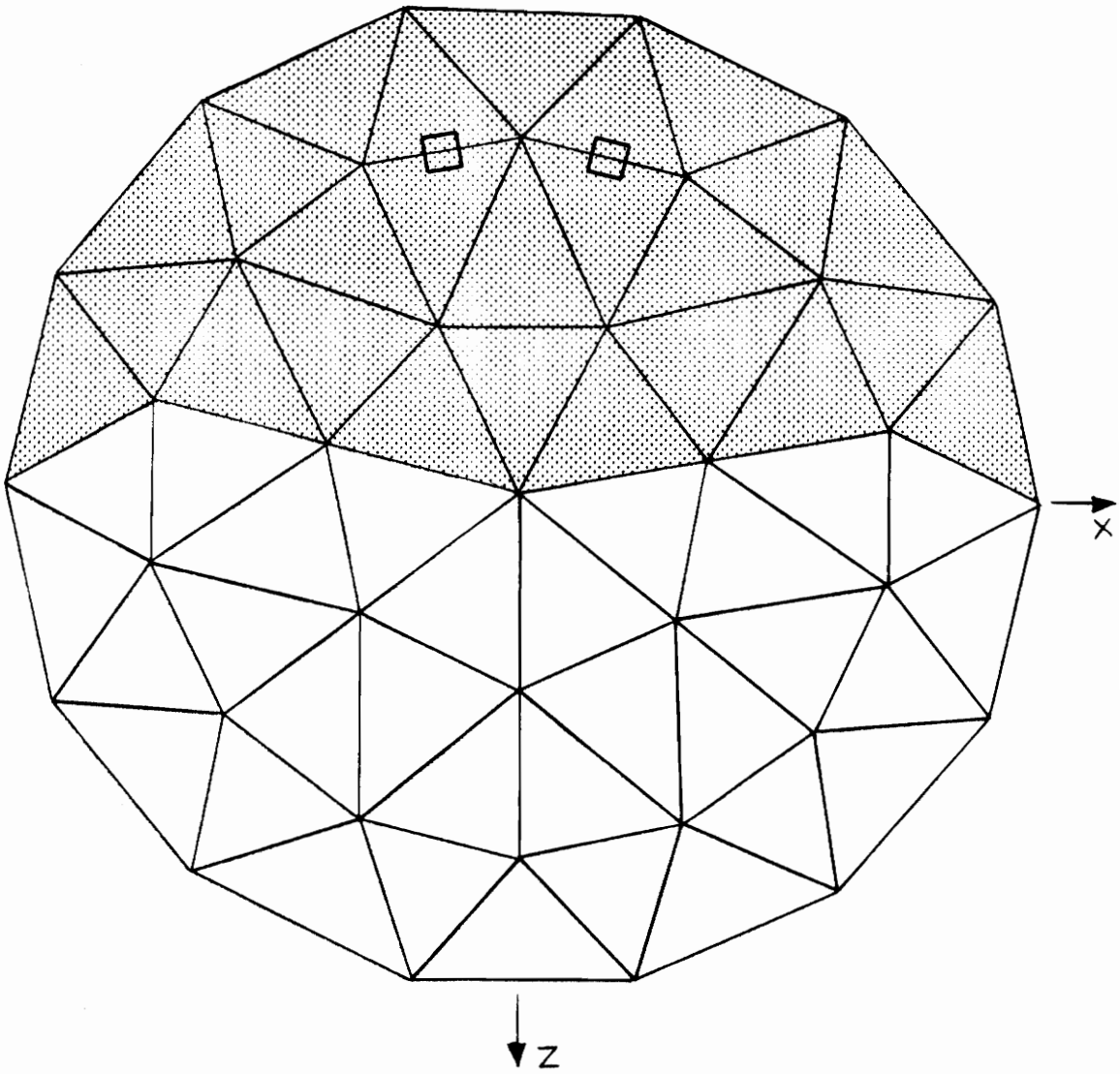

Highest Compression

Figure 5.24
Unbalanced Snow:
Position of Members with Highest Compression

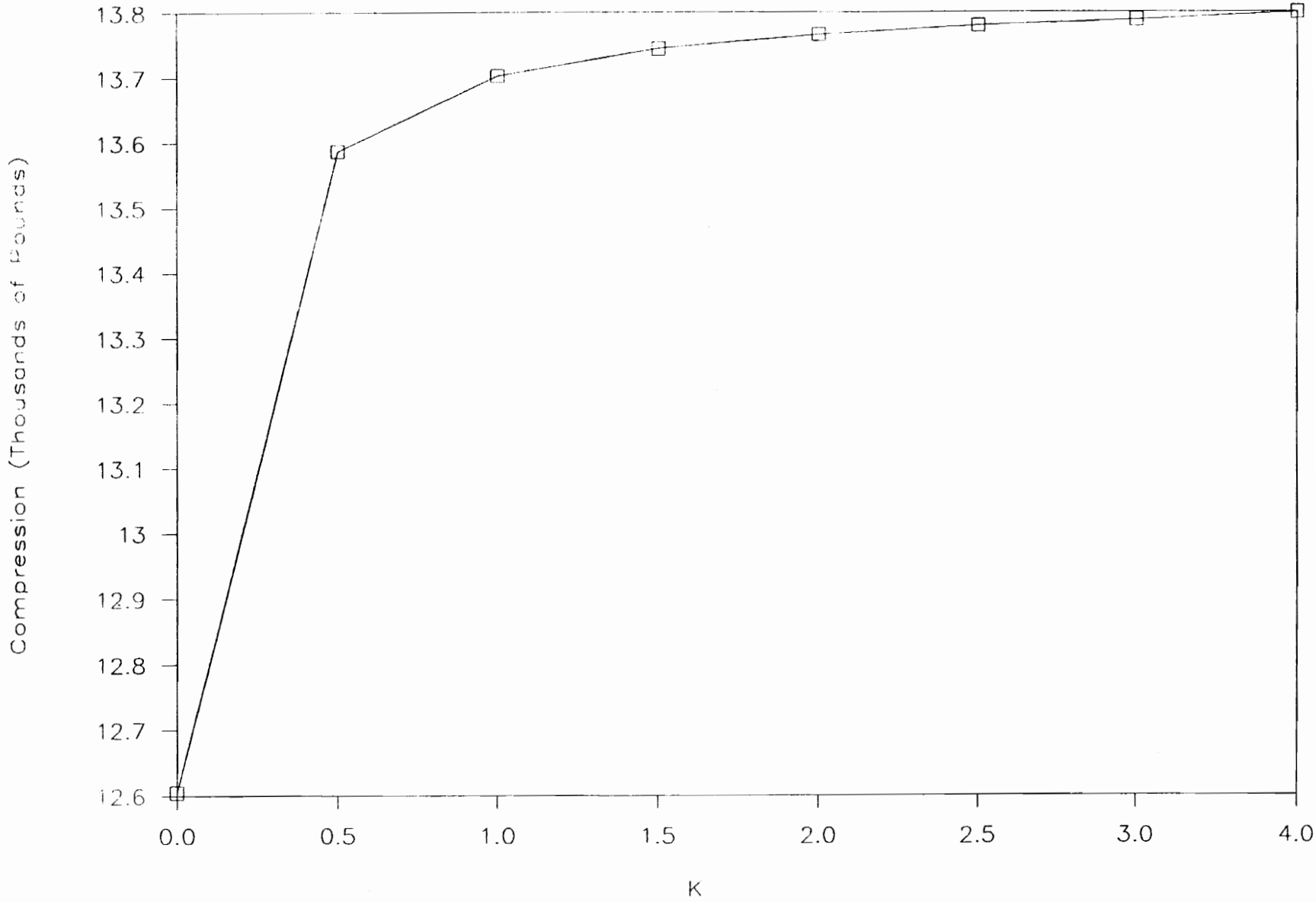

Figure 5.25
Unbalanced Snow: Stiffness-Compression Curve

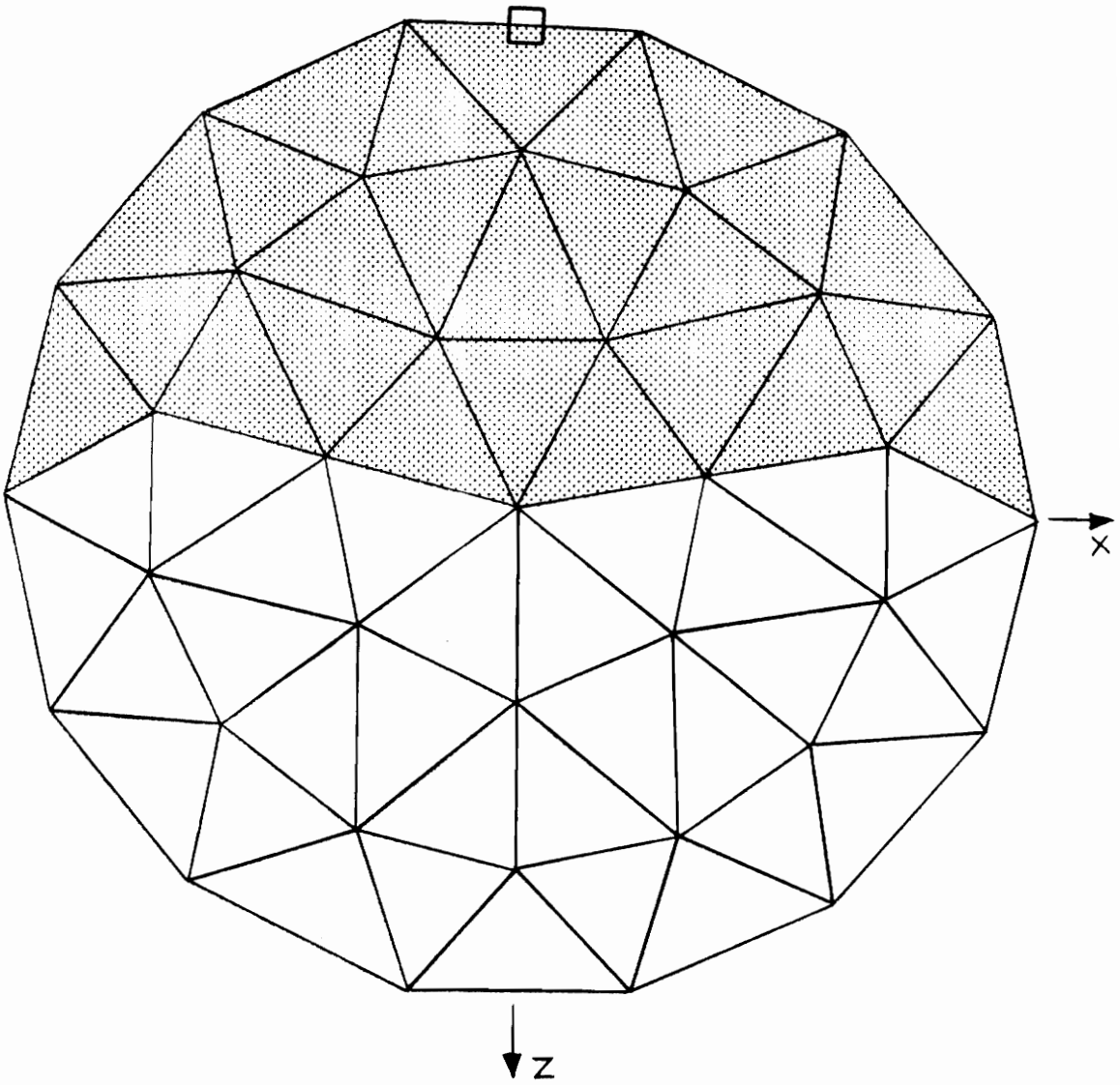

Figure 5.26
Unbalanced Snow:
Position of Member with Highest Tension

big jump from K=0 to K=0.5 and it levels off afterwards, see Figure 5.25. There is only a 1.57% difference of compression force between K=0.5 and K=4.0.

The maximum tension is located on the tension ring at the center of the loading area; see Figure 5.26. There again, the stiffness-tension curve is similar to the balanced snow stiffness-tension curve in that there is a big jump from K=0 to K=0.5 and it levels off afterwards, see Figure 5.27. There is a 0.68% difference for the maximum tension between K=0.5 and K=4.0.

The location of the member with the maximum major moment is dependent on the connector stiffness. For K=0, the pinned model, the location of the maximum major moment is in the second tier at the first member with load on both sides from the unloaded portion of the dome, see Figure 5.28. For the connector stiffness of K=0.5 to K=4.0 the maximum major moment here is 26,533 lb. in. The location of the members with the maximum major moment is on the bottom tier at the first member with load on both, see Figure 5.29. The location of the maximum major moment for the unbalanced snow is similar to the balanced snow in that for K=0, the member with the maximum major moment is in the second tier and for K=0.5 to K=4.0, the member with the maximum major moment is in the bottom tier.

The major moment at midspan for K=0 at the same location as the maximum moment for K=0.5 to K=4.0 is 26,227 lb. in.

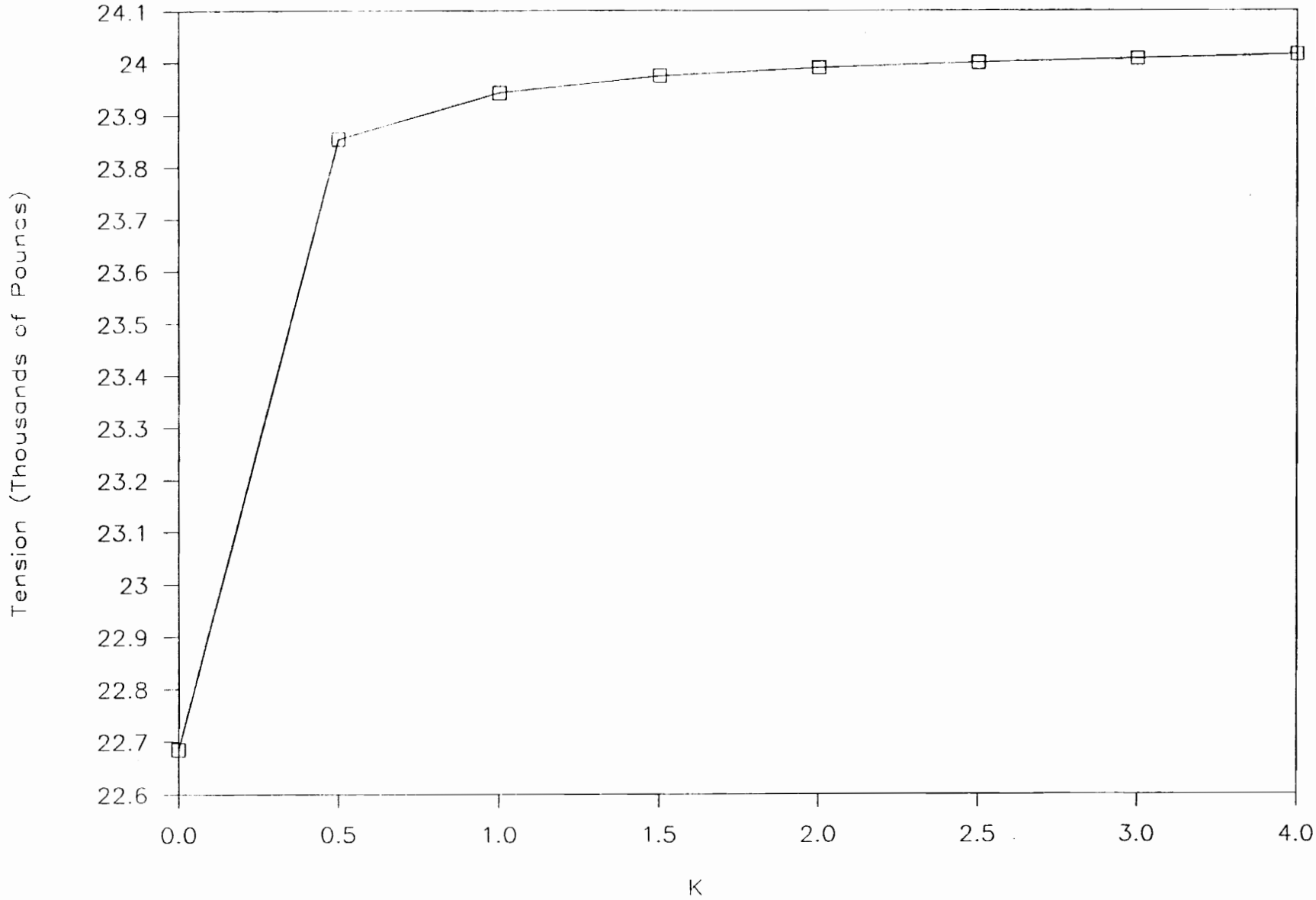

Figure 5.27
Unbalanced Snow: Stiffness-Tension Curve

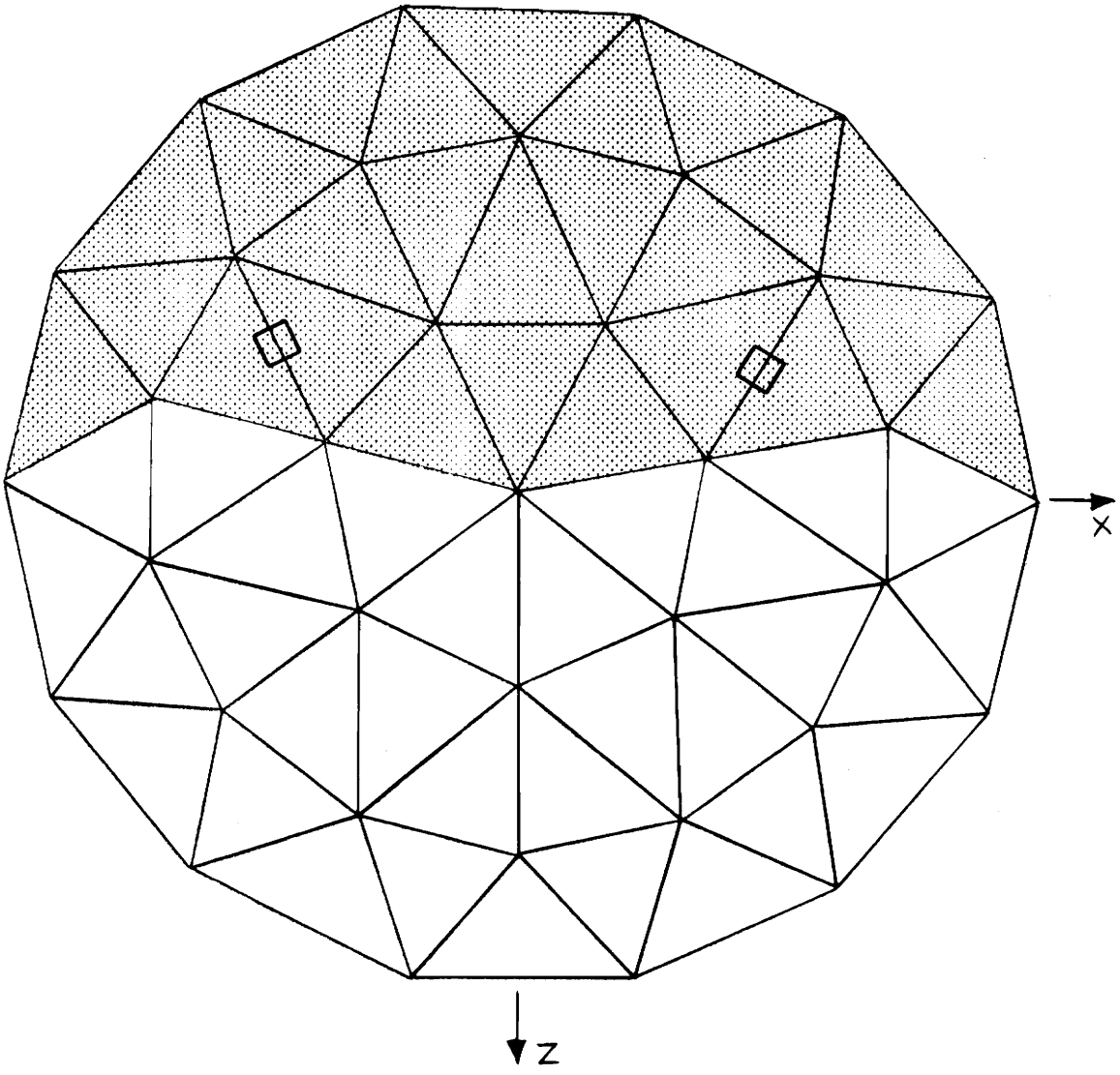

Highest Major Moment

Figure 5.28
Unbalanced Snow: Position of Members
with Highest Major Moment for Pinned-End Model (K=0)

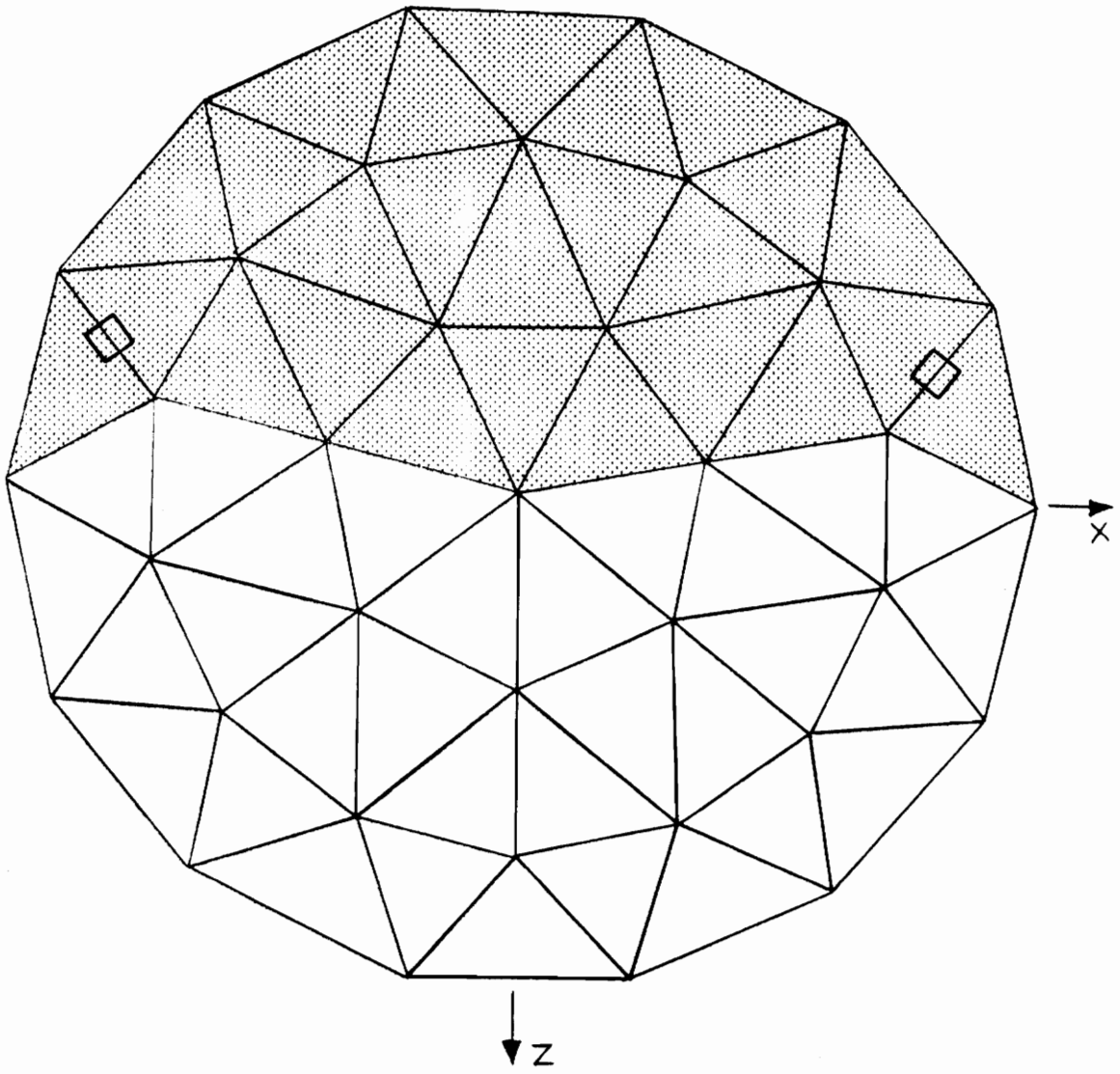

Highest Major Moment

Figure 5.29
Unbalanced Snow:
Position of Members with Highest Major Moment

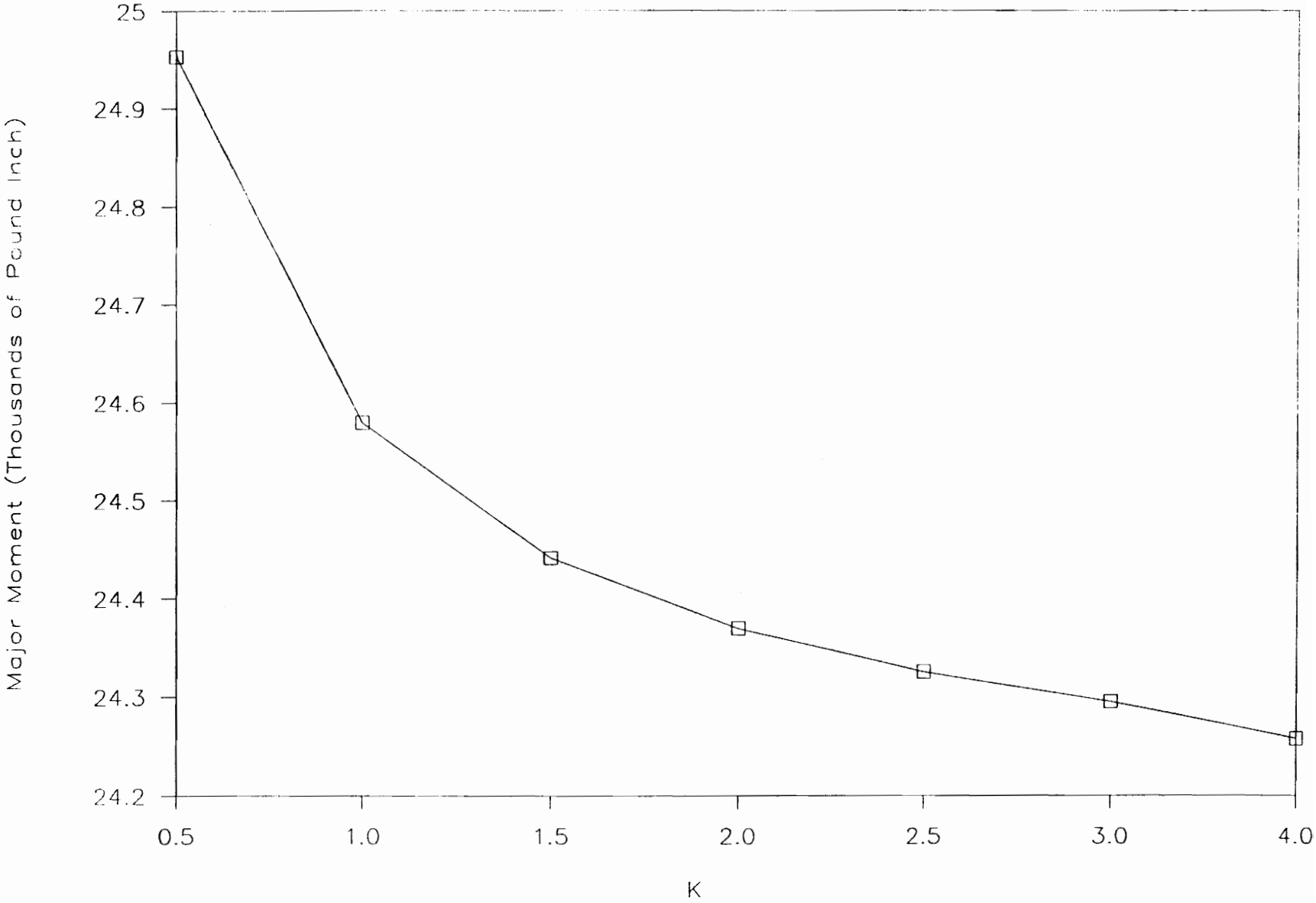

Figure 5.30
Unbalanced Snow: Stiffness-Major Moment Curve

There is a 4.86% difference of the major moment between K=0 versus K=0.5 and there is a 7.51% difference of the major moment between K=0 and K=4.0, as Figure 5.30 shows. The major moment at midspan decreases as the connector element stiffness increases. This is similar to the balanced snow load case.

The location of the member with the maximum minor moment is dependent on the connector stiffness like the major moment. For K=0, the pinned end model, the location of the maximum minor moment is in the tension ring at the center of the loading area. The same member has the maximum tension load, see Figure 5.31. For the connector stiffness of K=0.5 to K=4.0, the location of the members with the maximum minor moment is in the tension ring at the ends of the loading area, see Figure 5.32. Like the major moment, the minor moment at midspan decreases as the connector element increases, see Figure 5.33.

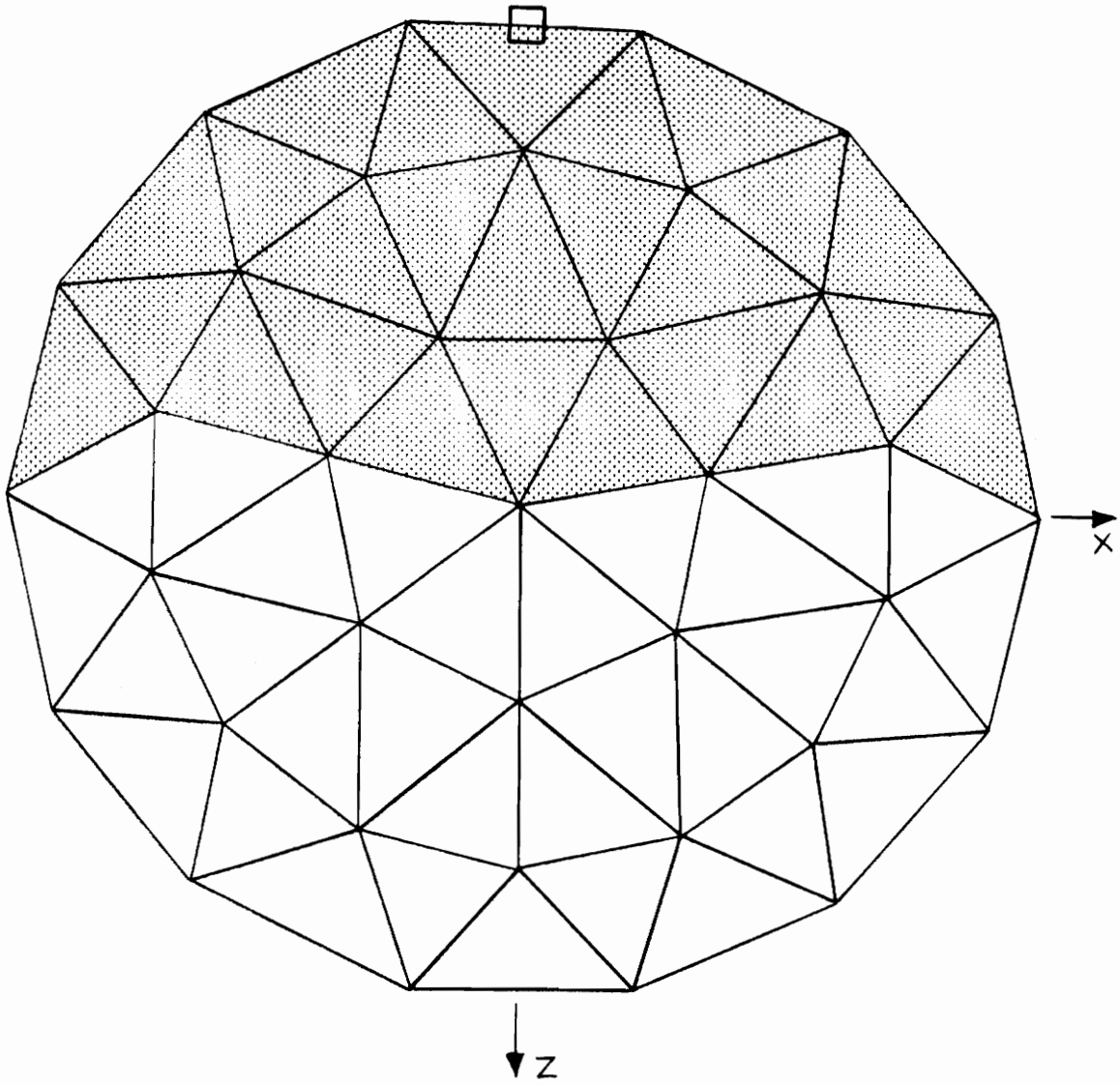

Highest Minor Moment

Figure 5.31
Unbalanced Snow: Position of Members
with Highest Minor Moment for Pinned-End Model (K=0)

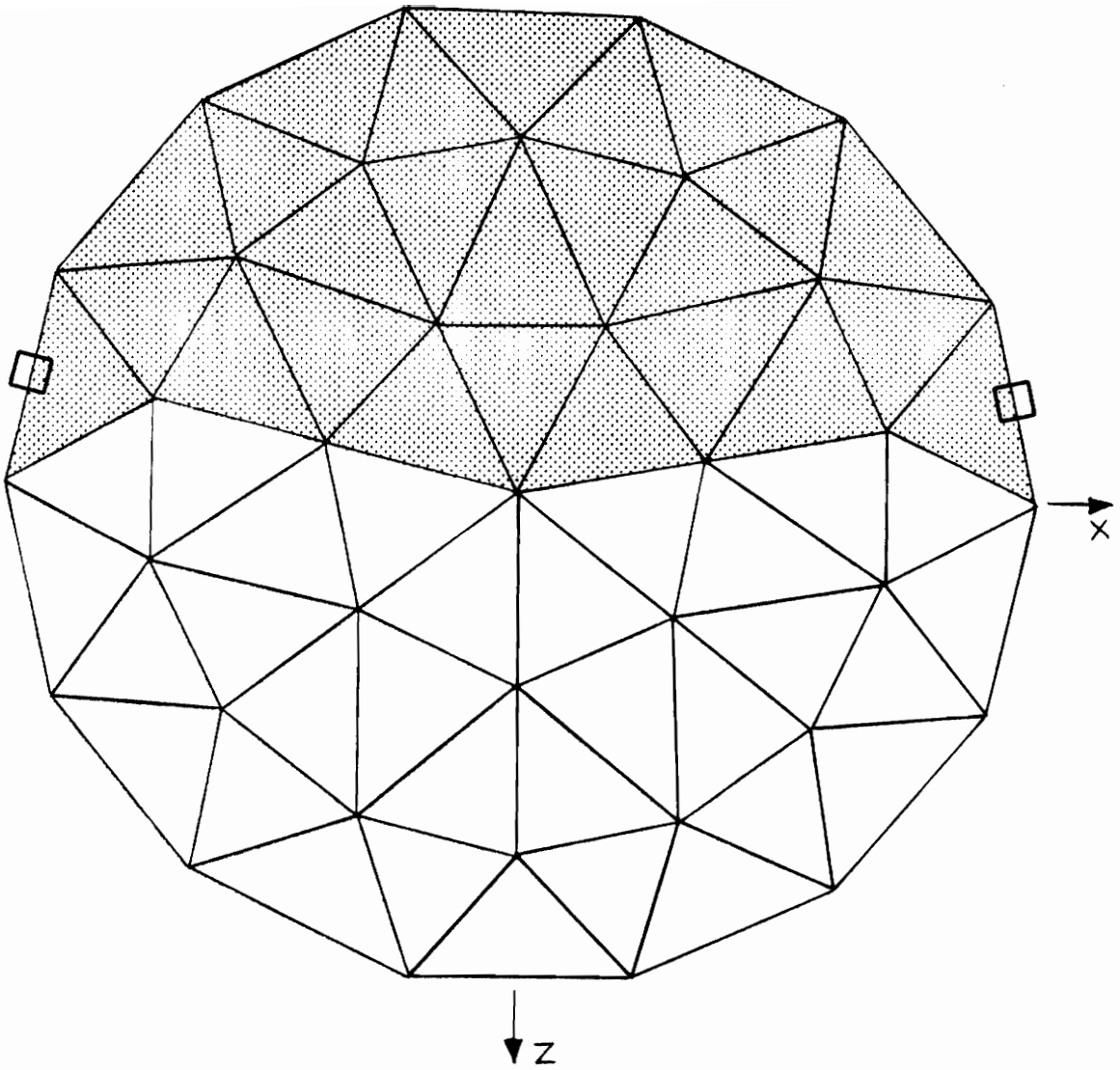

Figure 5.32
Unbalanced Snow:
Position of Members with Highest Minor Moment

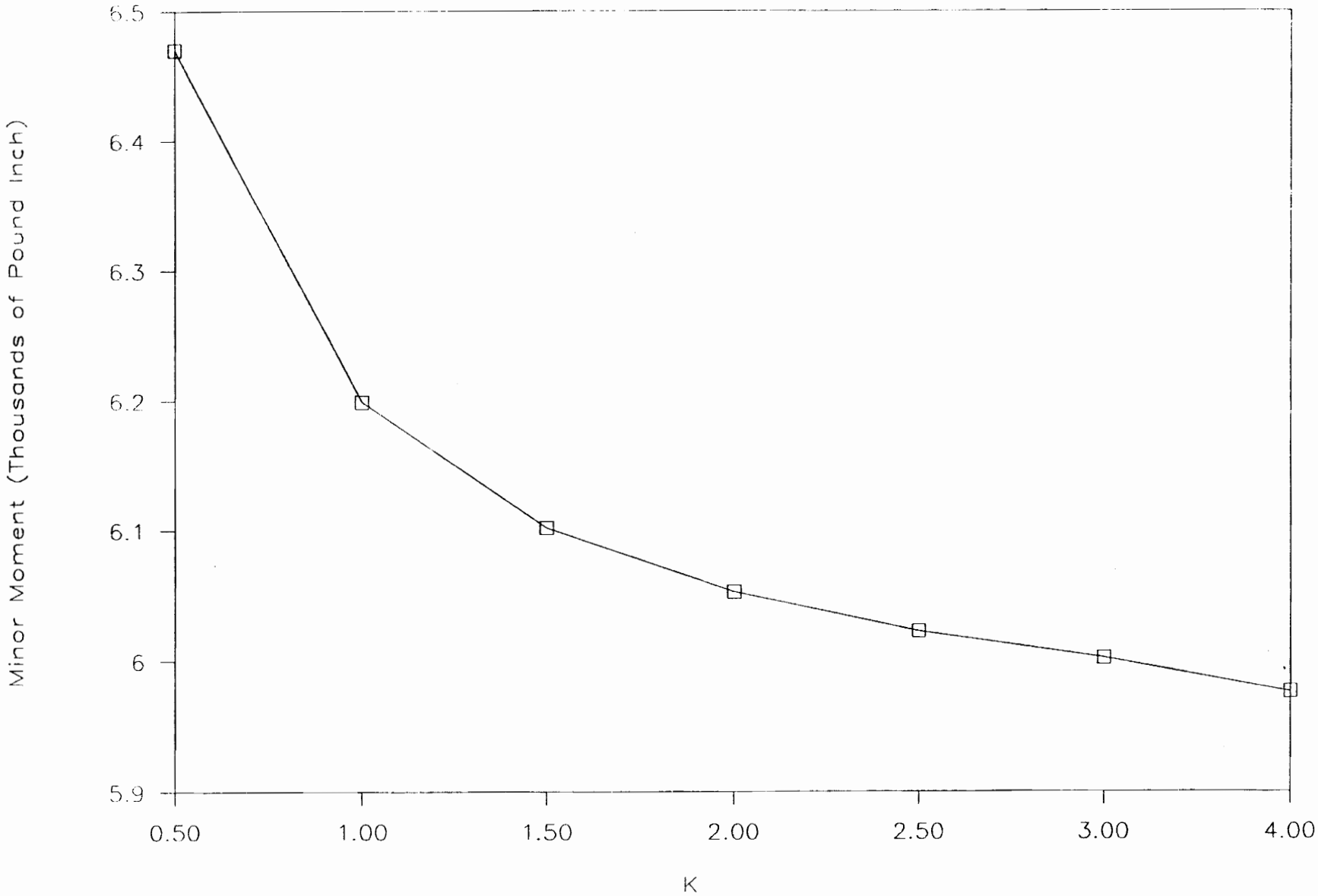

Figure 5.33
Unbalanced Snow: Stiffness-Minor Moment Curve

CHAPTER 6

CONCLUSIONS AND RECOMMENDATIONS

6.1 Conclusions

This thesis was concerned with a commercially available dome. A transformation of pressure loads into a distributed load along the member was derived. Two loads were applied to the structure. The resultant stresses were compared with the allowable stresses. A parametric study of joint stiffness to deflection and internal forces was performed.

In the parametric study, only certain areas were examined. The node at the center of the joint was used for the deflection-stiffness comparison. The midpoint of each member was used for the internal force-stiffness comparison. Only the axial force, the major moment, and the minor moment were studied.

The maximum deflection occurred when the joint stiffness was one-half of the member stiffness in both loading cases. For the balanced snow load, the nodes with the maximum deflection occurred along the first ring below the apex of the dome. However, under the unbalanced load the maximum deflection occurred on the second ring, one ring lower than for the balanced snow load. Axial compression and tension were treated as separate categories. The maximum compression and the maximum tension occurred when the joint stiffness was

four times the member stiffness in both loading cases. Also, the maximum axial load increased very little after the joint stiffness was one-half of the member stiffness. The location of the maximum axial tension naturally occurred at the tension ring for both loading cases. For the balanced snow load, the maximum axial compression was in the top ring of the dome. The second ring of the dome had the maximum compression for the unbalanced snow load.

The major moment and the minor moment at the midpoint of the member had its maximum value for K=0 which was the pinned end model. For the pinned end model with both the balanced and unbalanced snow, the maximum major moment occurred along diagonal members of the second tier. When the dome had any frame action (K=0.5 to K=4.0), the members with the maximum moment shifted down a tier to the bottom tier. For the minor moment, the maximum minor moment occurred along the tension ring for both the balanced and unbalanced snow.

6.2 Recommendations for Future Research

During this study, many questions were raised during the research that could not be answered due to the constraints on time. Other students may wish to pursue the various topics which resulted from this particular thesis topic.

One topic may be a parametric study of the joint stiffness for K=0 to K=0.5. The stiffness curves show a large

jump at K=0.5 and small increments between these values might be interesting.

Other topics are the following: a study of the stability boundaries subjected to multiple independent loads; comparison of concentrated loads at the joints with distributed loads along the member; a study of the joint connection using a plate element instead of a beam element; an analysis of the dome under the action of dynamic loads to the base; or the analysis of the dome subject to various wind loads and local concentrated loads.

REFERENCES

1. Abatan, A.O., Stability of Reticulated Domes Under Multiple Static and Dynamic Loads, Ph.d. Dissertation, Virginia Polytechnic Institute and State University, Blacksburg, VA, 1976

2. Aluminum Standards and Data, 8th Ed., The Aluminum Association, Washington D.C., 1984.

3. Arciszewski, T., "Design of Joints in Steel Space Structures," Third International Conference on Space Structures, Elsevier Applied Science Publishers, New York, 1984.

4. Baker, S., "A Comparison of the Codes of Practice Used in Different Countries for the Determination of Wind Loads on Domes, "Analysis, Design and Construction of Lattice Domes, Z.S. Makowski, ed., Nichols Publishing Co., New York, 1984, pp. 315-336.

5. Bass L., "Lamella Domes in the United States, "The International Conference on Space Structures, University of Surrey, Sept. 1966, John Wiley & Sons, Inc., New York, 1967, pp. 955-964.

6. Davies, R.M., The International Conference on Space Structures, University of Surrey, Sept. 1966, John Wiley & Sons, Inc., New York, 1967.

7. Dib, M.W., Analysis of Reticulated Domes with Automatic Mesh Generation and Bandwidth Reduction, M.S. Thesis, Virginia Polytechnic Institute and State University, Blacksburg, VA, 1984.

8. Dickson,III,W.L., Structural Analysis of Reticulated Domes, M.S. Thesis, Virginia Polytechnic Institute and State University, Blacksburg, VA 1984.

9. "Dome," Civil Engineering, July 1984, pp. 46-47.

10. Domebook 2, 2nd Ed., Shelter Publications, Bolinas, CA, 1972.

11. Eberlein, H., "Single and Double-layer MERO Domes," Analysis, Design, and Construction of Lattice Domes, Z.S. Makowski, ed., Nichols Publishing Co., New York, 1984.

12. Elliott, A.W., "Triodetic Domes," Analysis, Design and Construction of Lattice Domes, Z.S. Makowski, ed., Nichols Publishing Co., New York, 1984.

13. Hayes, T.S., Evaluation of a Refined Lattice Dome Model, M.S. Thesis, Virginia Polytechnic Institute and State University, Blacksburg, VA, 1985.

14. Hao, N.A., Parallel Lamella Dome Under Wind and Snow Loads, M.S. Thesis, Virginia Polytechnic Institute and State University, Blacksburg, VA, 1986.

15. Holzer, Siegrfied M., Computer Analysis of Structures Matrix Structural Analysis Structured Programming, Elsevier Science Publishing Co., Inc., 1985.

16. Jones, C.A., Design and Automated Parametric Study of Geodesic Domes, M.S. Thesis, Virginia Polytechnic Institute and State University, Blacksburg, VA, 1978.

17. Maher, F.J., "Wind Loads on Basic Dome Shapes," Journal of the Structural Division, ASCE, Vol. 91, No. ST3, june 1965, pp. 219-228.

18. Makowski, Z.S., ed., Analysis, Design and Construction of Lattice Domes, Nichols Publishing Co., New York, 1984.

19. Makowski, Z.S., Steel Space Structures, Michael Joseph Ltd., London, 1965.

20. Matsushita, F., "Diamond Dome Systems," Analysis, Design and Construction of Lattice Domes, Z.S. Makowski, ed., Nichols Publishing Co., New York, 1984.

21. McConnel and Klimke, "Geometrically Nonlinear Pin-Jointed Space Frames," Numerical Methods for Nonlinear Problems, C. Taylor, E. Hinton, & D.R.J. Owen, ed., Vol 1,pp.33.

22. Minimum Design Loads for Buildings and Other Structures, ANSI A58.1-1982, American National Standards Institute, Inc., New York, 1982.

23. Nooshin, H., ed., Third International Conference on Space Structures, Elsevier Applied Science Publishers, New York, 1984.

24. Platt, G.D., Wind Effects on a Hemispherical Dome, M.S. Thesis, Virginia Polytechnic Institute and State University, Blacksburg, VA, 1986.

25. Popko, E., Geodesics, University of Detroit Press, Detroit, Michigan, 1968.

26. Renton, J.D., "The Beam-Like Behavior of Space Trusses," AIAA Journal, Vol 22, no. 2, Feb. 1984, pp 273-79.

27. Richter, D.L., "Geodesic Domes: The Rational and Reality," Architectural Forum, Vol. 136, no. 1, Jan. 1972, pp. 84-86.

28. Schaefer, E.R., "Dome Structures," The International Conference on Space Structures, University of Surrey, Sept. 1966, John Wiley & Sons, Inc., New York, 1967, pp. 1045-58.

29. Schueller, W., Horizontal-Span Building Structures, John Wiley & Sons, Inc., New York, 1983.

30. Shen,S.H., Stability Boundaries for Four Reticulated Domes, M.S. Thesis, Virginia Polytechnic Institute and State University, Blacksburg, VA, 1979.

31. Shu-t'ien,L.F., "Metallic Dome Structural Systems," Journal of the Structural Division ASCE, Vol. 88, no. ST6, Dec. 1962, pp. 201-226.

32. Soare, "Investigation of the Collapse of a Large-Span Lattice Dome," Analysis, Design and Construction of Lattice Domes, Z.S. Makowski, ed., Nichols Publishing Co., New York, 1984.

33. Specifications for Aluminum Structures, 5th Ed., The Aluminum Association, Washington D.C., 1986.

34. STAAD-III, Version 12, Research Engineers, Inc.

35. Subramanian, N., Principles of Space Structures, Allahabad, Wheeler, 1983.

36. Uliana, D.A., The Effects of Earthquake Excitations on Reticulated Domes, M.S. Thesis, Virginia Polytechnic Institute and State University, Blacksburg, VA, 1985.

37. Wendel, W.R., Spaceframe Basics, Space Structures International Corp., Plainview, New York, 1984.

38. White,III, W.S., Stability of a Reticulated Dome Under Multiple Independent Loads, M.S. Thesis, Virginia Polytechnic Institute and State University, Blacksburg, VA, 1978.

39. Zetlin, L., "A Space Frame Forecast," Civil Engineering, Vol. 55, no. 8, August 1985, pp.50-54.

APPENDIX A

ALTERNATE SOLUTION FOR MEMBER LOADS

APPENDIX A

ALTERNATE SOLUTION FOR MEMBER LOADS

An alternate solution for the member loads uses simple beam theory. The normal forces at each node are

$$R_1 = \frac{2}{12}P_1A + \frac{1}{12}P_2A + \frac{1}{12}P_3A \tag{A.1}$$

$$R_2 = \frac{1}{12}P_1A + \frac{2}{12}P_2A + \frac{1}{12}P_3A \tag{A.2}$$

$$R_3 = \frac{1}{12}P_1A + \frac{1}{12}P_2A + \frac{2}{12}P_3A \tag{A.3}$$

where P_1, P_2, P_3, and A are defined in section 3.2. By reversing the direction of the reactive forces at the nodes, these loads are the equivalent loads applied at the nodes.

With the aid of Figure A.1, the triangular panel is divided into three beams. For each beam, the reaction forces are found.

For beam element 1-2, the moment about node 2 is the following:

$$\frac{1}{2}F_1(3)l_3\left(\frac{2}{3}l_3\right) + \frac{1}{2}F_2(3)l_3\left(\frac{1}{3}l_3\right) - l_3R_13 = 0 \tag{A.4}$$

which simplifies to

$$R_1^3 = \frac{1}{3}l_3F_1(3) + \frac{1}{6}l_3F_2(3) \tag{A.5}$$

The moment about node 1 is the following:

$$\frac{1}{2}F_1(3)l_3\left(\frac{1}{3}l_3\right) + \frac{1}{2}F_2(3)l_3\left(\frac{2}{3}l_3\right) - l_3R_2^3 = 0 \tag{A.6}$$

which simplifies to

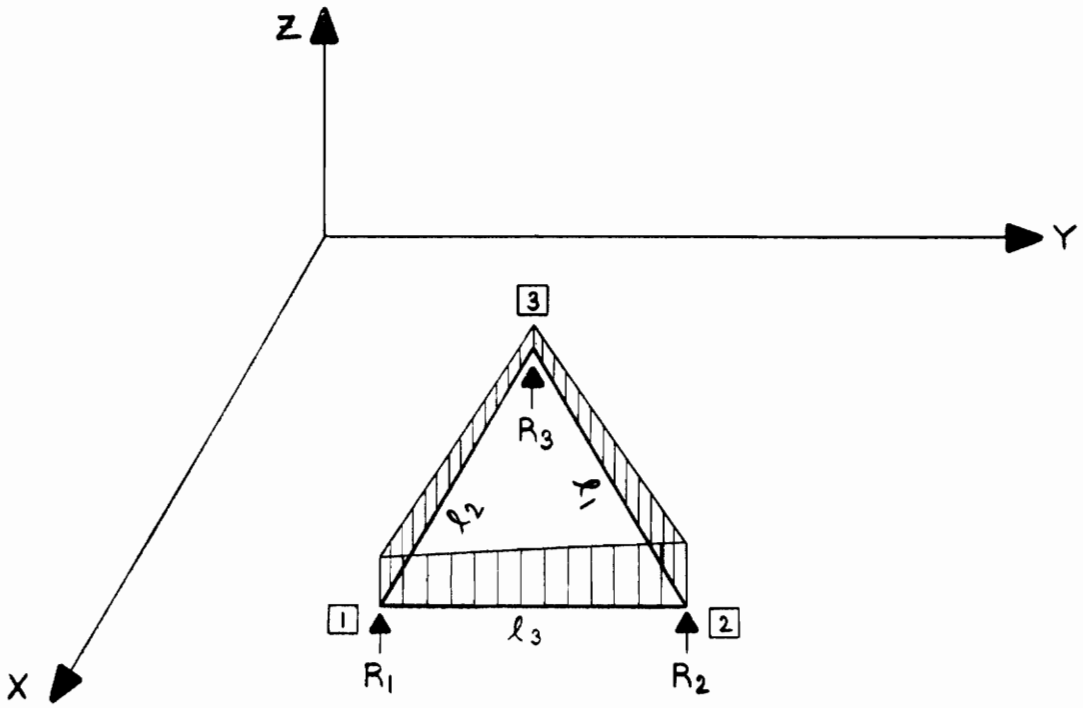

(a) Domain

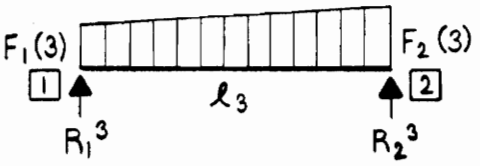

(b-1) Beam Element 1-2

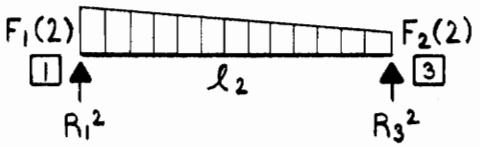

(b-2) Beam Element 1-3

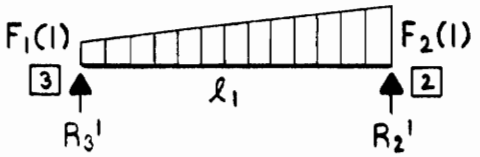

(b-3) Beam Element 2-3

Figure A.1 Panel Load Coordinates

$$R_2^3 = \frac{1}{6} l_3 F_1(3) + \frac{1}{3} l_3 F_2(3) \quad (A.7)$$

For beam element 1-3, the moment about node 3 is the following:

$$\frac{1}{2} F_1(2)\, l_2 \left(\frac{2}{3} l_2\right) + \frac{1}{2} F_2(2)\, l_2 \left(\frac{1}{3} l_2\right) - l_2 R_1^2 = 0 \quad (A.8)$$

which simplifies to

$$R_1^2 = \frac{1}{3} l_2 F_1(2) + \frac{1}{6} l_2 F_2(2) \quad (A.9)$$

The moment about node 1 is the following:

$$\frac{1}{2} F_1(2)\, l_2 \left(\frac{1}{3} l_2\right) + \frac{1}{2} F_2(2)\, l_2 \left(\frac{2}{3} l_2\right) - l_2 R_3^2 = 0 \quad (A.10)$$

which simplifies to

$$R_3^2 = \frac{1}{6} l_2 F_1(2) + \frac{1}{3} l_2 F_2(2) \quad (A.11)$$

For beam element 2-3, the moment about node 2 is the following:

$$\frac{1}{2} F_1(1)\, l_1 \left(\frac{2}{3}\right) l_1 + \frac{1}{2} F_2(1)\, l_1 \left(\frac{1}{3} l_1\right) - l_1 R_3^1 = 0 \quad (A.12)$$

which simplifies to

$$R_3^1 = \frac{1}{3} l_1 F_1(1) + \frac{1}{6} l_1 F_2(1) \quad (A.13)$$

The moment about node 3 is the following:

$$\frac{1}{2} F_1(1)\, l_1 \left(\frac{1}{3} l_1\right) + \frac{1}{2} F_2(1)\, l_1 \left(\frac{2}{3} l_1\right) - l_1 R_2^1 = 0 \quad (A.14)$$

which simplifies to

$$R_2^1 = \frac{1}{6} l_1 F_1(1) + \frac{1}{3} l_1 F_2(1) \quad (A.15)$$

When joining the three beam element to create the

triangular member, the reaction forces at each node of the beam element are added together for each node of the triangular member. Therefore,

$$R_1^3 + R_1^1 = R_1 \tag{A.16}$$

$$R_2^1 + R_2^3 = R_2 \tag{A.17}$$

$$R_3^1 + R_3^1 = R_3 \tag{A.18}$$

By substituting Eqs. A.5, A.7, A.9, A.11, A.13, and A.15 into Eqs. A.16, A.17 and A.18 give the following results:

$$\frac{1}{3}l_2F_1(2) + \frac{1}{6}l_2F_2(2) + \frac{1}{3}l_3F_1(3) + \frac{1}{6}l_3F_2(3) = R_1 \tag{A.19}$$

$$\frac{1}{6}l_1F_1(1) + \frac{1}{3}l_1F_2(1) + \frac{1}{6}l_3F_1(3) + \frac{1}{3}l_3F_2(3) = R_2 \tag{A.20}$$

$$\frac{1}{3}l_1F_1(1) + \frac{1}{6}l_1F_2(1) + \frac{1}{6}l_2F_1(2) + \frac{1}{3}l_2F_2(2) = R_3 \tag{A.21}$$

Since the applied load is continuous, the beam loading has to be continuous, therefore,

$$F_1(3) = F_1(2) = F_1 \tag{A.22}$$

$$F_2(3) = F_2(3) = F_2 \tag{A.23}$$

$$F_2(2) = F_1(1) = F_3 \tag{A.24}$$

By substituting Eqs., A.22, A.23, and A.24 into Eq. A.19, A.20, and A.21, one obtains the following equations:

$$\frac{2}{6}(l_2 + l_3)F_1 + \frac{1}{6}l_3F_2 + \frac{1}{6}l_2F_3 = R_1 \tag{A.25}$$

$$\frac{1}{6}l_3F_1 + \frac{2}{6}(l_1 + l_3)F_3 + \frac{1}{6}l_1F_3 = R_2 \tag{A.26}$$

$$\frac{1}{6}l_2F_1 + \frac{1}{6}l_1F_2 + \frac{2}{6}(l_1 + l_2)F_3 = R_3 \tag{A.27}$$

which are the same Eqs. as 3.43, 3.44 and 3.45 in section 3.2.

APPENDIX B:

TEST PROBLEM STAAD-III LISTING

```
STAAD SPACE
UNIT INCHES POUND
JOINT COORDINATES
    1          .000      644.290          .000
    2          .000      643.980         2.984
    3         2.984      643.980          .000
    4          .000      643.980        -2.984
    5        -2.984      643.980          .000
    6          .000      637.630        65.166
    7        65.166      637.630          .000
    8          .000      637.630       -65.166
    9       -65.166      637.630          .000
   10          .000      631.280       127.350
   11       127.350      631.280          .000
   12          .000      631.280      -127.350
   13      -127.350      631.280          .000
   14          .000      630.970       130.330
   15         2.121      630.970       128.210
   16        65.166      630.970        65.166
   17       128.210      630.970         2.121
   18       130.330      630.970          .000
   19       128.210      630.970        -2.121
   20        65.166      630.970       -65.166
   21         2.121      630.970      -128.210
   22          .000      630.970      -130.330
   23        -2.121      630.970      -128.210
   24       -65.166      630.970       -65.166
   25      -128.210      630.970        -2.121
   26      -130.330      630.970          .000
   27      -128.210      630.970         2.121
   28       -65.166      630.970        65.166
   29        -2.121      630.970       128.210
MEMBER INCIDENCES
    1     1     2
    2     1     3
    3     1     4
    4     1     5
    5    10    14
    6    11    18
    7    12    22
    8    13    26
    9    14    15
   10    17    18
   11    18    19
   12    21    22
   13    22    23
   14    25    26
   15    26    27
   16    29    14
```

```
   17     2     6
   18     6    10
   19     3     7
   20     7    11
   21     4     8
   22     8    12
   23     5     9
   24     9    13
   25    15    16
   26    16    17
   27    19    20
   28    20    21
   29    23    24
   30    24    25
   31    27    28
   32    28    29
MEMBER PROPERTIES
1 TO 8 PRISMATIC AX 2.114 IX 0.014 IY 0.728 IZ 10.46 YD 6.
9 TO 16 PRISMATIC AX 3.68 IX 0.064 IY 3.81 IZ 21.52 YD 6.
17 TO 24 PRISMATIC AX 2.114 IX 0.014 IY 0.728 IZ 10.46 YD 6.
25 TO 32 PRISMATIC AX 3.68 IX 0.064 IY 3.81 IZ 21.52 YD 6.
SUPPORTS
14 22 FIXED BUT MX MY MZ FZ
18 26 FIXED BUT MX MY MZ FX
CONSTANTS
E 10100000. ALL
REF 0. 0. 0. ALL
LOAD 1 (UNBALANCED SNOW)
MEMBER LOAD
1 3 TRAP GY -3.522643,-3.519473
2 TRAP GY -7.045287,7.038946
17 21 TRAP GY -3.519473,-3.453417
19 TRAP GY -7.038946,-6.9068345
18 22 TRAP GY -3.453417,-3.387361
20 TRAP GY -6.9068345,-6.774723
5 7 TRAP GY -3.387361,-3.384191
6 TRAP GY -6.774723,-6.768382
9 TO 12 UNI GY -3.384191
25 TO 28 UNI GY -3.384191
PERFORM ANALYSIS PRINT BOTH
PRINT ALL
PRINT ANALYSIS
PRINT MAXF ENV ALL
PLOT BENDING FILE
PLOT DISPLACEMENT FILE
FINISH
```

APPENDIX C

TRUSS DOME STAAD-III LISTING

```
STAAD TRUSS
UNIT INCHES POUND
JOINT COORDINATES
    1         .000      644.290         .000
    2         .000      630.970      130.331
    3      101.897      630.970       81.260
    4      127.064      630.970      -29.001
    5       56.549      630.970     -117.420
    6      -56.849      630.970     -117.420
    7     -127.060      630.970      -29.001
    8     -101.900      630.970       81.260
    9         .000      592.057      254.123
   10      110.260      592.057      228.957
   11      198.681      592.057      158.443
   12      247.752      592.057       56.548
   13      247.752      592.057      -56.548
   14      198.681      592.057     -158.440
   15      110.260      592.057     -228.960
   16         .000      592.057     -254.120
   17     -110.260      592.057     -228.960
   18     -198.680      592.057     -158.440
   19     -247.750      592.057      -56.548
   20     -247.750      592.057       56.548
   21     -198.680      592.057      158.443
   22     -110.260      592.057      228.957
   23      -78.608      538.811      344.403
   24       78.608      538.811      344.403
   25      220.254      538.811      276.190
   26      318.276      538.811      153.274
   27      353.260      538.811         .000
   28      318.276      538.811     -153.270
   29      220.254      538.811     -276.190
   30       78.608      538.811     -344.400
   31      -78.608      538.811     -344.400
   32     -220.250      538.811     -276.190
   33     -318.280      538.811     -153.270
   34     -353.260      538.811         .000
   35     -318.280      538.811      153.274
   36     -220.250      538.811      276.190
MEMBER INCIDENCES
    1     1     2
    2     1     3
    3     1     4
    4     1     5
    5     1     6
    6     1     7
    7     1     8
    8     2     3
```

9	3	4
10	4	5
11	5	6
12	6	7
13	7	8
14	8	2
15	2	9
16	2	10
17	3	10
18	3	11
19	3	12
20	4	12
21	4	13
22	4	14
23	5	14
24	5	15
25	5	16
26	6	16
27	6	17
28	6	18
29	7	18
30	7	19
31	7	20
32	8	20
33	8	21
34	8	22
35	2	22
36	9	10
37	10	11
38	11	12
39	12	13
40	13	14
41	14	15
42	15	16
43	16	17
44	17	18
45	18	19
46	19	20
47	20	21
48	21	22
49	22	9
50	9	24
51	10	24
52	10	25
53	11	25
54	11	26
55	12	26
56	12	27

```
    57    13    27
    58    13    28
    59    14    28
    60    14    29
    61    15    29
    62    15    30
    63    16    30
    64    16    31
    65    17    31
    66    17    32
    67    18    32
    68    18    33
    69    19    33
    70    19    34
    71    20    34
    72    20    35
    73    21    35
    74    21    36
    75    22    36
    76    22    23
    77     9    23
    78    23    24
    79    24    25
    80    25    26
    81    26    27
    82    27    28
    83    28    29
    84    29    30
    85    30    31
    86    31    32
    87    32    33
    88    33    34
    89    34    35
    90    35    36
    91    36    23
MEMBER PROPERTIES
1 TO 77 PRISMATIC AX 2.114
78 TO 91 PRISMATIC AX 3.68
SUPPORTS
27 34 FIXED BUT FX MX MY MZ
23 24 25 26 FIXED BUT FX FZ MX MY MZ
28 TO 33 FIXED BUT FX FZ MX MY MZ
35 36 FIXED BUT FX FZ MX MY MZ
CONSTANTS
E 10100000. ALL
UNITS INCH KIPS
LOAD 1 (BALANCED SNOW)
```

```
JOINT LOAD
1 FY -3.19668
2 TO 8 FY -2.740011
9 11 13 15 17 19 21 FY -2.283343
10 12 14 16 18 20 22 FY -2.740011
23 TO 36 FY -1.370006
LOAD 2 (UNBALANCED SNOW)
JOINT LOAD
1 FY -1.311863
4 7 FY -1.923269
5 6 FY -3.846539
13 19 FY -2.770759
14 16 18 FY -5.275053
15 17 FY -4.534019
27 34 FY -1.066751
28 TO 33 FY -3.141001
PERFORM ANALYSIS PRINT STATICS CHECK
PRINT ANALYSIS RESULTS
FINISH
```

APPENDIX D

BEAM DOME STAAD-III LISTING

```
STAAD SPACE
UNIT INCHES POUND
JOINT COORDINATES
```

1	.000	644.290	.000
2	.000	630.970	130.331
3	101.897	630.970	81.260
4	127.064	630.970	-29.001
5	56.549	630.970	-117.424
6	-56.549	630.970	-117.424
7	-127.064	630.970	-29.001
8	-101.897	630.970	81.260
9	.000	592.057	254.123
10	110.260	592.057	228.957
11	198.681	592.057	158.443
12	247.752	592.057	56.548
13	247.752	592.057	-56.548
14	198.681	592.057	-158.443
15	110.260	592.057	-228.957
16	.000	592.057	-254.123
17	-110.260	592.057	-228.957
18	-198.681	592.057	-158.443
19	-247.752	592.057	-56.548
20	-247.752	592.057	56.548
21	-198.681	592.057	158.443
22	-110.260	592.057	228.957
23	-78.608	538.811	344.403
24	78.608	538.811	344.403
25	220.254	538.811	276.190
26	318.276	538.811	153.274
27	353.260	538.811	.000
28	318.276	538.811	-153.274
29	220.254	538.811	-276.190
30	78.608	538.811	-344.403
31	-78.608	538.811	-344.403
32	-220.254	538.811	-276.190
33	-318.276	538.811	-153.274
34	-353.260	538.811	.000
35	-318.276	538.811	153.274
36	-220.254	538.811	276.190
37	.000	643.985	2.984
38	2.333	643.985	1.861
39	2.910	643.985	-.664
40	1.295	643.985	-2.689
41	-1.295	643.985	-2.689
42	-2.910	643.985	-.664
43	-2.333	643.985	1.861
44	.000	631.275	127.347
45	2.703	630.970	129.030

46	2.162	630.207	132.265
47	.000	630.071	133.193
48	-2.162	630.207	132.265
49	-2.703	630.970	129.030
50	99.564	631.275	79.399
51	99.194	630.970	82.562
52	102.061	630.207	84.157
53	104.134	630.071	83.045
54	104.758	630.207	80.776
55	102.564	630.970	78.335
56	124.154	631.275	-28.337
57	126.396	630.970	-26.077
58	129.430	630.207	-27.324
59	129.854	630.071	-29.638
60	128.468	630.207	-31.540
61	125.193	630.970	-31.347
62	55.254	631.275	-114.735
63	58.419	630.970	-115.079
64	59.336	630.207	-118.229
65	57.790	630.071	-120.003
66	55.440	630.207	-120.105
67	53.549	630.970	-117.424
68	-55.254	631.275	-114.735
69	-53.549	630.970	-117.424
70	-55.440	630.207	-120.105
71	-57.790	630.071	-120.003
72	-59.336	630.207	-118.229
73	-58.419	630.970	-115.079
74	-124.154	631.275	-28.337
75	-125.193	630.970	-31.347
76	-128.468	630.207	-31.540
77	-129.854	630.071	-29.638
78	-129.430	630.207	-27.324
79	-126.396	630.970	-26.077
80	-99.564	631.275	79.399
81	-102.564	630.970	78.335
82	-104.758	630.207	80.776
83	-104.134	630.071	83.045
84	-102.061	630.207	84.157
85	-99.194	630.970	82.562
86	.000	592.956	251.261
87	2.925	592.057	253.455
88	1.800	590.838	256.190
89	-1.800	590.838	256.190
90	-2.925	592.057	253.455
91	108.097	592.820	227.023
92	107.335	592.057	229.624
93	109.535	590.838	231.600

94	112.778	590.838	230.038
95	112.605	592.057	227.086
96	110.096	592.820	226.060
97	196.444	592.956	156.659
98	196.336	592.057	160.314
99	199.175	590.838	161.139
100	201.420	590.838	158.325
101	199.983	592.057	155.740
102	244.891	592.820	57.032
103	246.450	592.057	59.251
104	249.366	590.838	58.763
105	250.168	590.838	55.253
106	247.752	592.057	53.548
107	245.385	592.820	54.870
108	244.961	592.956	-55.911
109	247.752	592.057	-53.548
110	250.168	590.838	-55.253
111	249.366	590.838	-58.763
112	246.450	592.057	-59.251
113	197.277	592.820	-155.904
114	199.983	592.057	-155.740
115	201.420	590.838	-158.325
116	199.175	590.838	-161.139
117	196.336	592.057	-160.314
118	195.894	592.820	-157.639
119	109.018	592.956	-226.378
120	112.605	592.057	-227.086
121	112.778	590.838	-230.038
122	109.535	590.838	-231.600
123	107.335	592.057	-229.624
124	1.109	592.820	-251.442
125	2.925	592.057	-253.455
126	1.800	590.838	-256.190
127	-1.800	590.838	-256.190
128	-2.925	592.057	-253.455
129	-1.109	592.820	-251.442
130	-109.018	592.956	-226.378
131	-107.335	592.057	-229.624
132	-109.535	590.838	-231.600
133	-112.778	590.838	-230.038
134	-112.605	592.057	-227.086
135	-195.894	592.820	-157.639
136	-196.336	592.057	-160.314
137	-199.175	590.838	-161.139
138	-201.420	590.838	-158.325
139	-199.983	592.057	-155.740
140	-197.277	592.820	-155.904
141	-244.961	592.956	-55.911

missing page

contact arthur

190	217.551	538.811	-277.491
191	81.311	538.811	-343.101
192	79.332	540.030	-341.760
193	76.808	540.030	-342.336
194	75.608	538.811	-344.403
195	-75.608	538.811	-344.403
196	-76.808	540.030	-342.336
197	-79.332	540.030	-341.760
198	-81.311	538.811	-343.101
199	-217.551	538.811	-277.491
200	-217.735	540.030	-275.108
201	-219.760	540.030	-273.494
202	-222.124	538.811	-273.844
203	-316.406	538.811	-155.619
204	-315.538	540.030	-153.392
205	-316.661	540.030	-151.059
206	-318.944	538.811	-150.349
207	-352.592	538.811	-2.925
208	-350.844	540.030	-1.295
209	-350.844	540.030	1.295
210	-352.592	538.811	2.925
211	-318.944	538.811	150.349
212	-316.661	540.030	151.059
213	-315.538	540.030	153.392
214	-316.406	538.811	155.619
215	-222.124	538.811	273.844
216	-219.760	540.030	273.493
217	-217.735	540.030	275.108
218	-217.551	538.811	277.491
219	.000	637.630	65.166
220	50.948	637.630	40.630
221	63.532	637.630	-14.501
222	28.274	637.630	-58.712
223	-28.274	637.630	-58.712
224	-63.532	637.630	-14.501
225	-50.948	637.630	40.630
226	50.948	630.970	105.796
227	114.480	630.970	26.129
228	91.806	630.970	-73.213
229	.000	630.970	-117.424
230	-91.806	630.970	-73.213
231	-114.480	630.970	26.129
232	-50.948	630.970	105.796
233	.000	611.514	192.227
234	55.130	611.514	179.644
235	106.078	611.514	155.108
236	150.289	611.514	119.852
237	174.824	611.514	68.904

238	187.408	611.514	13.773
239	187.408	611.514	-42.774
240	162.872	611.514	-93.722
241	127.615	611.514	-137.934
242	83.404	611.514	-173.191
243	28.274	611.514	-185.774
244	-28.274	611.514	-185.774
245	-83.404	611.514	-173.191
246	-127.615	611.514	-137.934
247	-162.872	611.514	-93.722
248	-187.408	611.514	-42.774
249	-187.408	611.514	13.773
250	-174.824	611.514	68.904
251	-150.289	611.514	119.852
252	-106.078	611.514	155.108
253	-55.130	611.514	179.644
254	55.130	592.057	241.540
255	154.471	592.057	193.700
256	223.216	592.057	107.495
257	247.752	592.057	.000
258	223.216	592.057	-107.495
259	154.471	592.057	-193.700
260	55.130	592.057	-241.540
261	-55.130	592.057	-241.540
262	-154.471	592.057	-193.700
263	-223.216	592.057	-107.495
264	-247.752	592.057	.000
265	-223.216	592.057	107.495
266	-154.471	592.057	193.700
267	-55.130	592.057	241.540
268	39.304	565.434	299.263
269	94.434	565.434	286.680
270	165.257	565.434	252.573
271	209.468	565.434	217.316
272	258.479	565.434	155.858
273	283.014	565.434	104.911
274	300.506	565.434	28.274
275	300.506	565.434	-28.274
276	283.014	565.434	-104.911
277	258.479	565.434	-155.858
278	209.468	565.434	-217.316
279	165.257	565.434	-252.573
280	94.434	565.434	-286.680
281	39.304	565.434	-299.263
282	-39.304	565.434	-299.263
283	-94.434	565.434	-286.680
284	-165.257	565.434	-252.573
285	-209.468	565.434	-217.316

286	-258.479	565.434	-155.858
287	-283.014	565.434	-104.911
288	-300.506	565.434	-28.274
289	-300.506	565.434	28.274
290	-283.014	565.434	104.911
291	-258.479	565.434	155.858
292	-209.468	565.434	217.316
293	-165.257	565.434	252.573
294	-94.434	565.434	286.680
295	-39.304	565.434	299.263
296	.000	538.811	344.403
297	149.431	538.811	310.296
298	269.265	538.811	214.732
299	335.768	538.811	76.637
300	335.768	538.811	-76.637
301	269.265	538.811	-214.732
302	149.431	538.811	-310.296
303	.000	538.811	-344.403
304	-149.431	538.811	-310.296
305	-269.265	538.811	-214.732
306	-335.768	538.811	-76.637
307	-335.768	538.811	76.637
308	-269.265	538.811	214.732
309	-149.431	538.811	310.296

MEMBER	INCIDENCES	
1	1	37
2	44	2
3	1	38
4	50	3
5	1	39
6	56	4
7	1	40
8	62	5
9	1	41
10	68	6
11	1	42
12	74	7
13	1	43
14	80	8
15	2	45
16	51	3
17	3	55
18	57	4
19	4	61
20	63	5
21	5	67
22	69	6
23	6	73

24	75	7
25	7	79
26	81	8
27	8	85
28	49	2
29	2	47
30	86	9
31	2	46
32	91	10
33	3	52
34	96	10
35	3	53
36	97	11
37	3	54
38	102	12
39	4	58
40	107	12
41	4	59
42	108	13
43	4	60
44	113	14
45	5	64
46	118	14
47	5	65
48	119	15
49	5	66
50	124	16
51	6	70
52	129	16
53	6	71
54	130	17
55	6	72
56	135	18
57	7	76
58	140	18
59	7	77
60	141	19
61	7	78
62	146	20
63	8	82
64	151	20
65	8	83
66	152	21
67	8	84
68	157	22
69	2	48
70	162	22
71	9	87

72	92	10
73	10	95
74	98	11
75	11	101
76	103	12
77	12	106
78	109	13
79	13	112
80	114	14
81	14	117
82	120	15
83	15	123
84	125	16
85	16	128
86	131	17
87	17	134
88	136	18
89	18	139
90	142	19
91	19	145
92	147	20
93	20	150
94	153	21
95	21	156
96	158	22
97	22	161
98	90	9
99	9	88
100	168	24
101	10	93
102	169	24
103	10	94
104	172	25
105	11	99
106	173	25
107	11	100
108	176	26
109	12	104
110	177	26
111	12	105
112	180	27
113	13	110
114	181	27
115	13	111
116	184	28
117	14	115
118	185	28
119	14	116

120	188	29
121	15	121
122	189	29
123	15	122
124	192	30
125	16	126
126	193	30
127	16	127
128	196	31
129	17	132
130	197	31
131	17	133
132	200	32
133	18	137
134	201	32
135	18	138
136	204	33
137	19	143
138	205	33
139	19	144
140	208	34
141	20	148
142	209	34
143	20	149
144	212	35
145	21	154
146	213	35
147	21	155
148	216	36
149	22	159
150	217	36
151	22	160
152	164	23
153	9	89
154	165	23
155	23	166
156	167	24
157	24	170
158	171	25
159	25	174
160	175	26
161	26	178
162	179	27
163	27	182
164	183	28
165	28	186
166	187	29
167	29	190

168	191	30
169	30	194
170	195	31
171	31	198
172	199	32
173	32	202
174	203	33
175	33	206
176	207	34
177	34	210
178	211	35
179	35	214
180	215	36
181	36	218
182	163	23
183	37	219
184	219	44
185	38	220
186	220	50
187	39	221
188	221	56
189	40	222
190	222	62
191	41	223
192	223	68
193	42	224
194	224	74
195	43	225
196	225	80
197	45	226
198	226	51
199	55	227
200	227	57
201	61	228
202	228	63
203	67	229
204	229	69
205	73	230
206	230	75
207	79	231
208	231	81
209	85	232
210	232	49
211	47	233
212	233	86
213	46	234
214	234	91
215	52	235

216	235	96
217	53	236
218	236	97
219	54	237
220	237	102
221	58	238
222	238	107
223	59	239
224	239	108
225	60	240
226	240	113
227	64	241
228	241	118
229	65	242
230	242	119
231	66	243
232	243	124
233	70	244
234	244	129
235	71	245
236	245	130
237	72	246
238	246	135
239	76	247
240	247	140
241	77	248
242	248	141
243	78	249
244	249	146
245	82	250
246	250	151
247	83	251
248	251	152
249	84	252
250	252	157
251	48	253
252	253	162
253	87	254
254	254	92
255	95	255
256	255	98
257	101	256
258	256	103
259	106	257
260	257	109
261	112	258
262	258	114
263	117	259

264	259	120
265	123	260
266	260	125
267	128	261
268	261	131
269	134	262
270	262	136
271	139	263
272	263	142
273	145	264
274	264	147
275	150	265
276	265	153
277	156	266
278	266	158
279	161	267
280	267	90
281	88	268
282	268	168
283	93	269
284	269	169
285	94	270
286	270	172
287	99	271
288	271	173
289	100	272
290	272	176
291	104	273
292	273	177
293	105	274
294	274	180
295	110	275
296	275	181
297	111	276
298	276	184
299	115	277
300	277	185
301	116	278
302	278	188
303	121	279
304	279	189
305	122	280
306	280	192
307	126	281
308	281	193
309	127	282
310	282	196
311	132	283

312	283	197
313	133	284
314	284	200
315	137	285
316	285	201
317	138	286
318	286	204
319	143	287
320	287	205
321	144	288
322	288	208
323	148	289
324	289	209
325	149	290
326	290	212
327	154	291
328	291	213
329	155	292
330	292	216
331	159	293
332	293	217
333	160	294
334	294	164
335	89	295
336	295	165
337	166	296
338	296	167
339	170	297
340	297	171
341	174	298
342	298	175
343	178	299
344	299	179
345	182	300
346	300	183
347	186	301
348	301	187
349	190	302
350	302	191
351	194	303
352	303	195
353	198	304
354	304	199
355	202	305
356	305	203
357	206	306
358	306	207
359	210	307

```
  360  307  211
  361  214  308
  362  308  215
  363  218  309
  364  309  163
MEMBER PROPERTIES
1 TO 154 PRISMATIC AX 8.456 IX 0.056 IY 2.912 IZ 41.84 YD 6.
155 TO 182 PRISMATIC AX 14.72 IX 0.256 IY 15.24 IZ 86.08 YD 6.
183 TO 336 PRISMATIC AX 2.114 IX 0.014 IY 0.728 IZ 10.46 YD 6.
337 TO 364 PRISMATIC AX 3.68 IX 0.064 IY 3.81 IZ 21.52 YD 6.
SUPPORTS
23 TO 26 FIXED BUT FX FZ MX MY MZ
27 34 FIXED BUT FX MX MY MZ
28 TO 33 FIXED BUT FX FZ MX MY MZ
35 36 FIXED BUT FX FZ MX MY MZ
CONSTANTS
E 10100000. ALL
REF 0. 0. 0. ALL
LOAD 1 (UNBALANCED SNOW)
MEMBER LOAD
5 11 TRAP GY -2.2178 -2.2514
7 9 TRAP GY -4.4356 -4.5029
6 12 TRAP GY -3.6528 -3.6864
8 10 TRAP GY -7.3054 -7.3727
19 TO 24 UNI GY -8.6446
41 59 TRAP GY -3.8974 -3.9563
47 53 TRAP GY -7.7454 -7.8643
43 49 55 TRAP GY -8.8557 -8.8806
45 51 57 TRAP GY -8.8062 -8.8321
48 54 TRAP GY -12.7677 -12.8866
42 60 TRAP GY -6.3844 -6.4433
44 50 56 TRAP GY -10.1000 -10.1249
46 52 58 TRAP GY -10.0990 -10.1249
79 82 83 86 87 90 TRAP GY -12.7685 -12.7439
80 81 84 85 88 89 TRAP GY -11.8652 -11.8406
113 139 TRAP GY -7.8763 -7.8635
114 140 TRAP GY -7.3302 -7.3174
115 117 119 121 123 125 TRAP GY -14.2015 -14.1857
127 129 131 133 135 137 TRAP GY -14.2015 -14.1857
116 118 120 122 124 126 TRAP GY -13.5270 -13.5112
128 130 132 134 136 138 TRAP GY -13.5270 -13.5112
163 TO 176 UNI GY -7.3174
187 193 TRAP GY -2.2514 -2.9521
189 191 TRAP GY -4.5029 -5.9042
188 194 TRAP GY -2.9521 -3.6528
190 192 TRAP GY -5.9042 -7.3054
201 TO 206 UNI GY -8.6446
223 241 TRAP GY -3.9563 -5.1704
```

```
224 242 TRAP GY -5.1704 -6.3844
225 231 237 TRAP GY -8.8806 -9.4903
227 233 239 TRAP GY -8.8321 -9.4656
226 232 238 TRAP GY -9.4903 -10.1000
228 234 240 TRAP GY -9.4656 -10.0990
229 235 TRAP GY -7.8643 -10.3160
230 236 TRAP GY -10.3160 -12.7677
261 264 265 268 269 272 TRAP GY -12.7439 -12.3046
262 263 266 267 270 271 TRAP GY -12.3046 -11.8652
295 321 TRAP GY -7.8635 -7.5969
296 322 TRAP GY -7.5969 -7.3302
297 299 301 303 305 307 TRAP GY -14.1857 -13.8564
309 311 313 315 317 319 TRAP GY -14.1857 -13.8564
298 300 302 304 306 308 TRAP GY -13.8564 -13.5270
310 312 314 316 318 320 TRAP GY -13.8564 -13.5270
345 TO 358 UNI GY -7.3174
PERFORM ANALYSIS
PRINT ANALYSIS
FINISH
```

APPENDIX E

COMPUTER PROGRAM LISTINGS

```
 10 DIM JC(50,4), MI(100,3), PEI(60,4), PJI(60,4)  JL(50,2), EL(100,2)
 11 DIM PA(60,2), CJL(50,2), MF(100,3), AMF(100,4), LMF(100,4)
 12 PRINT "                    ******************"
 13 PRINT "                    *                  *"
 14 PRINT "                    *  PANEL LOADS     *"
 15 PRINT "                    *                  *"
 16 PRINT "                    ******************"
 17 PRINT:PRINT
 18 PRINT "   TRANSFORMS PRESSURE LOADS INTO CONCENTRATED LOADS AT JOINTS"
 19 PRINT "   AND DISTRIBUTED LOADS ALONG MEMBERS":PRINT:PRINT:PRINT
 20 INPUT "DATE": DT$
 30 PRINT
 40 INPUT "NUMBER OF JOINTS=",NJ%
 50 INPUT "NUMBER OF ELEMENTS=",NE%
 60 INPUT "NUMBER OF PANELS=",NP%
 70 PRINT
 72 PRINT
 80 PRINT "   UNITS: INCH, POUNDS "
 90 PRINT
100 PRINT "ENTER JOINT NUMBER AND JOINT COORDINATES FOR NUMBER OF JOINTS"
110 PRINT "JOINT#,X,Y,Z"
120 FOR I=1 TO NJ%
130 INPUT JC(I,1),JC(I,2),JC(I,3),JC(I,4)
140 NEXT I
150 PRINT
160 PRINT "ENTER MEMBER NUMBER AND MEMBER INCIDENCE FOR NUMBER OF ELEMENTS"
170 PRINT "ELEMENT#,A-END,B-END"
180 FOR J=1 TO NE%
190 INPUT MI(J,1),MI(J,2),MI(J,3)
200 NEXT J
210 PRINT
220 PRINT "ENTER PANEL NUMBER AND PANEL ELEMENT INCINDENCE FOR NUMBER OF"
225 PRINT "PANELS"
230 PRINT "PANEL#,ELEMENT#1,ELEMENT#2,ELEMENT#3"
240 FOR K=1 TO NP%
250 INPUT PEI(K,1),PEI(K,2),PEI(K,3),PEI(K,4)
260 NEXT K
270 PRINT
280 PRINT "ENTER PANEL NUMBER AND PANEL JOINT INCIDENCE FOR NUMBER OF PANELS"
290 PRINT "PANEL#,JOINT#1,JOINT#2,JOINT#3"
300 FOR I=1 TO NP%
310 INPUT PJI(I,1),PJI(I,2),PJI(I,3),PJI(I,4)
320 NEXT I
330 PRINT
340 PRINT "ENTER JOINT NUMBER AND PRESSURE AT JOINT FOR NUMBER OF JOINTS"
350 PRINT "JOINT# PRESSURE"
360 FOR J=1 TO NJ%
370 INPUT JL(J,1),JL(J,2)
380 NEXT J
390 PRINT
400 REM
410 REM    CALCULATE ELEMENT LENGTHS
420 REM
430 FOR K=1 TO NE%
440 EL(K,1)=MI(K,1)
450 AE=MI(K,2)
460 BE=MI(K,3)
470 FOR I=1 TO NJ%
480 IF AE=JC(I,1) THEN X1=JC(I,2):Y1=JC(I,3):Z1=JC(I,4)
490 IF BE=JC(I,1) THEN X2=JC(I,2):Y2=JC(I,3):Z2=JC(I,4)
500 NEXT I
510 EL(K,2)=((X2-X1)^2+(Y2-Y1)^2+(Z2-Z1)^2)^0.5
520 NEXT K
530 REM
540 REM    CALCULATE PANEL AREAS
```

```
550 REM
560 FOR I=1 TO NP%
570 PA(I,1)=PEI(I,1)
575 FOR J=1 TO NE%
580 IF PEI(I,2)=EL(J,1) THEN LA1=EL(J,2)
590 IF PEI(I,3)=EL(J,1) THEN LA2=EL(J,2)
600 IF PEI(I,4)=EL(J,1) THEN LA3=EL(J,2)
605 NEXT J
610 S=0.5*(LA1+LA2+LA3)
620 PA(I,2)=(S*(S-LA1)*(S-LA2)*(S-LA3))^0.5
630 NEXT I
640 REM
650 REM   CLCULATE EQUIVALENT CONCENTRATED LOAD AT JOINTS
660 REM
670 FOR I=1 TO NP%
680 J1=PJI(I,2)
690 J2=PJI(I,3)
700 J3=PJI(I,4)
710 FOR J=1 TO NJ%
720 IF J1=JL(J,1) THEN P1=JL(J,2):C1=J:CJL(J,1)=JL(J,1)
730 IF J2=JL(J,1) THEN P2=JL(J,2):C2=J:CJL(J,1)=JL(J,1)
740 IF J3=JL(J,1) THEN P3=JL(J,2):C3=J:CJL(J,1)=JL(J,1)
750 NEXT J
760 FOR K=1 TO NP%
770 IF PJI(K,1)=PA(K,1) THEN AC=PA(K,2)
780 NEXT K
790 R1=(2*P1*AC)/12+(P2*AC)/12+(P3*AC)/12
800 R2=(P1*AC)/12+(2*P2*AC)/12+(P3*AC)/12
810 R3=(P1*AC)/12+(P2*AC)/12+(2*P3*AC)/12
820 CJL(C1,2)=R1+CJL(C1,2)
830 CJL(C2,2)=R2+CJL(C2,2)
840 CJL(C3,2)=R3+CJL(C3,2)
850 NEXT I
860 REM
870 REM    CALCULATE EQUIVALENT NON-UNIFORM DISTRIBUTED LOAD
875 REM    ALONG ELEMENTS
880 REM
890 FOR K=1 TO NP%
894 FOR H=1 TO NP%
895 IF PEI(K,1)=PJI(H,1) GOTO 900
896 NEXT H
900 EN1=PEI(K,2)
910 EN2=PEI(K,3)
920 EN3=PEI(K,4)
930 DJ1=PJI(H,2)
940 DJ2=PJI(H,3)
950 DJ3=PJI(H,4)
960 FOR I=1 TO NE%
970 IF EN1=EL(I,1) THEN L1=EL(I,2)
980 IF EN2=EL(I,1) THEN L2=EL(I,2)
990 IF EN3=EL(I,1) THEN L3=EL(I,2)
1000 NEXT I
1010 FOR J=1 TO NP%
1020 IF PA(J,1)=PEI(K,1) THEN AP=PA(J,2)
1030 NEXT J
1040 L=(L1+L2)*(L1+L3)*(L2+L3)+L1*L2*L3
1050 F11=6*L1^2+7*L1*L2+7*L1*L3+4*L2*L3
1060 F12=3*L1^2+4*L1*L2+L1*L2-2*L2*L3
1070 F13=3*L1^2+L1*L2+4*L1*L3-2*L2*L3
1080 F21=3*L2^2+4*L1*L2-2*L1*L3+L2*L3
1090 F22=6*L2^2+7*L1*L2+4*L1*L3+7*L2*L3
1100 F23=3*L2^2+L1*L2-2*L1*L3+4*L2*L3
1110 F31=3*L3^2-2*L1*L2+4*L1*L3+L2*L3
1120 F32=3*L3^2-2*L1*L2+L1*L3+4*L2*L3
1130 F33=6*L3^2+4*L1*L2+7*L1*L3+7*L2*L3
1140 FOR I=1 TO NJ%
```

```
1150 IF DJ1=JL(I,1) THEN DP1=JL(I,2)
1160 IF DJ2=JL(I,1) THEN DP2=JL(I,2)
1170 IF DJ3=JL(I,1) THEN DP3=JL(I,2)
1180 NEXT I
1190 DF1=((DP1*F11+DP2*F12+DP3*F13)*AP)/(12*L)
1200 DF2=((DP1*F21+DP2*F22+DP3*F23)*AP)/(12*L)
1210 DF3=((DP1*F31+DP2*F32+DP3*F33)*AP)/(12*L)
1220 FOR H=1 TO NE%
1230 IF EN1=MI(H,1) GOTO 1270
1240 IF EN2=MI(H,1) GOTO 1400
1250 IF EN3=MI(H,1) GOTO 1530
1260 GOTO 1650
1270 IF DJ2=MI(H,2) GOTO 1340
1280 DMFA=DF3
1290 DMFB=DF2
1300 MF(H,1)=EN1
1310 MF(H,2)=DMFA+MF(H,2)
1320 MF(H,3)=DMFB+MF(H,3)
1330 GOTO 1650
1340 DMFA=DF2
1350 DMFB=DF3
1360 MF(H,1)=EN1
1370 MF(H,2)=DMFA+MF(H,2)
1380 MF(H,3)=DMFB+MF(H,3)
1390 GOTO 1650
1400 IF DJ3=MI(H,2) GOTO 1470
1410 DMFA=DF1
1420 DMFB=DF3
1430 MF(H,1)=EN2
1440 MF(H,2)=DMFA+MF(H,2)
1450 MF(H,3)=DMFB+MF(H,3)
1460 GOTO 1650
1470 DMFA=DF3
1480 DMFB=DF1
1490 MF(H,1)=EN2
1500 MF(H,2)=DMFA+MF(H,2)
1510 MF(H,3)=DMFB+MF(H,3)
1520 GOTO 1650
1530 IF DJ1=MI(H,2) GOTO 1600
1540 DMFA=DF2
1550 DMFB=DF1
1560 MF(H,1)=EN3
1570 MF(H,2)=DMFA+MF(H,2)
1580 MF(H,3)=DMFB+MF(H,3)
1590 GOTO 1650
1600 DMFA=DF1
1610 DMFB=DF2
1620 MF(H,1)=EN3
1630 MF(H,2)=DMFA+MF(H,2)
1640 MF(H,3)=DMFB+MF(H,3)
1650 REM     END OF IF-GOTO STATEMENTS
1660 NEXT H
1670 NEXT K
1680 REM
2070 REM     CALCULATE NON-UNIFORM DISTRIBUTED LOAD LINEAR EQUATION
2080 REM
2090 FOR I=1 TO NE%
2100 LN=MI(I,1)
2110 LJ1=MI(I,2)
2120 LJ2=MI(I,3)
2130 FOR J=1 TO NJ%
2140 IF LJ1=JC(J,1) THEN LX1=JC(J,2):LZ1=JC(J,4)
2150 IF LJ2=JC(J,1) THEN LX2=JC(J,2):LZ2=JC(J,4)
2160 NEXT J
2170 FOR K=1 TO NE%
2180 IF LN=MF(K,1) THEN LF1=MF(K,2):LF2=MF(K,3)
```

```
2190 NEXT K
2200 IF LX1=LX2 GOTO 2280
2210 M=(LF2-LF1)/(LX2-LX1)
2220 B=(LX2*LF1-LX1*LF2)/(LX2-LX1)
2230 LMF(I,1)=LN
2240 LMF(I,2)=1
2250 LMF(I,3)=M
2260 LMF(I,4)=B
2270 GOTO 2340
2280 M=(LF2-LF1)/(LZ2-LZ1)
2290 B=(LZ2*LF1-LZ1*LF2)/(LZ2-LZ1)
2300 LMF(I,1)=LN
2310 LMF(I,2)=3
2320 LMF(I,3)=M
2330 LMF(I,4)=B
2340 REM END OF IF-GOTO STATEMENTS
2350 NEXT I
2360 REM
2370 REM    PRINT OUTPUT
2380 REM
2400 REM
2410 REM    PRINT INPUT
2420 REM
2423 PRINT "                ************************************"
2427 PRINT "                *                                  *"
2430 PRINT "                *          PANEL LOADS             *"
2433 PRINT "                *                                  *"
2437 PRINT "                ************************************"
2440 PRINT : PRINT
2445 PRINT "   *****  UNITS: INCH, POUNDS  *****":PRINT
2450 PRINT "   DATE=";DT$
2460 PRINT
2465 PRINT "................................................................"
2467 PRINT
2470 PRINT "               ********** ECHO INPUT **********
2480 PRINT
2490 PRINT "   NUMBER OF JOINTS  =";NJ%
2500 PRINT "   NUMBER OF ELEMENTS=";NE%
2510 PRINT "   NUMBER OF PANELS  =";NP%
2520 PRINT
2530 PRINT "   HUB RADIUS=";HR;" INCH"
2540 PRINT
2550 PRINT
2560 PRINT "-----  JOINT COORDINATES(INCH)  -----"
2570 PRINT "JOINT#","X","Y","Z"
2580 FOR I=1 TO NJ%
2590 PRINT JC(I,1),JC(I,2),JC(I,3),JC(I,4)
2600 NEXT I
2610 PRINT:PRINT
2626 PRINT "-----  MEMBER INCIDENCE  -----"
2630 PRINT "ELEMENT#","A-END","B-END","LENGTH(INCH)"
2640 FOR J=1 TO NE%
2650 FOR K=1 TO NE%
2660 IF MI(J,1)=EL(K,1) GOTO 2680
2670 NEXT K
2680 PRINT MI(J,1),MI(J,2),MI(J,3),EL(K,2)
2690 NEXT J
2700 PRINT:PRINT
2710 PRINT "-----  PANEL ELEMENT INCIDENCE  -----'
2720 PRINT "PANEL#","ELEMENT#1","ELEMENT#2","ELEMENT#3","AREA(SQ. IN)'
2730 FOR I=1 TO NP%
2740 FOR J=1 TO NP%
2750 IF PEI(I,1)=PA(J,1) GOTO 2770
2760 NEXT J
2770 PRINT PEI(I,1),PEI(I,2),PEI(I,3),PEI(I,4),PA(J,2)
2780 NEXT I
```

```
2790 PRINT:PRINT
2800 PRINT "-----  PANEL JOINT INCIDENCE  -----"
2810 PRINT "PANEL#","JOINT#1","JOINT#2","JOINT#3"
2820 FOR K=1 TO NP%
2830 PRINT PJI(K,1),PJI(K,2),PJI(K,3),PJI(K,4)
2840 NEXT K
2850 PRINT:PRINT
2860 PRINT "-----  PRESSURE LOAD AT JOINTS  -----"
2870 PRINT "JOINT#","PRESSURE(PSI)"
2880 FOR I=1 TO NJ%
2890 PRINT JL(I,1),JL(I,2)
2900 NEXT I
2910 PRINT
2915 PRINT "................................................................."
2920 PRINT
2930 PRINT "               **********  OUTPUT  **********"
2940 PRINT
2950 PRINT
2960 PRINT "-----  EQUIVALENT CONCENTRATED LOAD AT JOINTS  -----"
2970 PRINT
2980 PRINT "JOINT#","LOAD(POUNDS)"
2990 FOR J=1 TO NJ%
3000 PRINT CJL(J,1),CJL(J,2)
3010 NEXT J
3020 PRINT
3030 PRINT
3040 PRINT "-----  EQUIVALENT DISTRIBUTED LOAD ALONG MEMBER  -----"
3050 PRINT
3060 PRINT "ELEMENT#","A-END","A-END FORCE","B-END FORCE","B-END"
3070 FOR K=1 TO NE%
3080 FOR I=1 TO NE%
3090 IF MF(K,1)=MI(I,1) GOTO 3110
3100 NEXT I
3110 PRINT MF(K,1),MI(I,2),MF(K,2),MF(K,3),MI(I,3)
3120 NEXT K
3130 PRINT
3140 PRINT "----- LINEAR FORCE EQUATION  -----"
3150 PRINT
3160 PRINT "ELEMENT#","FORCE EQUATION"
3170 FOR J=1 TO NE%
3180 PRINT LMF(J,1),"F=";LMF(J,3);"*COORD(";LMF(J,2);")+";LMF(J,4)
3190 NEXT J
3310 PRINT
3315 PRINT "................................................................."
20 PRINT
3330 PRINT "           **********  END OF PROGRAM  **********"
3340 PRINT
3350 END
3360 REM
3370 REM ***** INPUT DATA *****
3380 REM
3390 REM  1. ENTER DATE IN THE FORM: MM/DD/YY
3400 REM     DT$
3410 REM
3420 REM  2. ENTER NUMBER OF JOINTS
3430 REM     NJ
3440 REM
3450 REM  3. ENTER NUMBER OF ELEMENTS
3460 REM     NE
3470 REM
3480 REM  4. ENTER NUMBER OF PANELS
3490 REM     NP
3500 REM
3540 REM  5. ENTER JOINT NUMBER AND JOINT COORDINATE (X,Y,Z)
3550 REM     JC(I,1), JC(I,2), JC(I,3), JC(I,4)        I=1 TO NJ
3560 REM
```

```
3570 REM  6. ENTER MEMBER NUMBER AND MEMBER INCIDENCE
3580 REM     MI(J,1), MI(J,2), MI(J,3)                  J=1 TO NE
3590 REM
3600 REM  7. ENTER PANEL NUMBER AND PANEL ELEMENT INCIDENCE
3610 REM     PEI(I,1), PEI(I,2), PEI(I,3), PEI(I,4)    I=1 TO NP
3620 REM
3630 REM  8. ENTER PANEL NUMBER AND PANEL JOINT INCIDENCE
3640 REM     PJI(J,1), PJI(J,2), PJI(J,3), PJI(J,4)    J=1 TO NP
3650 REM
3660 REM  9. ENTER JOINT NUMBER AND PRESSURE LOAD AT JOINT
3670 REM     JL(I,1), JL(I,2)                          I=1 TO NJ
3680 REM
3690 REM ***** END OF INPUT *****
3700 REM
```

```
 10 DIM MF(100,4), IMF(100,11)
 20 PRINT
 30 PRINT "          ****************************"
 40 PRINT "          *                          *"
 50 PRINT "          *  TRAPEZOIDAL LOAD VALUES *"
 60 PRINT "          *                          *"
 70 PRINT "          ****************************"
 80 PRINT:PRINT:PRINT
 90 INPUT "DATE=";DT$
100 PRINT
110 PRINT "  UNITS: INCH, POUNDS"
120 PRINT
130 PRINT
140 INPUT "NUMBER OF MEMBERS=",NM
150 PRINT
160 PRINT
170 INPUT "HUB RADIUS=",HR
180 PRINT
190 PRINT " ENTER MEMBER NUMBER, LENGTH, A-END FORCE, AND B-END FORCE"
195 PRINT " FOR NUMBER OF MEMBERS."
200 PRINT
210 PRINT
220 FOR K=1 TO NM
230 INPUT "MEMBER NUMBER=",MF(K,1)
240 INPUT "LENGTH=",MF(K,2)
250 INPUT "A-END FORCE=",MF(K,3)
260 INPUT "B-END FORCE=",MF(K,4)
270 PRINT
280 NEXT K
290 FOR J=1 TO NM
300 IMF(J,1)=MF(J,1)
310 IMF(J,2)=MF(J,2)
320 IMF(J,3)=HR
330 IMF(J,4)=0.5*MF(J,2)-HR
340 IMF(J,5)=0.5*MF(J,2)-HR
350 IMF(J,6)=HR
360 IMF(J,7)=MF(J,3)
370 IMF(J,11)=MF(J,4)
380 REM
390 IF MF(J,3)>MF(J,4) GOTO 500
400 FH=MF(J,4)
410 FL=MF(J,3)
420 L=MF(J,2)
430 FL1=(HR*FH+FL*(L-HR))/L
440 FH1=(FH*(L-HR)+HR*FL)/L
450 FM=0.5*(FH+FL)
460 IMF(J,8)=FL1
470 IMF(J,9)=FM
480 IMF(J,10)=FH1
490 GOTO 590
500 FH=MF(J,3)
510 FL=MF(J,4)
520 L=MF(J,2)
530 FL1=(HR*FH+FL*(L-HR))/L
540 FH1=(FH*(L-HR)+HR*FL)/L
550 FM=0.5*(FH+FL)
560 IMF(J,8)=FH1
570 IMF(J,9)=FM
580 IMF(J,10)=FL1
590 REM
600 NEXT J
610 REM
620 REM PRINT OUTPUT
630 REM
640 PRINT
```

```
650 PRINT "           ******************************"
660 PRINT "           *                            *"
670 PRINT "           *  TRAPEZOIDAL LOAD VALUES   *"
680 PRINT "           *                            *"
690 PRINT "           ******************************"
700 PRINT:PRINT:PRINT
710 PRINT "           DATE=";DT$
720 PRINT:PRINT
730 PRINT "           UNITS: INCH, POUNDS"
740 PRINT:PRINT
750 PRINT "..........................................................................."
760 FOR I=1 TO NM
770 PRINT
780 PRINT "MEMBER NUMBER=";IMF(I,1),"LENGTH=";IMF(I,2)
790 PRINT "ELEMENT #1","L=";IMF(I,3),"A-END=";IMF(I,7),"B-END=";IMF(I,8)
800 PRINT "ELEMENT #2","L=";IMF(I,4),"A-END=";IMF(I,8),"B-END=";IMF(I,9)
810 PRINT "ELEMENT #3","L=";IMF(I,5),"A-END=";IMF(I,9),"B-END=";IMF(I,10)
820 PRINT "ELEMENT #4","L=";IMF(I,6),"A-END=";IMF(I,10),"B-END=";IMF(I,11)
830 PRINT
840 PRINT "..........................................................................."
850 NEXT I
860 PRINT
870 PRINT "           **********  END OF PROGRAM  **********"
880 PRINT
890 END
900 REM
910 REM *****  INPUT DATA  *****
920 REM
930 REM 1. ENTER DATE IN THE FORM: MM/DD/YY
940 REM    DT$
950 REM
960 REM 2. ENTER NUMBER OF MEMBERS
970 REM    NM
980 REM
990 REM 3. ENTER HUB RADIUS
1000 REM    HR
1010 REM
1020 REM 4. FOR NUMBER OF MEMBERS ENTER THE FOLLOWING:      I=1 TO NM
1030 REM
1040 REM    A. ENTER MEMBER NUMBER
1050 REM       MF(I,1)
1060 REM
1070 REM    B. ENTER MEMBER LENGTH
1080 REM       MF(I,2)
1090 REM
1100 REM    C. ENTER A-END FORCE
1110 REM       MF(I,3)
1120 REM
1130 REM    D. ENTER B-END FORCE
1140 REM       MF(I,4)
1150 REM
1160 REM *****  END OF INPUT  *****
1170 REM
```

VITA

The author was born on October 2, 1962, in Denver, Colorado. His parents are Charles F. and JaNell F., and he has two younger brothers, David and Philip. His wife, Julia Lynn, completed a Bachelor of Science in Psychology at Virginia Tech. The author attended Arlington County public schools, graduating in June 1981. He next attended Old Dominion University for one year before he transferred to Virginia Tech. In June 1985, he obtained a Bachelor of Science degree in Civil Engineering. After graduation, he enrolled in the graduate program at Virginia Tech. He is currently completing the requirements for the Master of Science degree in Civil Engineering (Structures).

ABSTRACT

A linear analysis of a commercial aluminum lattice dome was performed with the loads prescribed by the American National Standards Institute. The pressure snow loads were transformed into a distributed load along the dome members. The analysis of the dome was performed with the structural analysis program STAAD-III. The dome was modeled as a space frame with the joint member stiffness range from pinned-end to four times the member stiffness. The internal forces in the pinned-end and framed-end models were compared to the specifications by the Aluminum Association. The pinned-end model under the unbalanced snow load were found to exceed the allowable. The maximum deflection occurred when the joint stiffness was one-half of the member stiffness. The maximum axial force occurred when the joint stiffness was four times the member stiffness. The maximum moment at the midpoint of the member occurs when the member ends are pinned.